

---

# CHAPTER 3

---

## TRANSMISSION LINES AND WAVEGUIDES

This chapter is a long one and for this reason has been divided into three parts, namely:

Part 1—Waves on transmission lines

Part 2—Field analysis of transmission lines

Part 3—Rectangular and circular waveguides

The three parts are closely related but independent with the exception of Sec. 3.7, which is needed as an introduction to both Parts 2 and 3. With the exception of this section, the three parts can be studied independently and in any order.

In Part 1 we give an introduction to waves on transmission lines using a distributed-circuit model of the transmission line. By using the distributed-circuit model, we are able to study the excitation and propagation of current and voltage waves on a transmission line without the need to invoke Maxwell's equations.

The electrical characteristics of a transmission line such as the propagation constant, attenuation constant, characteristic impedance, and the distributed-circuit parameters can only be determined from a knowledge of the fields surrounding the transmission line. Thus in Part 2 we carry out a detailed field analysis of transmission lines. This part also includes an extensive discussion of planar transmission-line structures such as the microstrip line.

Part 3 presents the theory for waves in hollow rectangular and circular waveguides (pipes). In the beginning section of Part 2, we show that Maxwell's equations can be separated into equations that describe three types of waves. These are transverse electromagnetic waves (TEM), transverse electric (TE), and transverse magnetic (TM) waves. The TEM wave is the principal wave that can exist on a transmission line. The TE and TM waves are characterized by having no axial component of electric and magnetic field respectively. The TE and TM waves are the fundamental wave types that can exist in hollow-pipe waveguides. Hollow-pipe waveguides do not support TEM waves. The ability to reduce Maxwell's equations into three set of equations, one set for each wave type, facilitates the analysis of transmission lines and waveguides. Thus this decomposition of Maxwell's equations is carried out in the first section of Part 2.

## PART 1 WAVES ON TRANSMISSION LINES

---

In this section we introduce the topic of voltage and current waves on a two-conductor transmission line by using a distributed-circuit model of the transmission line. This allows us to explore a number of fundamental properties of one-dimensional waves without having to consider the electromagnetic fields in detail. The distributed-circuit-model approach has limitations and in general must be replaced by a detailed solution for the electromagnetic field associated with the guiding structure if we want to determine the distributed-circuit parameters. The field analysis of transmission lines is presented in Part 2.

### 3.1 WAVES ON AN IDEAL TRANSMISSION LINE

In Fig. 3.1a we show a two-conductor transmission line consisting of two parallel round conductors (wires). The conductors will be assumed to be perfect, i.e., have infinite conductivity. The conductors extend from  $z = 0$  to infinity, thus forming a semiinfinite transmission line. At  $z = 0$  a voltage generator with internal resistance  $R_g$  is connected to the transmission line. The generator produces a voltage  $\mathcal{V}_g(t)$  that is impressed across the transmission line. If the generator is switched on at time  $t = 0$ , a current  $\mathcal{I}(t)$  will begin to flow into the upper conductor. A return current  $-\mathcal{I}(t)$  must then flow on the lower conductor since current flow through the generator must be continuous. The return current is produced by the action of the electric field established between the two conductors. Since the transmission line is semiinfinite in length, there is no direct conducting path between the upper and lower conductors. However, there is a distributed capacitance  $C$

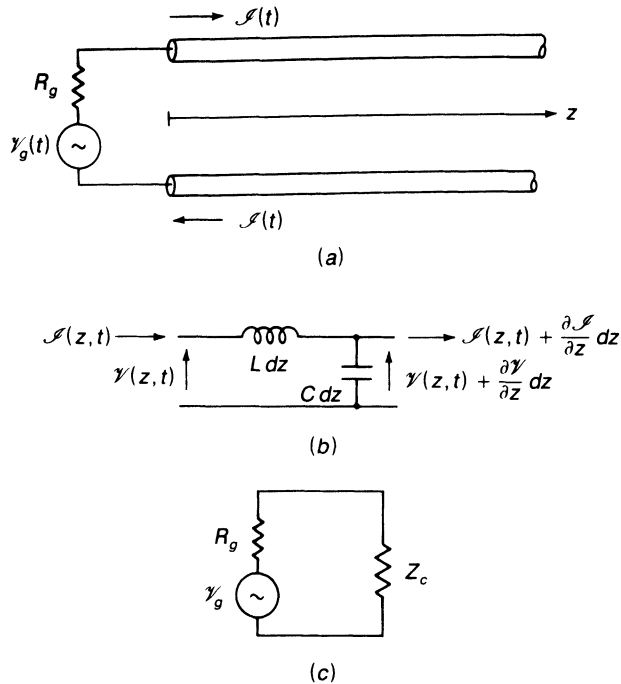


**FIGURE 3.1**  
 (a) An ideal two-conductor transmission line connected to a voltage generator; (b) equivalent circuit of a differential section of the transmission line with no loss; (c) equivalent circuit seen by the generator.

per meter between the two conductors; so we have a capacitive or displacement current flowing from the upper conductor to the lower conductor.

The electric current results in a magnetic field around the conductors and consequently the transmission line will also have a distributed series inductance  $L$  per meter. We can model a differential section  $dz$  of this transmission line as a series inductance  $L dz$  and a shunt capacitance  $C dz$  as shown in Fig. 3.1b. If the conductors had finite conductivity, we would also need to include a series resistance in the equivalent circuit of a differential section. However, we are assuming that the conductors are perfect; so the series distributed resistance  $R$  per meter is zero.

Since electrical effects propagate with a finite velocity  $v$  (the speed of light in vacuum), it should be clear that the voltage  $\mathcal{V}(z, t)$  and current  $\mathcal{I}(z, t)$  at some arbitrary point  $z$  on the transmission line will be zero until a time  $z/v$  has elapsed after switching the generator on. We will show that the generator launches voltage and current waves on the transmission line that propagate with a finite velocity. The equations that describe these waves are established by applying Kirchhoff's circuit laws to the equivalent circuit of a differential section of the transmission line, along with a specification of the terminal relationships (boundary conditions) that must hold at the generator end.

At some arbitrary point  $z$  on the transmission line, let the voltage and current be given by  $\mathcal{V}(z, t)$ ,  $\mathcal{I}(z, t)$ . At a differential distance  $dz$  further

along, the voltage and current have changed by small amounts  $(\partial\mathcal{V}/\partial z) dz$  and  $(\partial\mathcal{I}/\partial z) dz$ ; so the output voltage and current at  $z + dz$  will be

$$\mathcal{V}(z + dz, t) = \mathcal{V}(z, t) + \frac{\partial\mathcal{V}(z, t)}{\partial z} dz$$

$$\mathcal{I}(z + dz, t) = \mathcal{I}(z, t) + \frac{\partial\mathcal{I}(z, t)}{\partial z} dz$$

The sum of all potential drops around the circuit must be zero; so we have

$$-\mathcal{V} + L dz \frac{\partial\mathcal{I}}{\partial t} + \mathcal{V} + \frac{\partial\mathcal{V}}{\partial z} dz = 0$$

$$\text{or} \quad \frac{\partial\mathcal{V}(z, t)}{\partial z} = -L \frac{\partial\mathcal{I}(z, t)}{\partial t} \quad (3.1a)$$

The sum of currents flowing into the output node must also be zero; so we can write

$$\mathcal{I} - C dz \frac{\partial\mathcal{V}}{\partial t} - \mathcal{I} - \frac{\partial\mathcal{I}}{\partial z} dz = 0$$

$$\text{or} \quad \frac{\partial\mathcal{I}(z, t)}{\partial z} = -C \frac{\partial\mathcal{V}(z, t)}{\partial t} \quad (3.1b)$$

These two partial differential equations describe the relationship between the voltage and current waves on the transmission line.

We can obtain an equation for the voltage  $\mathcal{V}(z, t)$  by differentiating (3.1a) with respect to  $z$  and using (3.1b) to eliminate the current; thus

$$\frac{\partial^2\mathcal{V}(z, t)}{\partial z^2} = -L \frac{\partial^2\mathcal{I}}{\partial z \partial t} = -L \left( -C \frac{\partial^2\mathcal{V}}{\partial t^2} \right)$$

$$\text{or} \quad \frac{\partial^2\mathcal{V}(z, t)}{\partial z^2} - LC \frac{\partial^2\mathcal{V}(z, t)}{\partial t^2} = 0 \quad (3.2a)$$

In a similar way we obtain

$$\frac{\partial^2\mathcal{I}(z, t)}{\partial z^2} - LC \frac{\partial^2\mathcal{I}(z, t)}{\partial t^2} = 0 \quad (3.2b)$$

The product  $LC$  has the dimensions of one over velocity squared. These two equations are one-dimensional wave equations and describe waves propagating with a velocity†

$$v = \frac{1}{\sqrt{LC}} \quad (3.3)$$

†For an ideal transmission line in air,  $v = c = 3 \times 10^8$  m/s, the velocity of light.

Consider the equation

$$\frac{\partial^2 \mathcal{V}}{\partial z^2} - \frac{1}{v^2} \frac{\partial^2 \mathcal{V}}{\partial t^2} = 0$$

We can readily show that any two arbitrary functions of the form  $f^+(t - z/v)$  and  $f^-(t + z/v)$  are solutions of this equation. If we let  $w = t - z/v$  then we have

$$\frac{\partial f^+(t - z/v)}{\partial z} = \frac{\partial f^+(w)}{\partial z} = \frac{\partial f^+(w)}{\partial w} \frac{\partial w}{\partial z} = -\frac{1}{v} \frac{\partial f^+(w)}{\partial w}$$

and

$$\frac{\partial^2 f^+(w)}{\partial z^2} = \frac{1}{v^2} \frac{\partial^2 f^+(w)}{\partial w^2}$$

For  $\partial^2 f^+ / \partial t^2$  we get  $\partial^2 f^+ / \partial w^2$ . Consequently,

$$\frac{\partial^2 f^+}{\partial z^2} - \frac{1}{v^2} \frac{\partial^2 f^+}{\partial t^2} = \frac{\partial^2 f^+}{\partial w^2} \left( \frac{1}{v^2} - \frac{1}{v^2} \right) = 0$$

so  $f^+(t - z/v)$  is clearly a solution of the one-dimensional wave equation, as is  $f^-(t + z/v)$ .

The function  $f^+(t - z/v)$  is the same as the function  $f^+(t)$  but delayed in time by an amount  $z/v$  which equals the distance  $z$  divided by the velocity of propagation  $v$ . We interpret this solution as a wave propagating in the positive  $z$  direction and identify this solution with a superscript  $+$  sign. The other solution represents a wave propagating in the  $-z$  direction and is identified by the  $-$  sign as a superscript.

The general solution for the voltage waves on the transmission line is

$$\mathcal{V}(z, t) = V^+ f^+ \left( t - \frac{z}{v} \right) + V^- f^- \left( t + \frac{z}{v} \right) \quad (3.4)$$

where  $V^+$  and  $V^-$  are amplitude constants. By using (3.1b) we see that

$$\frac{\partial \mathcal{I}}{\partial z} = -C \left( V^+ \frac{\partial f^+}{\partial t} + V^- \frac{\partial f^-}{\partial t} \right)$$

If we assume that  $\mathcal{I}$  is of the form

$$\mathcal{I}(z) = I^+ f^+ \left( t - \frac{z}{v} \right) - I^- f^- \left( t + \frac{z}{v} \right)$$

then

$$\frac{\partial \mathcal{I}}{\partial z} = -\frac{1}{v} \left( I^+ \frac{\partial f^+}{\partial t} + I^- \frac{\partial f^-}{\partial t} \right)$$

upon using

$$\frac{\partial f^\pm}{\partial z} = \frac{\partial f^\pm}{\partial(t \mp z/v)} \frac{\partial(t \mp z/v)}{\partial z} = \mp \frac{1}{v} \frac{\partial f^\pm}{\partial t}$$

An examination of these equations shows that the assumed solution for

$\mathcal{I}(z, t)$  is compatible with that for the voltage  $\mathcal{V}(z, t)$  if we choose

$$I^+ = vCV^+ \quad I^- = vCV^-$$

The parameter  $vC$  has the dimensions of an admittance and is also equal to  $C/\sqrt{LC} = \sqrt{C/L}$ . The characteristic admittance  $Y_c$  of the transmission line is defined by this parameter. The reciprocal parameter is called the characteristic or surge impedance of the transmission line. It is given by

$$Z_c = \sqrt{\frac{L}{C}} = Y_c^{-1} \quad (3.5)$$

By using this parameter the solution for the current waves on the transmission line can be expressed in the form

$$\mathcal{I}(z, t) = \frac{V^+}{Z_c} f^+ \left( t - \frac{z}{v} \right) - \frac{V^-}{Z_c} f^- \left( t + \frac{z}{v} \right) \quad (3.6)$$

The negative sign preceding the wave with amplitude  $V^-$  indicates a reversal in the direction of current flow for the wave propagating in the  $-z$  direction.

For the transmission-line circuit shown in Fig. 3.1, the generator will launch voltage and current waves propagating in the  $+z$  direction. Since the transmission line extends to infinity, no waves propagating in the  $-z$  direction will be present. Later on we will consider a transmission line that is terminated at  $z = l$  with either a resistance, capacitance, or a combination of these elements. Waves propagating in both the  $+z$  and  $-z$  directions will then exist. For the present case the voltage and current waves on the transmission line are assumed to be

$$\mathcal{V}(z, t) = V^+ f^+ \left( t - \frac{z}{v} \right)$$

$$\mathcal{I}(z, t) = I^+ f^+ \left( t - \frac{z}{v} \right)$$

with  $V^+ = I^+ Z_c$ . At the generator end  $z = 0$  the terminal conditions require that

$$\mathcal{V}_g(t) = \mathcal{I}_g R_g + \mathcal{V}(0, t)$$

$$\mathcal{I}(0, t) = \mathcal{I}_g$$

where  $\mathcal{I}_g$  is the current supplied by the generator. These terminal conditions can be expressed in the form

$$\mathcal{V}_g(t) = R_g \frac{V^+}{Z_c} f^+(t) + V^+ f^+(t)$$

$$\frac{V^+}{Z_c} f^+(t) = \mathcal{I}_g$$

from which we find that

$$V^+ f^+(t) = \frac{Z_c}{Z_c + R_g} \mathcal{V}_g(t) \quad (3.7)$$

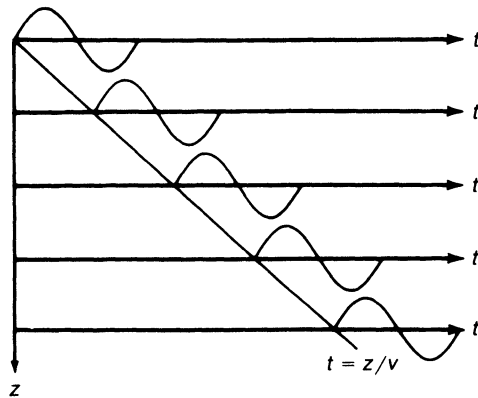
The voltage wave launched on the transmission line is thus given by

$$\mathcal{V}(z, t) = \frac{Z_c}{Z_c + R_g} \mathcal{V}_g\left(t - \frac{z}{v}\right) \quad (3.8a)$$

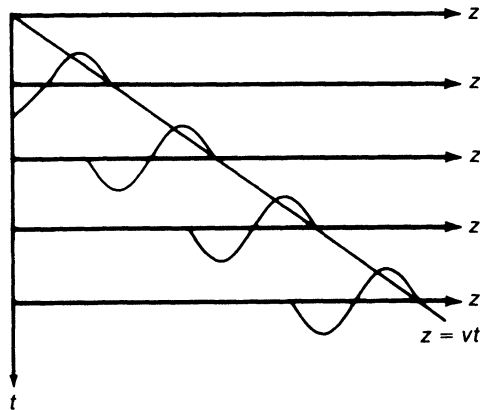
with a corresponding current wave

$$\mathcal{I}(z, t) = \frac{1}{Z_c + R_g} \mathcal{V}_g\left(t - \frac{z}{v}\right) \quad (3.8b)$$

At any point on the transmission line, the voltage waveform is the same as that produced by the generator but delayed in time and reduced in amplitude by the factor  $Z_c/(R_g + Z_c)$ . The voltage reduction is the usual voltage



(a)



(b)

**FIGURE 3.2**  
Time-distance and distance-time plots of voltage waveform  $\mathcal{V}(z, t)$  on a transmission line for a single-cycle sinusoidal generator voltage pulse.

division factor associated with the equivalent circuit shown in Fig. 3.1c. For the infinite line the generator sees only an equivalent impedance  $Z_c$  equal to the transmission-line characteristic impedance.

In Fig. 3.2a we show a time-distance plot of the voltage waveform on a transmission line for the case when the generator produces a single cycle of a sinusoidal waveform, i.e.,

$$\mathcal{V}_g(t) = V_0 \sin t \quad 0 \leq t \leq 2\pi$$

Figure 3.2a shows  $\mathcal{V}(z, t)$  as a function of  $t$  at various distances  $z$ , while Fig. 3.2b shows  $\mathcal{V}(z, t)$  as a function of  $z$  for various values of  $t$ . In the latter plot note that the leading edge of the waveform is the initial voltage produced by the generator at time  $t = 0$  and hence the waveform appears reversed when plotted as a function of  $z$ .

### 3.2 TERMINATED TRANSMISSION LINE: RESISTIVE LOAD

In Fig. 3.3 we show a transmission line terminated at a distance  $l$  from the generator in a load resistance  $R_L$ . At the load end the terminal conditions are

$$\mathcal{V}(l, t) = \mathcal{V}_L = \mathcal{I}_L R_L \quad (3.9a)$$

$$\mathcal{I}(l, t) = \mathcal{I}_L \quad (3.9b)$$

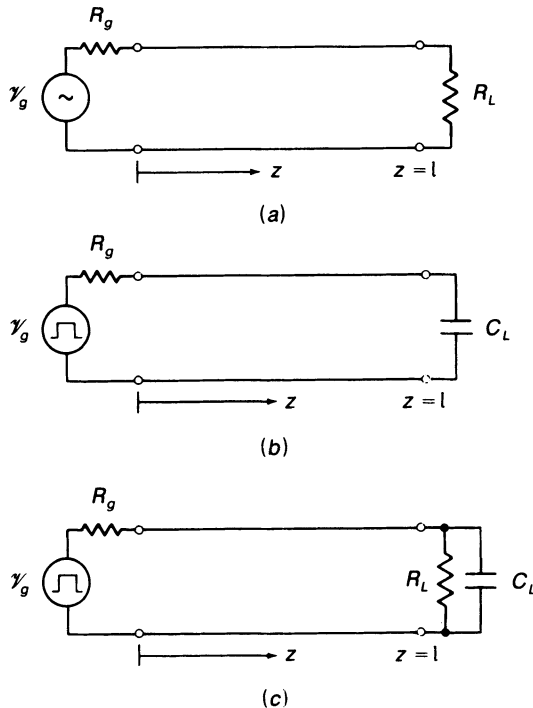


**FIGURE 3.3**  
The terminated transmission line.



If we choose  $R_L$  equal to the characteristic impedance  $Z_c$ , then  $\mathcal{V}_L = \mathcal{I}_L R_L = \mathcal{I}_L Z_c$ . For a wave propagating in the  $+z$  direction,  $\mathcal{V}(z, t) = Z_c \mathcal{I}(z, t)$ , so that at  $z = l$ ,  $\mathcal{V}(l, t) = Z_c \mathcal{I}(l, t)$ , which satisfies the load terminal condition. Thus by choosing  $R_L = Z_c$  the forward propagating wave will be completely absorbed by the load resistor and no reflected wave will be generated at the load end. Thus, in order to avoid a reflected wave, such as a reflected pulse in a digital circuit application, the transmission line should be terminated in its characteristic impedance.

When  $R_L \neq Z_c$  the terminal conditions at the load end cannot be satisfied without introducing a reflected wave. The incident wave at  $z = l$  is given by

$$\mathcal{V}_i(l, t) = \frac{Z_c}{Z_c + R_g} \mathcal{V}_g \left( t - \frac{l}{v} \right) = V^+ \mathcal{V}_g \left( t - \frac{l}{v} \right)$$

$$\mathcal{I}_i(l, t) = \frac{1}{Z_c} \mathcal{V}_i(l, t)$$

where  $V^+$  is the amplitude of  $\mathcal{V}_i$  relative to  $\mathcal{V}_g$ . In order for a reflected wave to combine with the incident wave so as to satisfy the terminal conditions (3.9), the reflected wave must have the same time dependence as that of the incident wave. Hence the form of the reflected wave will be

$$\mathcal{V}_r(z, t) = V^- \mathcal{V}_g \left( t - \frac{l}{v} + \frac{(z - l)}{v} \right)$$

$$= V^- \mathcal{V}_g \left( t + \frac{z}{v} - \frac{2l}{v} \right)$$

The argument must contain the factor  $t + z/v$  plus additional delay factors, so that at  $z = l$  the reflected wave has the form  $\mathcal{V}_g(t - l/v)$ . The reflected current wave is given by

$$\mathcal{I}_r(z, t) = -\frac{1}{Z_c} \mathcal{V}_r(z, t)$$

At the load end the total current on the transmission line must equal the current  $\mathcal{I}_L$  flowing through  $R_L$ ; thus

$$\frac{1}{Z_c} (V^+ - V^-) \mathcal{V}_g \left( t - \frac{l}{v} \right) = \mathcal{I}_L$$

The total voltage on the transmission line must equal the load voltage; so

$$(V^+ + V^-) \mathcal{V}_g \left( t - \frac{l}{v} \right) = V_L = \mathcal{I}_L R_L$$

When we divide this equation by the first one, we obtain

$$\frac{V^+ + V^-}{V^+ - V^-} = \frac{R_L}{Z_c}$$

which gives

$$\frac{V^-}{V^+} = \frac{R_L - Z_c}{R_L + Z_c} = \Gamma_L \quad (3.10)$$

The parameter  $\Gamma_L$  is called the load voltage reflection coefficient. The amplitude  $V^-$  is that of the reflected voltage wave and  $V^+$  is the amplitude of the incident voltage wave. The ratio is determined by the *conditions at the load end only*.

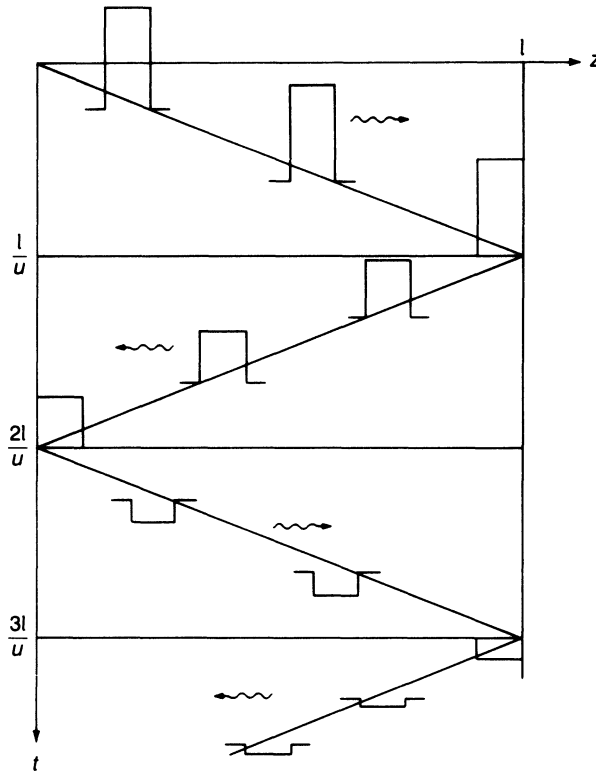
Once a reflected wave has been launched from the load termination, the total voltage on the transmission line will consist of the incident voltage wave plus the reflected voltage wave until the time at which the reflected wave reaches the generator end. If the generator internal impedance  $R_g$  equals the characteristic impedance  $Z_c$ , then the reflected wave is absorbed at the generator end. If  $R_g \neq Z_c$  then the reflected wave is reflected at the generator end to produce another forward propagating wave. For the reflected wave at the generator end, the terminal conditions are obtained by short-circuiting the voltage generator. Thus the reflected wave sees a termination  $R_g$  and will be reflected with a reflection coefficient  $\Gamma_g$  given by

$$\Gamma_g = \frac{R_g - Z_c}{R_g + Z_c} \quad (3.11)$$

As long as the generator continues to produce a voltage  $\mathcal{V}_g(t)$ , it continues to launch a first forward propagating wave with voltage  $\mathcal{V}_i(0, t) = Z_c \mathcal{V}_g(t) / (R_g + Z_c)$  and with current  $\mathcal{I}_i(0, t) = \mathcal{I}_g$ . Thus the superposition of a reflected wave at the generator end requires the launching of a second forward propagating wave with a voltage amplitude that cancels that of the reflected wave at the generator terminals, i.e., the generator is treated as being short-circuited. The second forward propagating wave will also undergo reflection at the load termination, so that as time proceeds we will end up with a multitude of forward propagating and reflected waves on the transmission line. This collection of waves can be described as follows:

$$\begin{aligned} \mathcal{V}(z, t) = & V^+ \mathcal{V}_g \left( t - \frac{z}{v} \right) + \Gamma_L V^+ \mathcal{V}_g \left( t + \frac{z - 2l}{v} \right) U \left( t - \frac{l}{v} \right) \\ & + \Gamma_g \Gamma_L V^+ \mathcal{V}_g \left( t - \frac{z + 2l}{v} \right) U \left( t - \frac{2l}{v} \right) \\ & + \Gamma_g \Gamma_L^2 V^+ \mathcal{V}_g \left( t + \frac{z - 4l}{v} \right) U \left( t - \frac{3l}{v} \right) \\ & + \Gamma_g^2 \Gamma_L^2 V^+ \mathcal{V}_g \left( t - \frac{z + 4l}{v} \right) U \left( t - \frac{4l}{v} \right) + \dots \quad (3.12) \end{aligned}$$

where  $V^+ = Z_c / (R_g + Z_c)$  and  $U(t - \alpha)$  is the unit step function which equals zero for  $t < \alpha$  and equals unity for  $t \geq \alpha$ . The unit step function is a

**FIGURE 3.4**

Distance-time plot of a pulse undergoing multiple reflection on a transmission line when  $\Gamma_L = -\Gamma_g = 0.5$ . Reflection at the generator end causes a reversal in the polarity of the pulse.

convenient function to use to specify when a waveform begins. In the case of multiple reflected waves on a transmission line, each reflected wave begins after time delays of  $l/v$ ,  $2l/v$ ,  $3l/v$ , etc., corresponding to the time delay to propagate a certain number of times back and forth between the generator end and load end.† The current wave can be obtained by multiplying the forward propagating waves by  $Y_c$  and the backward propagating waves by  $-Y_c$ . When the generator voltage  $\mathcal{V}_g(t)$  exists for only a finite time interval, the total voltage wave on the line will decay toward zero since each successive reflected wave is multiplied by a reflection coefficient, either  $\Gamma_L$  or  $\Gamma_g$ , which is less than one in magnitude, and hence successive waves are of diminishing amplitude.

The sequence of multiple reflected waves can be illustrated in a distance-time plot. In Fig. 3.4 we show this type of plot for a generator producing a rectangular pulse. We have chosen  $R_L = 3Z_c$  and  $R_g = Z_c/3$  so that  $\Gamma_L = 0.5$ ,  $\Gamma_g = -0.5$ . When the reflection coefficient is negative, the

†The unit step functions were introduced for clarity in describing the physical process but are actually not required in (3.12) since  $\mathcal{V}_g(t - \tau) = 0$  for  $t < \tau$ .

sign of the reflected voltage wave is reversed and this is illustrated in Fig. 3.4. In high-speed digital circuits using interconnecting transmission lines, multiple reflected pulses are undesirable and can be avoided by terminating each transmission line in a resistance equal to its characteristic impedance.

### 3.3 CAPACITIVE TERMINATION

When the transmission line is terminated in a reactive element such as a capacitor as shown in Fig. 3.3*b*, the reflected wave will have a waveform different from that of the incident wave. The solution for the reflected wave is readily found from the condition that the sum of the incident plus reflected voltage wave at  $z = l$  must satisfy the terminal conditions. The incident wave is again chosen to be  $\mathcal{V}_i(l, t) = V^+ \mathcal{V}_g(t - l/v)$ . The reflected wave is initiated at time  $t = l/v$  and will propagate from the point  $z = l$  toward the generator. Therefore it is of the form

$$\mathcal{V}_r\left(t - \frac{l}{v} + \frac{z - l}{v}\right) = \mathcal{V}_r\left(t + \frac{z - 2l}{v}\right)$$

For a capacitor we require

$$\mathcal{I}_L = C_L \frac{d\mathcal{V}_L}{dt} = C_L \left[ \frac{d\mathcal{V}_i(l, t)}{dt} + \frac{d\mathcal{V}_r(t - l/v)}{dt} \right]$$

where  $\mathcal{V}_r(t - l/v)$  is the reflected voltage wave at  $z = l$ . In addition, we use the condition

$$\mathcal{I}_L = Y_c \left[ \mathcal{V}_i(l, t) - \mathcal{V}_r\left(t - \frac{l}{v}\right) \right]$$

From these two equations we obtain

$$\begin{aligned} & \frac{d\mathcal{V}_r(t - l/v)}{dt} + \frac{1}{C_L Z_c} \mathcal{V}_r\left(t - \frac{l}{v}\right) \\ &= -\frac{d\mathcal{V}_i}{dt} + \frac{1}{C_L Z_c} \mathcal{V}_i \\ &= -V^+ \frac{d\mathcal{V}_g(t - l/v)}{dt} + \frac{V^+}{C_L Z_c} \mathcal{V}_g\left(t - \frac{l}{v}\right) \end{aligned} \quad (3.13)$$

For a specific example we will consider the case when the generator produces a rectangular pulse given by

$$\mathcal{V}_g(t) = 1 \quad 0 \leq t \leq T$$

The right-hand side of (3.13) will now become the source function

$$V^+ \left\{ \frac{1}{C_L Z_c} \left[ U\left(t - \frac{l}{v}\right) - U\left(t - \frac{l}{v} - T\right) \right] - \delta\left(t - \frac{l}{v}\right) + \delta\left(t - \frac{l}{v} - T\right) \right\}$$

where  $\delta(t - \alpha)$  is the Dirac delta function or impulse function that arises from the derivative of the rectangular pulse. We can integrate (3.13) by introducing the integrating factor  $e^{t/\tau}$  where  $\tau = C_L Z_c$ . We note that

$$\frac{d}{dt} (\mathcal{V}_r e^{t/\tau}) = e^{t/\tau} \left( \frac{d\mathcal{V}_r}{dt} + \frac{1}{\tau} \mathcal{V}_r \right)$$

so consequently

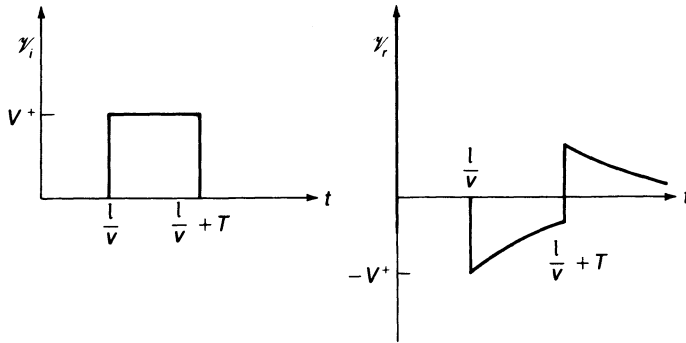
$$\begin{aligned} \int_{l/v}^t \frac{d}{dt} \mathcal{V}_r e^{t/\tau} dt &= \mathcal{V}_r \left( t - \frac{l}{v} \right) e^{t/\tau} - \mathcal{V}_r(0) e^{l/v\tau} \\ &= \frac{V^+}{\tau} \int_{l/v}^t \left[ U\left(t - \frac{l}{v}\right) - U\left(t - \frac{l}{v} - T\right) \right] e^{t/\tau} dt \\ &\quad - V^+ \int_{l/v}^t \left[ \delta\left(t - \frac{l}{v}\right) - \delta\left(t - \frac{l}{v} - T\right) \right] e^{t/\tau} dt \\ &= \begin{cases} V^+ (e^{t/\tau} - 2e^{l/v\tau}) & \frac{l}{v} \leq t \leq \frac{l}{v} + T \\ V^+ (-2e^{l/v\tau} + 2e^{(l+vT)/v\tau}) & t > \frac{l}{v} + T \end{cases} \end{aligned}$$

Since we have included the impulse functions as derivatives of the applied rectangular pulse, the lower limit of integration is regarded to be just before  $t = l/v$  and thus  $\mathcal{V}_r(0)$  is equal to zero since it corresponds to  $\mathcal{V}_r(0^-)$ . Hence we obtain

$$\mathcal{V}_r \left( t - \frac{l}{v} \right) = \begin{cases} V^+ (1 - 2e^{-(vt-l)/v\tau}) & \frac{l}{v} < t \leq \frac{l}{v} + T \\ V^+ (-2e^{l/v\tau} + 2e^{(l+vT)/v\tau}) e^{-t/\tau} & t > \frac{l}{v} + T \end{cases} \quad (3.14)$$

At  $t = l/v$  the reflected wave has an amplitude equal to  $-V^+$  which cancels that of the incident pulse. This is consistent with the requirement that initially the capacitor  $C_L$  is uncharged and must have a zero voltage across it. The capacitor charges to a final voltage level

$$\begin{aligned} V_c &= \mathcal{V}_i \left( l, t = \frac{l}{v} + T \right) + \mathcal{V}_r(T) \\ &= 2V^+ (1 - e^{-T/\tau}) \end{aligned}$$


**FIGURE 3.5**

Incident and reflected voltage waveforms at  $z = l$ .

at  $t = l/v + T$  and then discharges toward zero. The apparent discontinuous change that occurs in the reflected voltage wave at  $t = l/v + T$  is caused by the sudden drop to zero volts for the incident pulse, and in order to match the voltage across the capacitor, the reflected voltage wave must have a positive jump of value  $V^+$ . The incident and reflected voltage waveforms at  $z = l$  are shown in Fig. 3.5. The reflected voltage waveform will propagate toward the generator and will begin to initiate a new forward propagating wave at time  $t = 2l/v$ . Clearly the capacitor has made a significant change in the waveform of the reflected wave.

The analysis for the case of a capacitor-resistor termination as shown in Fig. 3.3c is similar. The terminal conditions are

$$\mathcal{J} = \mathcal{V}_L G_L + C_L \frac{d\mathcal{V}_L}{dt} = Y_c \left[ \mathcal{V}_i(l, t) - \mathcal{V}_r \left( t - \frac{l}{v} \right) \right]$$

$$\mathcal{V}_L = \mathcal{V}_i(l, t) + \mathcal{V}_r \left( t - \frac{l}{v} \right)$$

so in place of (3.13) we have

$$\frac{d\mathcal{V}_r}{dt} + \left( \frac{1}{C_L Z_c} + \frac{1}{C_L R_L} \right) \mathcal{V}_r = -\frac{d\mathcal{V}_i}{dt} + \left( \frac{1}{C_L Z_c} - \frac{1}{C_L R_L} \right) \mathcal{V}_i \quad (3.15)$$

The solution is similar to that for (3.13) except that the charging time constant is now  $\tau_1 = C_L R_L Z_c / (R_L + Z_c)$ . Initially,  $\mathcal{V}_r$  has a value equal to  $-V^+$  as before. In this case the capacitor charges toward a final voltage equal to

$$V^+ \left( 1 + \frac{R_L - Z_c}{R_L + Z_c} \right) = \frac{2R_L}{R_L + Z_c} V^+$$

determined by the steady-state voltage across  $R_L$  if  $C_L$  was absent. At

$t = l/v + T$  the capacitor voltage will be

$$V_c = V^+ \frac{2R_L}{R_L + Z_c} (1 - e^{-T/\tau_1})$$

The reflected-wave voltage at this time will be  $V_c - V^+$ . When  $t$  becomes greater than  $l/v + T$  the incident voltage wave pulse drops to zero volts so the reflected-wave voltage jumps to a value equal to  $V_c$  and will then decay toward zero with a time constant  $\tau_1$ .

### 3.4 STEADY-STATE SINUSOIDAL WAVES

When the generator produces a sinusoidal voltage  $\mathcal{V}_g(t) = V_g \cos \omega t$ , the steady-state voltage waves on the transmission line will be of the form  $\cos \omega(t - z/v)$  and  $\cos \omega(t + z/v)$ . The steady state is achieved, for all practical purposes, after a few multiple reflections have occurred, since the amplitude of the successive reflected wave decreases quite rapidly because it is multiplied by  $\Gamma_g$  or  $\Gamma_L$  upon each reflection. The solution for steady-state sinusoidal waves is most conveniently obtained using phasor analysis. The generator voltage is represented by  $V_g e^{j\omega t}$ . The voltage and current waves on the transmission line will then also have an  $e^{j\omega t}$  time dependence. The differential equations (3.1a) and (3.1b) now become (the common time factor  $e^{j\omega t}$  is dropped)

$$\frac{\partial V(z)}{\partial z} = -j\omega LI(z) \quad (3.16a)$$

$$\frac{\partial I(z)}{\partial z} = -j\omega CV(z) \quad (3.16b)$$

where  $V(z)$  and  $I(z)$  are complex phasor amplitudes. By eliminating the current we find that  $V(z)$  satisfies the equation

$$\frac{d^2 V(z)}{dz^2} + \frac{\omega^2}{v^2} V(z) = 0 \quad (3.16c)$$

The solution for  $V(z)$  is of the form

$$V(z) = V^+ e^{-j\beta z} + V^- e^{j\beta z} \quad (3.17a)$$

with a corresponding solution

$$I(z) = I^+ e^{-j\beta z} - I^- e^{j\beta z} \quad (3.17b)$$

for the current waves. The constant  $\beta = \omega/v$  is the propagation phase constant. As before the current amplitudes are related to the voltage amplitudes through the characteristic impedance of the line, i.e.,

$$I^+ = Y_c V^+ \quad I^- = Y_c V^-$$

When the time factor is restored, it is readily seen that  $e^{-j\beta z + j\omega t} = e^{j\omega(t - z/v)}$

corresponds to a wave propagating in the  $+z$  direction, while  $e^{j\beta z + j\omega t}$  is a wave propagating in the  $-z$  direction. In the next section we will show that for a transmission line with finite conducting wires and possibly also surrounded with lossy dielectric materials, the waves attenuate in amplitude as they propagate. For this case the wave solutions are of the form

$$V = V^+ e^{-j\beta z - \alpha z} + V^- e^{j\beta z + \alpha z} \quad (3.18a)$$

$$I = I^+ e^{-j\beta z - \alpha z} - I^- e^{j\beta z + \alpha z} \quad (3.18b)$$

where  $\alpha$  is the attenuation constant.

### 3.5 WAVES ON A LOSSY TRANSMISSION LINE

Conductors used in a transmission line will always have a finite conductivity and will therefore exhibit some series resistance. Furthermore, because of the skin effect the current flows in a thin layer at the surface of the conductor, the effective thickness of the layer being equal to the skin depth  $\delta_s$  given by  $(2/\omega\mu\sigma)^{1/2}$  [see (2.104)]. Consequently, the series resistance increases with an increase in the frequency of operation. In order to account for this resistance, a distributed series resistance  $R$  per meter must be included in the distributed circuit used to model the transmission line.

The two conductors in a transmission line are usually maintained parallel to each other by supporting them in a dielectric structure. For example, a coaxial transmission line is filled with a dielectric medium in order to keep the center conductor coaxial with the outer shield. Dielectric materials usually have a negligible conductance but do have a small amount of dielectric loss due to polarization loss in the dielectric. Consequently, a shunt conductance  $G$  per meter is added to the distributed circuit to account for this loss. Thus, for a lossy transmission line, the equivalent circuit of a differential length  $dz$  is chosen to be that shown in Fig. 3.6.

If the voltage and current at the input are  $\mathcal{V}(z, t)$ ,  $\mathcal{I}(z, t)$  and if the voltage and current at the output are

$$\mathcal{V} + \frac{\partial \mathcal{V}}{\partial z} dz \quad \mathcal{I} + \frac{\partial \mathcal{I}}{\partial z} dz$$

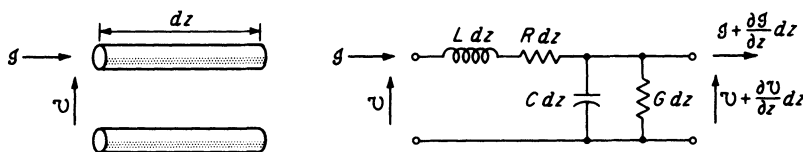


**FIGURE 3.6**  
Equivalent circuit of a differential length of transmission line.



then Kirchhoff's laws give

$$\mathcal{V} - \left( \mathcal{V} + \frac{\partial \mathcal{V}}{\partial z} dz \right) = \mathcal{I} R dz + L dz \frac{\partial \mathcal{I}}{\partial t}$$

$$\text{or} \quad \frac{\partial \mathcal{V}}{\partial z} = -\mathcal{I} R - L \frac{\partial \mathcal{I}}{\partial t} \quad (3.19a)$$

Similarly,

$$\mathcal{I} - \left( \mathcal{I} + \frac{\partial \mathcal{I}}{\partial z} dz \right) = \mathcal{V} G dz + C dz \frac{\partial \mathcal{V}}{\partial t}$$

$$\text{or} \quad \frac{\partial \mathcal{I}}{\partial z} = -\mathcal{V} G - C \frac{\partial \mathcal{V}}{\partial t} \quad (3.19b)$$

The first equation states that the potential difference between the input and output is equal to the potential drop across  $R$  and  $L$ . The second equation states that the output current is less than the input current by an amount equal to the shunt current flowing through  $C$  and  $G$ . Differentiating (3.19a) with respect to  $z$  and (3.19b) with respect to time  $t$  gives

$$\frac{\partial^2 \mathcal{V}}{\partial z^2} = -R \frac{\partial \mathcal{I}}{\partial z} - L \frac{\partial^2 \mathcal{I}}{\partial t \partial z} \quad (3.20a)$$

$$\frac{\partial^2 \mathcal{I}}{\partial t \partial z} = -G \frac{\partial \mathcal{V}}{\partial t} - C \frac{\partial^2 \mathcal{V}}{\partial t^2} \quad (3.20b)$$

Using (3.19b) and (3.20b) in (3.20a) now gives the following equation for the line voltage  $\mathcal{V}$ :

$$\frac{\partial^2 \mathcal{V}}{\partial z^2} = R \left( G \mathcal{V} + C \frac{\partial \mathcal{V}}{\partial t} \right) + L \left( G \frac{\partial \mathcal{V}}{\partial t} + C \frac{\partial^2 \mathcal{V}}{\partial t^2} \right)$$

$$\text{or} \quad \frac{\partial^2 \mathcal{V}}{\partial z^2} - (RC + LG) \frac{\partial \mathcal{V}}{\partial t} - LC \frac{\partial^2 \mathcal{V}}{\partial t^2} - RG \mathcal{V} = 0 \quad (3.21)$$

The current  $\mathcal{I}$  satisfies this one-dimensional wave equation also. If a solution in the form of a propagating wave

$$\mathcal{V} = \text{Re}(V e^{-\gamma z + j\omega t})$$

is assumed, substitution into (3.21) shows that the propagation constant  $\gamma$  must be a solution of

$$\gamma^2 - j\omega(RC + LG) + \omega^2 LC - RG = 0 \quad (3.22)$$

If only the steady-state sinusoidally time-varying solution is desired, phasor notation may be used. If we let  $V$  and  $I$  represent the voltage and current without the time dependence  $e^{j\omega t}$ , the basic equations (3.19) may be

written as

$$\frac{\partial V}{\partial z} = -(R + j\omega L)I \quad (3.23a)$$

$$\frac{\partial I}{\partial z} = -(G + j\omega C)V \quad (3.23b)$$

The wave equation (3.21) becomes

$$\frac{\partial^2 V}{\partial z^2} - (RG - \omega^2 LC)V - j\omega(RC + LG)V = 0 \quad (3.24)$$

The general solution to (3.24) is

$$V = V^+ e^{-\gamma z} + V^- e^{\gamma z} \quad (3.25)$$

where  $\gamma = \alpha + j\beta$  is given by

$$\gamma = [-\omega^2 LC + RG + j\omega(RC + LG)]^{1/2} \quad (3.26)$$

from (3.22). The constants  $V^+$  and  $V^-$  are arbitrary amplitude constants for waves propagating in the  $+z$  and  $-z$  directions, respectively. The solution for the current  $I$  may be found from (3.23a), that is

$$I = I^+ e^{-\gamma z} - I^- e^{\gamma z} = \frac{\gamma}{R + j\omega L} (V^+ e^{-\gamma z} - V^- e^{\gamma z}) \quad (3.27)$$

The parameter

$$Z_c = \frac{R + j\omega L}{\gamma} = \left( \frac{R + j\omega L}{G + j\omega C} \right)^{1/2} \quad (3.28)$$

is the characteristic impedance of the line since it is equal to the ratio  $V^+/I^+$  and  $V^-/I^-$ . Note that  $\gamma = [(R + j\omega L)(G + j\omega C)]^{1/2}$ .

### Loss-Free Transmission Line

For a line without loss, i.e., for which  $R = G = 0$ , the propagation constant is

$$\gamma = j\beta = j\omega\sqrt{LC} \quad (3.29)$$

and the characteristic impedance is pure real and given by

$$Z_c = \sqrt{\frac{L}{C}} \quad (3.30)$$

According to the field analysis,  $\beta$  is also equal to  $\omega(\mu\epsilon)^{1/2}$ , and hence

$$LC = \mu\epsilon \quad (3.31)$$

for a transmission line. This result may also be verified from the solutions for  $L$  and  $C$ , as shown later in the section on transmission-line parameters.

Using (3.31) in (3.30) shows that the characteristic impedance is also given by

$$Z_c = \sqrt{\frac{L}{C}} = \sqrt{\frac{\mu\epsilon}{C^2}} = \frac{\epsilon}{C} \sqrt{\frac{\mu}{\epsilon}} = Z \frac{\epsilon}{C} \quad (3.32)$$

where  $Z$  is the intrinsic impedance of the medium. The characteristic impedance differs from the intrinsic impedance  $Z$  by a factor  $\epsilon/C$ , which is a function of the line configuration only.

### Low-Loss Transmission Line

For most microwave transmission lines the losses are very small; that is,  $R \ll \omega L$  and  $G \ll \omega C$ . When this is the case, the term  $RG$  in the expression (3.26) for  $\gamma$  may be neglected. A binomial expansion then gives

$$\gamma \approx j\omega\sqrt{LC} + \frac{1}{2}\sqrt{LC} \left( \frac{R}{L} + \frac{G}{C} \right) = \alpha + j\beta \quad (3.33)$$

To first order the characteristic impedance is still given by (3.30) or (3.32). Thus the phase constant for a low-loss line is

$$\beta = \omega\sqrt{LC} \quad (3.34a)$$

and the attenuation constant  $\alpha$  is

$$\alpha = \frac{1}{2}\sqrt{LC} \left( \frac{R}{L} + \frac{G}{C} \right) = \frac{1}{2}(RY_c + GZ_c) \quad (3.34b)$$

where  $Y_c = Z_c^{-1} = \sqrt{C/L}$  is the characteristic admittance of the transmission line.

### 3.6 TERMINATED TRANSMISSION LINE: SINUSOIDAL WAVES

In this section the properties of a transmission line terminated in an arbitrary load impedance  $Z_L$  are examined. This will serve to illustrate how the forward and backward propagating waves can be combined to satisfy the boundary conditions at a termination. Figure 3.7 illustrates schematically a transmission line terminated in a load impedance  $Z_L$ . The line is assumed lossless and with a characteristic impedance  $Z_c$  and a propagation constant

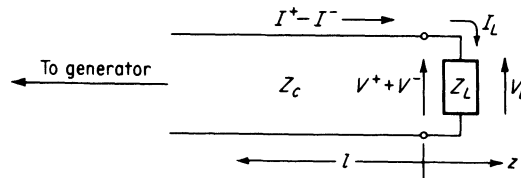


**FIGURE 3.7**  
Terminated transmission line.

$\gamma = j\beta$ . It should be noted that at microwave frequencies conventional low-frequency resistors, inductors, or capacitors, when connected across the two conductors of a transmission line, may behave as impedance elements with quite different characteristics from the low-frequency behavior.

If a voltage wave  $V^+ e^{-j\beta z}$  with an associated current  $I^+ e^{-j\beta z}$  is incident on the termination, a reflected voltage wave  $V^- e^{j\beta z}$  with a current  $-I^- e^{j\beta z}$  will, in general, be created. The ratio of the reflected and incident wave amplitudes is determined by the load impedance only. At the load the total line voltage must equal the impressed voltage across the load and the line current must be continuous through the load. Hence, if  $Z_L$  is located at  $z = 0$ ,

$$V = V^+ + V^- = V_L \quad (3.35a)$$

$$I = I^+ - I^- = I_L \quad (3.35b)$$

But  $I^+ = Y_c V^+$ ,  $I^- = Y_c V^-$ , and  $V_L/I_L = Z_L$  by definition of load impedance. Therefore

$$V^+ + V^- = V_L \quad (3.36a)$$

$$V^+ - V^- = \frac{Z_c}{Z_L} V_L \quad (3.36b)$$

The ratio of  $V^-$  to  $V^+$  is usually described by a voltage reflection coefficient  $\Gamma$  defined as

$$\Gamma_L = \frac{V^-}{V^+} \quad (3.37)$$

In place of (3.36) we may write

$$V^+(1 + \Gamma_L) = V_L$$

$$V^+(1 - \Gamma_L) = \frac{Z_c}{Z_L} V_L$$

Dividing one equation by the other yields

$$\frac{1 + \Gamma_L}{1 - \Gamma_L} = \frac{Z_L}{Z_c} \quad (3.38)$$

The quantity  $Z_L/Z_c$  is called the normalized load impedance (load impedance measured in units of  $Z_c$ ), and  $(1 + \Gamma_L)/(1 - \Gamma_L)$  is then the normalized input impedance seen looking toward the load at  $z = 0$ . The normalized load impedance will be expressed as  $\bar{Z}_L$ , with the bar on top signifying a normalized impedance in general. Solving for the voltage reflection coefficient  $\Gamma$  gives

$$\Gamma_L = \frac{Z_L - Z_c}{Z_L + Z_c} = \frac{Z_L/Z_c - 1}{Z_L/Z_c + 1} = \frac{\bar{Z}_L - 1}{\bar{Z}_L + 1} \quad (3.39)$$

Analogous to a voltage reflection coefficient, a current reflection coefficient  $\Gamma_I$  could also be introduced. In the present case

$$\Gamma_I = \frac{-I^-}{I^+} = -\frac{Y_c V^-}{Y_c V^+} = -\Gamma_L$$

In this text, however, only the voltage reflection coefficient will be used; so the adjective “voltage” can be dropped without confusion.

The incident voltage wave can be considered as transmitting a voltage  $V_L$  across the load, and a voltage transmission coefficient  $T$  can be defined as giving  $V_L$  in terms of  $V^+$ ; thus

$$V_L = TV^+ = (1 + \Gamma_L)V^+$$

$$\text{So} \quad T = 1 + \Gamma_L \quad (3.40)$$

A corresponding current transmission coefficient is not used in this book.

Returning to (3.39), it is seen that if  $Z_L = Z_c$ , the reflection coefficient is zero. In this case all the power in the incident wave is transmitted to the load and none of it is reflected back toward the generator. The power delivered to the load in this case is

$$P = \frac{1}{2} \text{Re}(VI^*) = \frac{1}{2} |V^+|^2 Y_c = \frac{1}{2} |V_L|^2 Y_L \quad (3.41)$$

The load is said to be matched to the transmission line when  $\Gamma_L = 0$ .

If  $Z_L$  does not equal  $Z_c$ , the load is mismatched to the line and a reflected wave is produced. The power delivered to the load is now given by

$$\begin{aligned} P &= \frac{1}{2} \text{Re}(V_L I_L^*) = \frac{1}{2} \text{Re}[(V^+ + V^-)(I^+ - I^-)^*] \\ &= \frac{1}{2} \text{Re}[Y_c(V^+ + V^-)(V^+ - V^-)^*] \\ &= \frac{1}{2} \text{Re}[Y_c |V^+|^2 (1 + \Gamma_L)(1 - \Gamma_L)^*] \\ &= \frac{1}{2} Y_c |V^+|^2 (1 - |\Gamma_L|^2) \end{aligned} \quad (3.42)$$

The final result states the physically obvious result that the power delivered to the load is the incident power minus that reflected from the load.

In the absence of reflection, the magnitude of the voltage along the line is a constant equal to  $|V^+|$ . When a reflected wave also exists, the incident and reflected waves interfere to produce a standing-wave pattern along the line. The voltage at any point on the line ( $z < 0$ ) is given by

$$V = V^+ e^{-j\beta z} + \Gamma_L V^+ e^{j\beta z}$$

and has a magnitude given by

$$|V| = |V^+| |1 + \Gamma_L e^{2j\beta z}| = |V^+| |1 + \Gamma_L e^{-2j\beta l}|$$

where  $l = -z$  is the positive distance measured from the load toward the

generator, as in Fig. 3.7. Let  $\Gamma_L$  be equal to  $\rho e^{j\theta}$ , where  $\rho = |\Gamma_L|$ ; then†

$$\begin{aligned}
 |V| &= |V^+| |1 + \rho e^{j(\theta - 2\beta l)}| \\
 &= |V^+| \left\{ [1 + \rho \cos(\theta - 2\beta l)]^2 + \rho^2 \sin^2(\theta - 2\beta l) \right\}^{1/2} \\
 &= |V^+| \left\{ (1 + \rho)^2 - 2\rho[1 - \cos(\theta - 2\beta l)] \right\}^{1/2} \\
 &= |V^+| \left[ (1 + \rho)^2 - 4\rho \sin^2\left(\beta l - \frac{\theta}{2}\right) \right]^{1/2} \tag{3.43}
 \end{aligned}$$

This result shows that  $|V|$  oscillates back and forth between maximum values of  $|V^+|(1 + \rho)$  when  $\beta l - \theta/2 = n\pi$  and minimum values  $|V^+|(1 - \rho)$  when  $\beta l - \theta/2 = n\pi + \pi/2$ , where  $n$  is an integer. These results also agree with physical intuition since they state that voltage maxima occur when the incident and reflected waves add in phase and that voltage minima occur when they add  $180^\circ$  out of phase. Successive maxima and minima are spaced a distance  $d = \pi/\beta = \lambda\pi/2\pi = \lambda/2$  apart, where  $\lambda$  is the wavelength for TEM waves in the medium surrounding the conductors. The distance between a maximum and the nearest minimum is  $\lambda/4$ .

Since the current reflection coefficient is equal to  $-\Gamma_L$  the current waves subtract whenever the voltage waves add up in phase. Hence current maxima and minima are displaced  $\lambda/4$  from the corresponding voltage maxima and minima. Figure 3.8 illustrates the voltage and current standing-wave patterns that result when  $Z_L$  is a pure resistance equal to  $3Z_c$ .

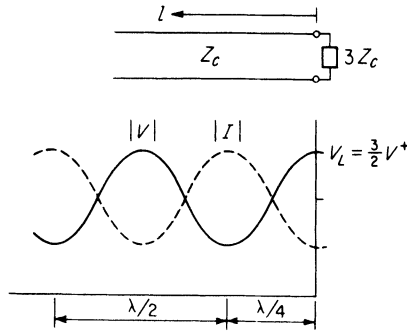
The ratio of the maximum line voltage to the minimum line voltage is called the voltage standing-wave ratio  $S$ ; thus

$$S = \frac{|V^+|(1 + \rho)}{|V^+|(1 - \rho)} = \frac{1 + \rho}{1 - \rho} \tag{3.44}$$

This is a parameter of considerable importance in practice for the following reasons: At microwave frequencies instruments for the direct absolute measurement of voltage or current are difficult to construct and use. On the other hand, devices to measure relative voltage or current (or electric or magnetic field) amplitudes are easy to construct. A typical device is a small probe inserted into the region of the electric field around a line. The output of the probe is connected to a crystal rectifier, and produces an output current which is a measure of the relative electric field or voltage at the probe position. By moving the probe along the line, the standing-wave ratio can be measured directly in terms of the maximum and minimum probe

---

†The symbol  $\rho$  denotes both charge density and the modulus of the reflection coefficient. The context makes it clear which quantity is under discussion; so confusion should not occur.


**FIGURE 3.8**

Voltage and current standing-wave patterns on a line terminated in a load impedance equal to  $3Z_c$ .

currents. The location of a voltage minimum can also be measured, and this permits the phase angle  $\theta$  of  $\Gamma_L$  to be calculated. Since  $\rho$  is known from the measured value of  $S$ ,  $\Gamma_L$  is specified, and the normalized load impedance may be calculated from (3.38).

Although the reflection coefficient was introduced as a measure of the ratio of reflected- to incident-wave amplitudes at the load, the definition may be extended to give the corresponding voltage ratio at any point on the line. Thus, at  $z = -l$ , the reflection coefficient is

$$\Gamma(l) = \frac{V^- e^{-j\beta l}}{V^+ e^{j\beta l}} = \frac{V^-}{V^+} e^{-2j\beta l} = \Gamma_L e^{-2j\beta l} \quad (3.45)$$

where  $\Gamma_L = V^-/V^+$  denotes the reflection coefficient of the load. The normalized impedance, seen looking toward the load, at  $z = -l$ , is

$$\begin{aligned} \bar{Z}_{\text{in}} &= \frac{Z_{\text{in}}}{Z_c} = \frac{V}{IZ_c} = \frac{V^+ e^{j\beta l} + V^- e^{-j\beta l}}{V^+ e^{j\beta l} - V^- e^{-j\beta l}} \\ &= \frac{1 + \Gamma(l)}{1 - \Gamma(l)} = \frac{1 + \Gamma_L e^{-2j\beta l}}{1 - \Gamma_L e^{-2j\beta l}} \end{aligned} \quad (3.46)$$

By replacing  $\Gamma_L$  by  $(Z_L - Z_c)/(Z_L + Z_c)$  and  $e^{\pm j\beta l}$  by  $\cos \beta l \pm j \sin \beta l$ , this result may be expressed as

$$\bar{Z}_{\text{in}} = \frac{Z_{\text{in}}}{Z_c} = \frac{Z_L + jZ_c \tan \beta l}{Z_c + jZ_L \tan \beta l} \quad (3.47)$$

A similar result holds for the normalized input admittance; so

$$\bar{Y}_{\text{in}} = \frac{Y_{\text{in}}}{Y_c} = \frac{Y_L + jY_c \tan \beta l}{Y_c + jY_L \tan \beta l} = \frac{\bar{Y}_L + j \tan \beta l}{1 + j\bar{Y}_L \tan \beta l} \quad (3.48)$$

Of particular interest are two special cases, namely,  $\beta l = \pi$  or  $l = \lambda/2$  and

$\beta l = \pi/2$  or  $l = \lambda/4$ , for which

$$Z_{\text{in}}\left(l = \frac{\lambda}{2}\right) = Z_L \quad (3.49a)$$

$$Z_{\text{in}}\left(l = \frac{\lambda}{4}\right) = \frac{Z_c^2}{Z_L} \quad (3.49b)$$

The first is equivalent to an ideal one-to-one impedance transformer, whereas in the second case the impedance has been inverted with respect to  $Z_c^2$ .

The terminal conditions at the generator end are readily established by using (3.47) to evaluate the input impedance  $Z_{\text{in}}$  seen looking toward the load at the generator end. If the generator with open-circuit voltage  $V_g$  has an internal impedance  $Z_g$ , then by the usual voltage division formula the total transmission-line voltage  $V$  at  $z = -l$  will be given by

$$V = \frac{Z_{\text{in}}}{Z_{\text{in}} + Z_g} V_g$$

But  $V$  is the sum of the forward-propagating-wave and reflected-wave voltages at  $z = -l$ , that is,

$$\begin{aligned} V &= V^+ e^{j\beta l} + V^- e^{-j\beta l} \\ &= V^+ e^{j\beta l} (1 + \Gamma_L e^{-2j\beta l}) \end{aligned}$$

By using this expression we can solve for  $V^+$  which is found to be

$$\begin{aligned} V^+ &= \frac{Z_{\text{in}} V_g}{(Z_{\text{in}} + Z_g)(e^{j\beta l} + \Gamma_L e^{-j\beta l})} \\ &= \frac{Z_{\text{in}}(Z_L + Z_c)V_g}{2(Z_{\text{in}} + Z_g)(Z_L \cos \beta l + jZ_c \sin \beta l)} \quad (3.50) \end{aligned}$$

## Terminated Lossy Line

In the case of a lossy line with propagation constant  $\gamma = j\beta + \alpha$ , the previous equations hold except that  $j\beta$  must be replaced by  $j\beta + \alpha$ , where  $\alpha$  is usually so small that, for the short lengths of line used in most experimental setups, the neglect of  $\alpha$  is justified. Nevertheless, it is of some interest to examine the behavior of a lossy transmission line terminated in a load  $Z_L$ . One simplifying assumption will be made, and this is that the characteristic impedance  $Z_c$  can still be considered real. This assumption is certainly valid for low-loss lines of the type used at microwave frequencies.



A detailed calculation justifying this assumption for a typical case is called for in Prob. 3.18.

Clearly, the presence of an attenuation constant  $\alpha$  does not affect the definition of the voltage reflection coefficient  $\Gamma_L$  for the load. However, at any other point a distance  $l$  toward the generator, the reflection coefficient is now given by

$$\Gamma(l) = \Gamma_L e^{-2j\beta l - 2\alpha l} \quad (3.51)$$

As  $l$  is increased,  $\Gamma$  decreases exponentially until, for large  $l$ , it essentially vanishes. Thus, whenever a load  $Z_L$  is viewed through a long section of lossy line, it appears to be matched to the line since  $\Gamma$  is negligible at the point considered. This effect may also be seen from the expression for the input impedance, namely,

$$Z_{in} = Z_c \frac{1 + \Gamma_L e^{-2j\beta l - 2\alpha l}}{1 - \Gamma_L e^{-2j\beta l - 2\alpha l}} = Z_c \frac{Z_L + Z_c \tanh(j\beta l + \alpha l)}{Z_c + Z_L \tanh(j\beta l + \alpha l)} \quad (3.52)$$

which approaches  $Z_c$  for  $l$  large since  $\tanh x$  approaches 1 for  $x$  large and not a pure imaginary quantity.

The losses also have the effect of reducing the standing-wave ratio  $S$  toward unity as the point of observation is moved away from the load toward the generator. As the generator is approached, the incident-wave amplitude increases exponentially whereas the reflected-wave amplitude decreases exponentially. The result is a standing-wave pattern of the type illustrated in Fig. 3.9. For illustrative purposes a relatively large value of  $\alpha$  has been assumed here.

The power delivered to the load is given by

$$P_L = \frac{1}{2} \operatorname{Re}(V_L I_L^*) = \frac{1}{2} |V_L|^2 G_L = \frac{Y_c}{2} |V^+|^2 (1 - |\Gamma_L|^2) \quad (3.53)$$

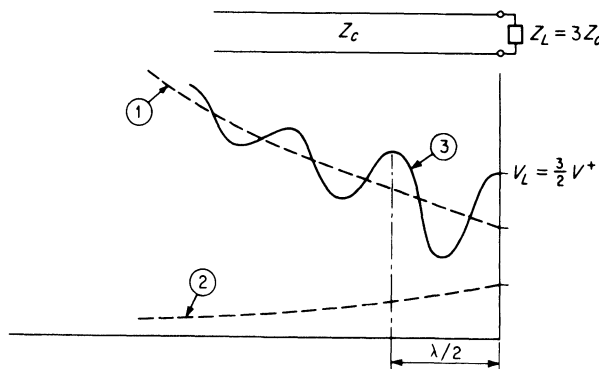


**FIGURE 3.9**  
Voltage standing-wave pattern on a lossy transmission line. (1) Envelope of incident-wave amplitude; (2) envelope of reflected-wave amplitude; (3) standing-wave pattern.

as before. At some point  $z = -l$ , the power directed toward the load is

$$\begin{aligned} P(l) &= \frac{1}{2} \operatorname{Re}(VI^*) = \frac{1}{2} |V|^2 Y_c = \frac{Y_c}{2} |V^+ e^{\alpha l}|^2 [1 - |\Gamma(l)|^2] \\ &= \frac{Y_c}{2} |V^+|^2 (e^{2\alpha l} - |\Gamma_L|^2) \end{aligned} \quad (3.54)$$

where  $|\Gamma|e^{\alpha l}$  has been replaced by  $|\Gamma_L|$ . Of the power given by (3.54) only that portion corresponding to  $P_L$  as given by (3.53) is delivered to the load. The remainder is dissipated in the lossy line, this remainder being given by

$$P(l) - P_L = \frac{Y_c}{2} |V^+|^2 (e^{2\alpha l} - 1) \quad (3.55)$$

## PART 2

### FIELD ANALYSIS OF TRANSMISSION LINES

---

The first section of this part will show that Maxwell's equations can be reformulated so as to describe three classes of waves, TEM, TE, and TM waves. The TEM wave is the principal wave on transmission lines. From the solution for the electric and magnetic fields for the TEM wave, we will be able to establish that there are unique voltage and current waves associated with the TEM wave. We will also be able to evaluate the distributed-circuit parameters  $R$ ,  $L$ ,  $C$ , and  $G$  for a transmission line. The field analysis thus provides a theoretical basis for treating the transmission line as a distributed circuit.

After the basic equations for TEM, TE, and TM waves have been derived, we present the field analysis for transmission lines that support TEM waves. This is followed by several sections dealing with planar transmission lines. Many of the planar lines that we examine support only quasi-TEM waves but can be analyzed as transmission lines once their equivalent distributed-circuit parameters have been determined.

### 3.7 CLASSIFICATION OF WAVE SOLUTIONS

The transmission lines and waveguides analyzed in this chapter are all characterized by having axial uniformity. Their cross-sectional shape and electrical properties do not vary along the axis, which is chosen as the  $z$  axis. Since sources are not considered, the electric and magnetic fields are

solutions of the homogeneous vector Helmholtz equation, i.e.,

$$\nabla^2 \mathbf{E} + k_0^2 \mathbf{E} = 0 \quad \nabla^2 \mathbf{H} + k_0^2 \mathbf{H} = 0$$

The type of solution sought is that corresponding to a wave that propagates along the  $z$  axis. Since the Helmholtz equation is separable, it is possible to find solutions of the form  $f(z)g(x, y)$ , where  $f$  is a function of  $z$  only and  $g$  is a function of  $x$  and  $y$  or other suitable transverse coordinates only. The second derivative with respect to  $z$  enters into the wave equation in a manner similar to the second derivative with respect to time. By analogy with  $e^{j\omega t}$  as the time dependence, the  $z$  dependence can be assumed to be  $e^{\pm j\beta z}$ . This assumption will lead to wave solutions of the form  $\cos(\omega t \pm \beta z)$  and  $\sin(\omega t \pm \beta z)$ , which are appropriate for describing wave propagation along the  $z$  axis. A wave propagating in the positive  $z$  direction is represented by  $e^{-j\beta z}$ , and  $e^{j\beta z}$  corresponds to a wave propagating in the negative  $z$  direction. With an assumed  $z$  dependence  $e^{-j\beta z}$ , the del operator becomes  $\nabla = \nabla_t + \nabla_z = \nabla_t - j\beta \mathbf{a}_z$ , since  $\nabla_z = \mathbf{a}_z \partial / \partial z$ . Note that  $\nabla_t$  is the transverse part and equals  $\mathbf{a}_x \partial / \partial x + \mathbf{a}_y \partial / \partial y$  in rectangular coordinates. The propagation phase constant  $\beta$  will turn out to depend on the waveguide configuration.

Considerable simplification of Maxwell's equations is obtained by decomposing all fields into transverse and axial components and separating out the  $z$  dependence. Thus let (the time dependence  $e^{j\omega t}$  is suppressed)

$$\begin{aligned} \mathbf{E}(x, y, z) &= \mathbf{E}_t(x, y, z) + \mathbf{E}_z(x, y, z) \\ &= \mathbf{e}(x, y)e^{-j\beta z} + \mathbf{e}_z(x, y)e^{-j\beta z} \end{aligned} \quad (3.56)$$

$$\begin{aligned} \mathbf{H}(x, y, z) &= \mathbf{H}_t(x, y, z) + \mathbf{H}_z(x, y, z) \\ &= \mathbf{h}(x, y)e^{-j\beta z} + \mathbf{h}_z(x, y)e^{-j\beta z} \end{aligned} \quad (3.57)$$

where  $\mathbf{E}_t, \mathbf{H}_t$  are the transverse ( $x$  and  $y$ ) components, and  $\mathbf{E}_z, \mathbf{H}_z$  are the axial components. Note also that  $\mathbf{e}(x, y), \mathbf{h}(x, y)$  are transverse vector functions of the transverse coordinates only, and  $\mathbf{e}_z(x, y), \mathbf{h}_z(x, y)$  are axial vector functions of the transverse coordinates.

Consider the  $\nabla \times \mathbf{E}$  equation, which may be expanded to give

$$\nabla \times \mathbf{E} = (\nabla_t - j\beta \mathbf{a}_z) \times (\mathbf{e} + \mathbf{e}_z)e^{-j\beta z} = -j\omega\mu_0(\mathbf{h} + \mathbf{h}_z)e^{-j\beta z}$$

$$\text{or} \quad \nabla_t \times \mathbf{e} - j\beta \mathbf{a}_z \times \mathbf{e} + \nabla_t \times \mathbf{e}_z - j\beta \mathbf{a}_z \times \mathbf{e}_z = -j\omega\mu_0 \mathbf{h} - j\omega\mu_0 \mathbf{h}_z$$

The term  $\mathbf{a}_z \times \mathbf{e}_z = 0$ , and  $\nabla_t \times \mathbf{e}_z = \nabla_t \times \mathbf{a}_z e_z = -\mathbf{a}_z \times \nabla_t e_z$ . Note also that  $\nabla_t \times \mathbf{e}$  is directed along the  $z$  axis only, since it involves factors such as  $\mathbf{a}_x \times \mathbf{a}_y, \mathbf{a}_x \times \mathbf{a}_x, \mathbf{a}_y \times \mathbf{a}_x$ , and  $\mathbf{a}_y \times \mathbf{a}_y$ , whereas  $\mathbf{a}_z \times \mathbf{e}$  and  $\nabla_t \times \mathbf{e}_z$  have transverse components only. Consequently, when the transverse and axial

components of the above equation are equated, there results

$$\nabla_t \times \mathbf{e} = -j\omega\mu_0 \mathbf{h}_z \quad (3.58a)$$

$$\nabla_t \times \mathbf{e}_z - j\beta \mathbf{a}_z \times \mathbf{e} = -\mathbf{a}_z \times \nabla_t e_z - j\beta \mathbf{a}_z \times \mathbf{e} = -j\omega\mu_0 \mathbf{h} \quad (3.58b)$$

In a similar manner the  $\nabla \times \mathbf{H}$  equation yields

$$\nabla_t \times \mathbf{h} = j\omega\epsilon_0 \mathbf{e}_z \quad (3.58c)$$

$$\mathbf{a}_z \times \nabla_t h_z + j\beta \mathbf{a}_z \times \mathbf{h} = -j\omega\epsilon_0 \mathbf{e} \quad (3.58d)$$

The divergence equation  $\nabla \cdot \mathbf{B} = 0$  becomes

$$\begin{aligned} \nabla \cdot \mathbf{B} &= \nabla \cdot \mu_0 \mathbf{H} = (\nabla_t - j\beta \mathbf{a}_z) \cdot (\mathbf{h} + \mathbf{h}_z) \mu_0 e^{-j\beta z} \\ &= (\nabla_t \cdot \mathbf{h} - j\beta \mathbf{a}_z \cdot \mathbf{h}_z) \mu_0 e^{-j\beta z} = 0 \end{aligned}$$

or

$$\nabla_t \cdot \mathbf{h} = j\beta h_z \quad (3.58e)$$

Similarly,  $\nabla \cdot \mathbf{D} = 0$  gives

$$\nabla_t \cdot \mathbf{e} = j\beta e_z \quad (3.58f)$$

This reduced form of Maxwell's equations will prove to be very useful in formulating the solutions for waveguiding systems.

For a large variety of waveguides of practical interest it turns out that all the boundary conditions can be satisfied by fields that do not have all components present. Specifically, for transmission lines, the solution of interest is a transverse electromagnetic wave with transverse components only, that is,  $E_z = H_z = 0$ , whereas for waveguides, solutions with  $E_z = 0$  or  $H_z = 0$  are possible. Because of the widespread occurrence of such field solutions, the following classification of solutions is of particular interest.

1. Transverse electromagnetic (TEM) waves. For TEM waves,  $E_z = H_z = 0$ . The electric field may be found from the transverse gradient of a scalar function  $\Phi(x, y)$ , which is a function of the transverse coordinates only and is a solution of the two-dimensional Laplace equation.
2. Transverse electric (TE), or  $H$ , modes. These solutions have  $E_z = 0$ , but  $H_z \neq 0$ . All the field components may be derived from the axial component  $H_z$  of magnetic field.
3. Transverse magnetic (TM), or  $E$ , modes. These solutions have  $H_z = 0$ , but  $E_z \neq 0$ . The field components may be derived from  $E_z$ .

In some cases it will be found that a TE or TM mode by itself will not satisfy all the boundary conditions. However, in such cases linear combinations of TE and TM modes may be used, since such linear combinations always provide a complete and general solution. Although other possible types of wave solutions may be constructed, the above three types are the most useful in practice and by far the most commonly used ones.

The appropriate equations to be solved to obtain TEM, TE, or TM modes will be derived below by placing  $E_z$  and  $H_z$ ,  $E_z$ , and  $H_z$ , respectively, equal to zero in Maxwell's equations.

## TEM Waves

For TEM waves  $e_z = h_z = 0$ ; so (3.3) reduces to

$$\nabla_t \times \mathbf{e} = 0 \quad (3.59a)$$

$$\beta \mathbf{a}_z \times \mathbf{e} = \omega \mu_0 \mathbf{h} \quad (3.59b)$$

$$\nabla_t \times \mathbf{h} = 0 \quad (3.59c)$$

$$\beta \mathbf{a}_z \times \mathbf{h} = -\omega \epsilon_0 \mathbf{e} \quad (3.59d)$$

$$\nabla_t \cdot \mathbf{h} = 0 \quad (3.59e)$$

$$\nabla_t \cdot \mathbf{e} = 0 \quad (3.59f)$$

The vanishing of the transverse curl of  $\mathbf{e}$  means that the line integral of  $\mathbf{e}$  around any closed path in the  $xy$  plane is zero. This must clearly be so since there is no axial magnetic flux passing through such a contour. Although  $\nabla_t \times \mathbf{h} = 0$  when there are no volume currents present, the line integral of  $\mathbf{h}$  will not vanish for a transmission line with conductors on which axial currents may exist. This point will be considered again later when transmission lines are analyzed. Equation (3.59a) is just the condition that permits  $\mathbf{e}$  to be expressed as the gradient of a scalar potential. Hence let

$$\mathbf{e}(x, y) = -\nabla_t \Phi(x, y) \quad (3.60)$$

Using (3.59f) shows that  $\Phi$  is a solution of the two-dimensional Laplace equation

$$\nabla_t^2 \Phi(x, y) = 0 \quad (3.61)$$

The electric field is thus given by

$$\mathbf{E}_t(x, y, z) = -\nabla_t \Phi(x, y) e^{-j\beta z}$$

But this field must also satisfy the Helmholtz equation

$$\nabla^2 \mathbf{E}_t + k_0^2 \mathbf{E}_t = 0$$

Since  $\nabla = \nabla_t - j\beta \mathbf{a}_z$ ,  $\nabla^2 = \nabla_t^2 - \beta^2$ , that is, the second derivative with respect to  $z$  gives a factor  $-\beta^2$ , this reduces to

$$\nabla_t^2 \mathbf{E}_t + (k_0^2 - \beta^2) \mathbf{E}_t = 0$$

or

$$\nabla_t [\nabla_t^2 \Phi + (k_0^2 - \beta^2) \Phi] = 0$$

This shows that  $\beta = \pm k_0$  for TEM waves, a result to be anticipated from the wave solutions discussed in Chap. 2. The magnetic field may be found

from the  $\nabla \times \mathbf{E}$  equation, i.e., from (3.59b); thus

$$\frac{\omega\mu_0}{k_0} \mathbf{h} = \mathbf{a}_z \times \mathbf{e} = Z_0 \mathbf{h} \quad (3.62)$$

In summary, for TEM waves, first find a scalar potential  $\Phi$  which is a solution of

$$\nabla_t^2 \Phi(x, y) = 0 \quad (3.63a)$$

and satisfies the proper boundary conditions. The fields are then given by

$$\mathbf{E} = \mathbf{E}_t = \mathbf{e} e^{\mp jk_0 z} = -\nabla_t \Phi e^{\mp jk_0 z} \quad (3.63b)$$

$$\mathbf{H} = \mathbf{H}_t = \pm \mathbf{h} e^{\mp jk_0 z} = \pm Y_0 \mathbf{a}_z \times \mathbf{e} e^{\mp jk_0 z} \quad (3.63c)$$

where  $k_0 = \omega(\mu_0 \epsilon_0)^{1/2}$ ,  $Y_0 = (\epsilon_0 / \mu_0)^{1/2}$ , and  $e^{-jk_0 z}$  represents a wave propagating in the  $+z$  direction and  $e^{jk_0 z}$  corresponds to wave propagation in the  $-z$  direction. For TEM waves,  $Z_0$  is the wave impedance, and from (3.63c) it is seen that, for wave propagation in the  $+z$  direction,

$$\frac{E_x}{H_y} = -\frac{E_y}{H_x} = Z_0 \quad (3.64a)$$

whereas for propagation in the  $-z$  direction,

$$\frac{E_x}{H_y} = -\frac{E_y}{H_x} = -Z_0 \quad (3.64b)$$

## TE Waves

For transverse electric (TE) waves,  $h_z$  plays the role of a potential function from which the rest of the field components may be obtained. The magnetic field  $\mathbf{H}$  is a solution of

$$\nabla^2 \mathbf{H} + k_0^2 \mathbf{H} = 0$$

Separating the above equation into transverse and axial parts and replacing  $\nabla^2$  by  $\nabla_t^2 - \beta^2$  yield

$$\nabla_t^2 h_z(x, y) + k_c^2 h_z(x, y) = 0 \quad (3.65a)$$

$$\nabla_t^2 \mathbf{h} + k_c^2 \mathbf{h} = 0 \quad (3.65b)$$

where  $k_c^2 = k_0^2 - \beta^2$  and a  $z$  dependence  $e^{-j\beta z}$  is assumed. Unlike the case of TEM waves,  $\beta^2$  will not equal  $k_0^2$  for TE waves. Instead,  $\beta$  is determined by the parameter  $k_c^2$  in (3.65a). When this equation is solved, subject to appropriate boundary conditions, the eigenvalue  $k_c^2$  will be found to be a function of the waveguide configuration.

The Maxwell equations (3.58) with  $\mathbf{e}_z = 0$  become

$$\nabla_t \times \mathbf{e} = -j\omega\mu_0 \mathbf{h}_z \quad (3.66a)$$

$$\beta \mathbf{a}_z \times \mathbf{e} = \omega\mu_0 \mathbf{h} \quad (3.66b)$$

$$\nabla_t \times \mathbf{h} = 0 \quad (3.66c)$$

$$\mathbf{a}_z \times \nabla_t h_z + j\beta \mathbf{a}_z \times \mathbf{h} = -j\omega\epsilon_0 \mathbf{e} \quad (3.66d)$$

$$\nabla_t \cdot \mathbf{h} = j\beta h_z \quad (3.66e)$$

$$\nabla_t \cdot \mathbf{e} = 0 \quad (3.66f)$$

The transverse curl of (3.66c) gives

$$\nabla_t \times (\nabla_t \times \mathbf{h}) = \nabla_t \nabla_t \cdot \mathbf{h} - \nabla_t^2 \mathbf{h} = 0$$

Replacing  $\nabla_t \cdot \mathbf{h}$  by  $j\beta h_z$  from (3.58e) and  $\nabla_t^2 \mathbf{h}$  by  $-k_c^2 \mathbf{h}$  from (3.65b) leads to the solution for  $\mathbf{h}$  in terms of  $h_z$ ; namely,

$$\mathbf{h} = -\frac{j\beta}{k_c^2} \nabla_t h_z \quad (3.67)$$

To find  $\mathbf{e}$  in terms of  $\mathbf{h}$ , take the vector product of (3.66b) with  $\mathbf{a}_z$  to obtain

$$\beta \mathbf{a}_z \times (\mathbf{a}_z \times \mathbf{e}) = \beta [(\mathbf{a}_z \cdot \mathbf{e}) \mathbf{a}_z - (\mathbf{a}_z \cdot \mathbf{a}_z) \mathbf{e}] = -\beta \mathbf{e} = \omega\mu_0 \mathbf{a}_z \times \mathbf{h}$$

$$\text{or} \quad \mathbf{e} = -\frac{\omega\mu_0}{\beta} \mathbf{a}_z \times \mathbf{h} = -\frac{k_0}{\beta} Z_0 \mathbf{a}_z \times \mathbf{h} \quad (3.68)$$

The factor  $k_0 Z_0 / \beta$  has the dimensions of an impedance, and is called the wave impedance of TE, or  $H$ , modes. It will be designated by the symbol  $Z_h$ , so that

$$Z_h = \frac{k_0}{\beta} Z_0 \quad (3.69)$$

Thus, in component form, (3.68) gives

$$\frac{e_x}{h_y} = -\frac{e_y}{h_x} = Z_h \quad (3.70)$$

for a wave with  $z$  dependence  $e^{-j\beta z}$ .

The remaining equations in the set (3.66) do not yield any new results; so the solution for TE waves may be summarized as follows: First find a solution for  $h_z$ , where

$$\nabla_t^2 h_z + k_c^2 h_z = 0 \quad (3.71a)$$

$$\text{Then} \quad \mathbf{h} = -\frac{j\beta}{k_c^2} \nabla_t h_z \quad (3.71b)$$

$$\text{and} \quad \mathbf{e} = -Z_h \mathbf{a}_z \times \mathbf{h} \quad (3.71c)$$

$$\text{where} \quad \beta = (k_0^2 - k_c^2)^{1/2} \quad \text{and} \quad Z_h = \frac{k_0 Z_0}{\beta}$$

Complete expressions for the fields are

$$\mathbf{H} = \pm \mathbf{h} e^{\mp j\beta z} + \mathbf{h}_z e^{\mp j\beta z} \quad (3.71d)$$

$$\mathbf{E} = \mathbf{E}_t = \mathbf{e} e^{\mp j\beta z} \quad (3.71e)$$

Note that in (3.71d) the sign in front of  $\mathbf{h}$  is reversed for a wave propagating in the  $-z$  direction since  $\mathbf{h}$  will be defined by (3.71b), with  $\beta$  positive regardless of whether propagation is in the  $+z$  or  $-z$  direction. The sign in front of  $\mathbf{e}$  does not change since it involves the factor  $\beta$  twice, once in the expression for  $\mathbf{h}$  and again in  $Z_h$ . Only the sign of one of  $\mathbf{e}$  or  $\mathbf{h}$  can change if a reversal in the direction of energy flow is to occur. That is, the solution for a wave propagating in the  $-z$  direction can be chosen as  $\mathbf{E} = -\mathbf{e} e^{j\beta z}$ ,  $\mathbf{H} = (\mathbf{h} - \mathbf{h}_z) e^{j\beta z}$  or as  $\mathbf{E} = \mathbf{e} e^{j\beta z}$ ,  $\mathbf{H} = (-\mathbf{h} + \mathbf{h}_z) e^{j\beta z}$ . One solution is the negative of the other. The latter solution is arbitrarily chosen as the standard in this text.

## TM Waves

The TM, or  $E$ , waves have  $\mathbf{h}_z = 0$ , but the axial electric field  $\mathbf{e}_z$  is not zero. These modes may be considered the dual of the TE modes in that the roles of electric and magnetic fields are interchanged. The derivation of the equations to be solved parallels that for TE waves, and hence only the final results will be given.

First obtain a solution for  $e_z$ , where

$$\nabla_t^2 e_z + k_c^2 e_z = 0 \quad (3.72a)$$

subject to the boundary conditions imposed. This will serve to determine the eigenvalue  $k_c^2$ . The transverse fields are then given by

$$\mathbf{E}_t = \mathbf{e} e^{\mp j\beta z} = -\frac{j\beta}{k_c^2} \nabla_t e_z e^{\mp j\beta z} \quad (3.72b)$$

$$\mathbf{H}_t = \pm \mathbf{h} e^{\mp j\beta z} = \pm Y_e \mathbf{a}_z \times \mathbf{e} e^{\mp j\beta z} \quad (3.72c)$$

where  $\beta = (k_0^2 - k_c^2)^{1/2}$  and the wave admittance  $Y_e$  for TM waves is given by

$$Y_e = Z_e^{-1} = \frac{k_0}{\beta} Y_0 \quad (3.72d)$$

The dual nature of TE and TM waves is exhibited by the relation

$$Z_e Z_h = Z_0^2 \quad (3.73)$$



which holds when both types of waves have the same value of  $\beta$  and is derivable from (3.69) and (3.72d). The complete expression for the electric field is

$$\begin{aligned}\mathbf{E} &= \mathbf{E}_t + \mathbf{E}_z = \mathbf{e}e^{\mp j\beta z} \pm \mathbf{e}_ze^{\mp j\beta z} \\ &= \left( -\frac{j\beta}{k_c^2} \nabla_t e_z \pm \mathbf{e}_z \right) e^{\mp j\beta z}\end{aligned}\quad (3.74)$$

It is convenient to keep the sign of  $\mathbf{e}$  the same for propagation in either the  $+z$  or  $-z$  direction. Since  $\nabla \cdot \mathbf{E} = 0$ , that is,  $\nabla_t \cdot \mathbf{E}_t + \partial E_z / \partial z = 0$ , this requires that the  $z$  component of electric field be  $-\mathbf{e}_ze^{j\beta z}$  for a wave propagating in the  $-z$  direction, because  $\nabla_t \cdot \mathbf{E}_t$  does not change sign, whereas  $\partial E_z / \partial z$  does, in view of the change in sign in front of  $\beta$ . The transverse magnetic field must also change sign upon reversal of the direction of propagation in order to obtain a change in the direction of energy flow. For reference, this sign convention is summarized below. The transverse variations of the fields are represented by the functions  $\mathbf{e}$ ,  $\mathbf{h}$ ,  $\mathbf{e}_z$ , and  $\mathbf{h}_z$ , independent of the direction of propagation. Waves propagating in the  $+z$  direction are then given by

$$\mathbf{E} = \mathbf{E}^+ = (\mathbf{e} + \mathbf{e}_z)e^{-j\beta z} \quad (3.75a)$$

$$\mathbf{H} = \mathbf{H}^+ = (\mathbf{h} + \mathbf{h}_z)e^{-j\beta z} \quad (3.75b)$$

For propagation in the  $-z$  direction the fields are

$$\mathbf{E} = \mathbf{E}^- = (\mathbf{e} - \mathbf{e}_z)e^{j\beta z} \quad (3.76a)$$

$$\mathbf{H} = \mathbf{H}^- = (-\mathbf{h} + \mathbf{h}_z)e^{j\beta z} \quad (3.76b)$$

Additional superscripts (+) or (-) will be used when it is necessary to indicate the direction of propagation. The previously derived equations for TEM, TE, and TM modes are valid in a medium with electrical constants  $\epsilon$ ,  $\mu$ , provided these are used to replace  $\epsilon_0$ ,  $\mu_0$ . A finite conductivity can also be taken into account by making  $\epsilon$  complex, i.e., replacing  $\epsilon$  by  $\epsilon - j\sigma/\omega$ .

The wave impedance introduced in the solutions is an extremely useful concept in practice. The wave impedance is always chosen to relate the transverse components of the electric and magnetic fields. The sign is always such that if  $i, j, k$  is a cyclic labeling of the coordinates and propagation is along the positive direction of coordinate  $k$ , the ratio  $E_i/H_j = (Z_w)_k$  is positive. Here  $(Z_w)_k$  is the wave impedance referred to the  $k$  axis as the direction of propagation. If  $i, j, k$  form an odd permutation of the coordinates, then  $E_i/H_j$  is negative. The usefulness of the wave-impedance concept stems from the fact that the power is given in terms of the

transverse fields alone. For example, for TE waves,

$$\begin{aligned}
 P &= \frac{1}{2} \operatorname{Re} \int_S \mathbf{E} \times \mathbf{H}^* \cdot \mathbf{a}_z \, dx \, dy \\
 &= \frac{1}{2} \operatorname{Re} \int_S \mathbf{e} \times \mathbf{h}^* \cdot \mathbf{a}_z \, dx \, dy \\
 &= -\frac{1}{2} \operatorname{Re} \int_S Z_h (\mathbf{a}_z \times \mathbf{h}) \times \mathbf{h}^* \cdot \mathbf{a}_z \, dx \, dy \\
 &= \frac{Z_h}{2} \int_S \mathbf{h} \cdot \mathbf{h}^* \, dx \, dy = \frac{Y_h}{2} \int_S \mathbf{e} \cdot \mathbf{e}^* \, dx \, dy
 \end{aligned}$$

upon expanding the integrand. Thus the wave impedance enables the power transmitted to be expressed in terms of one of the transverse fields alone. A further property of the wave impedance, which will be dealt with later, is that it provides a basis for an analogy between conventional multiconductor transmission lines and waveguides.

### 3.8 TRANSMISSION LINES (FIELD ANALYSIS)

#### Lossless Transmission Line

A transmission line consists of two or more parallel conductors. Typical examples are the two-conductor line, shielded two-conductor line, and coaxial line with cross sections, as illustrated in Fig. 3.10. Initially, it will be assumed that the conductors are perfectly conducting and that the medium surrounding the conductors is air, with  $\epsilon \approx \epsilon_0$ ,  $\mu \approx \mu_0$ . The effect of small losses will be considered later.

When the conductors are completely surrounded by a uniform dielectric medium, the principal wave that can exist on the transmission line is a TEM wave. The electric field for this wave can be found from the scalar potential which is a solution of Laplace's equation in the transverse plane. Microstrip lines and other planar transmission lines do not have the dielectric medium completely surrounding the conductors and therefore do not support a pure TEM wave. In this case it is found that only in the low-frequency limit does the dominant mode of propagation approach that of a TEM wave. We refer to the principal wave on these lines as a

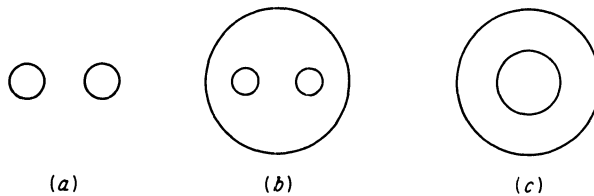


**FIGURE 3.10**  
Cross sections of typical transmission lines. (a) Two-conductor line; (b) shielded two-conductor line; (c) coaxial line.

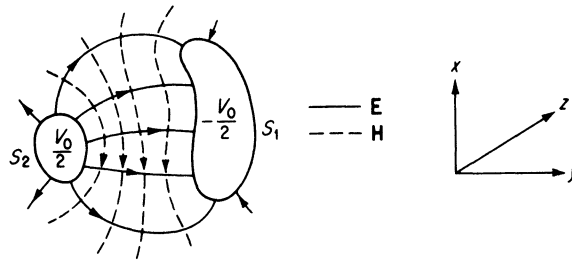


**FIGURE 3.11**  
Cross section of a general two-conductor line showing transverse field patterns.

quasi-TEM wave. The solution for the electric and magnetic fields of the quasi-TEM wave requires a separate solution for both the electric and magnetic fields in order to determine the distributed-circuit line parameters  $R$ ,  $L$ ,  $C$ , and  $G$ . This is because the electric and magnetic fields are no longer related in the simple way that they are for the TEM wave. The solution for the magnetic field can be found by solving for the vector potential function as will be shown later. In this section and the following one, we consider only transmission lines that support a TEM wave.

With reference to Fig. 3.11, let the one conductor be at a potential  $V_0/2$  and the other conductor at  $-V_0/2$ . To determine the field of a TEM wave, a suitable potential  $\Phi(x, y)$  must be found first. It is necessary that  $\Phi$  be a solution of

$$\nabla_t^2 \Phi = 0$$

and satisfy the boundary conditions

$$\Phi = \begin{cases} \frac{V_0}{2} & \text{on } S_2 \\ -\frac{V_0}{2} & \text{on } S_1 \end{cases}$$

Since  $\Phi$  is unique only to within an additive constant, we could equally well choose  $\Phi = V_0$  on  $S_2$  and  $\Phi = 0$  on  $S_1$ . If a solution for  $\Phi$  is possible, a TEM mode or field solution is also possible. When two or more conductors are present, this is always the case. The solution for  $\Phi$  is an electrostatic problem that can be solved when the line configuration is simple enough, as exemplified in Fig. 3.10.

The fields are given by (3.63), and for propagation in the  $+z$  direction are

$$\mathbf{E} = \mathbf{E}_t = \mathbf{e} e^{-jk_0 z} = -\nabla_t \Phi e^{-jk_0 z} \quad (3.77a)$$

$$\mathbf{H} = \mathbf{H}_t = Y_0 \mathbf{a}_z \times \mathbf{e} e^{-jk_0 z} \quad (3.77b)$$

The line integral of  $\mathbf{e}$  between the two conductors is

$$\begin{aligned}\int_{S_1}^{S_2} \mathbf{e} \cdot d\mathbf{l} &= \int_{S_1}^{S_2} -\nabla_t \Phi \cdot d\mathbf{l} \\ &= -\int_{S_1}^{S_2} \frac{d\Phi}{dl} dl = -[\Phi(S_2) - \Phi(S_1)] = -V_0\end{aligned}$$

Associated with the electric field is a unique voltage wave

$$V = V_0 e^{-jk_0 z} \quad (3.78)$$

since the line integral of  $\mathbf{e}$  between  $S_1$  and  $S_2$  is independent of the path chosen because  $\mathbf{e}$  is the gradient of a scalar potential.

The line integral of  $\mathbf{h}$  around one conductor, say  $S_2$ , gives

$$\oint_{S_2} \mathbf{h} \cdot d\mathbf{l} = \oint_{S_2} \mathbf{J}_s \cdot d\mathbf{l} = I_0$$

by application of Ampère's law,  $\nabla \times \mathbf{H} = j\omega \mathbf{D} + \mathbf{J}$ , and noting that there is no axial displacement flux  $D_z$  for a TEM mode. On the conductors the boundary conditions require  $\mathbf{n} \times \mathbf{e} = 0$  and  $\mathbf{n} \times \mathbf{h} = \mathbf{J}_s$ , where  $\mathbf{n}$  is a unit outward normal and  $\mathbf{J}_s$  is the surface current density. Since  $\mathbf{n}$  and  $\mathbf{h}$  lie in a transverse plane, the current  $\mathbf{J}_s$  is in the axial direction. In the region remote from the conductors,  $\nabla_t \times \mathbf{h} = 0$ , but the line integral around a conductor is not zero because of the current that exists. The current on the two conductors is oppositely directed, as may be verified from the expression  $\mathbf{n} \times \mathbf{h} = \mathbf{J}_s$ . Associated with the magnetic field there is a unique current wave

$$I = I_0 e^{-jk_0 z} \quad (3.79)$$

Since the potential  $\Phi$  is independent of frequency, it follows that the transverse fields  $\mathbf{e}$  and  $\mathbf{h}$  are also independent of frequency and are, in actual fact, the static field distributions which exist between the conductors if the potential difference is  $V_0$  and currents  $I_0, -I_0$  exist on  $S_2, S_1$ , respectively. The magnetic lines of flux coincide with the equipotential lines, since  $\mathbf{e}$  and  $\mathbf{h}$  are orthogonal, as seen from (3.77b).

**Example 3.1 Coaxial line.** Figure 3.12 illustrates a coaxial transmission line for which the solution for a TEM mode will be constructed. In cylindrical coordinates  $r, \phi, z$ , the two-dimensional Laplace equation is

$$\frac{1}{r} \frac{\partial}{\partial r} \left( r \frac{\partial \Phi}{\partial r} \right) + \frac{1}{r^2} \frac{\partial^2 \Phi}{\partial \phi^2} = 0$$

or for a potential function independent of the angular coordinate  $\phi$ ,

$$\frac{1}{r} \frac{\partial}{\partial r} \left( r \frac{\partial \Phi}{\partial r} \right) = 0$$

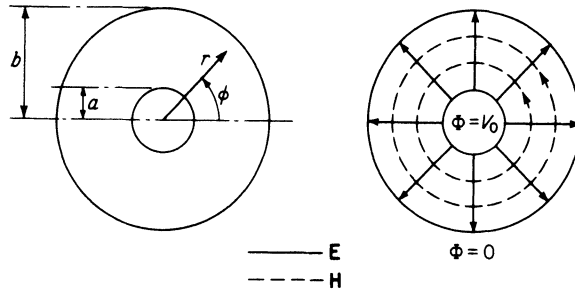


**FIGURE 3.12**  
Coaxial transmission line.

Integrating this equation twice gives

$$\Phi = C_1 \ln r + C_2$$

Imposing the boundary conditions  $\Phi = V_0$  at  $r = a$ ,  $\Phi = 0$  at  $r = b$ , gives

$$V_0 = C_1 \ln a + C_2 \quad 0 = C_1 \ln b + C_2$$

and hence  $C_2 = -C_1 \ln b$ ,  $C_1 = V_0 / [\ln(a/b)]$ ,

$$\Phi = V_0 \frac{\ln(r/b)}{\ln(a/b)} \quad (3.80)$$

The electric and magnetic fields of a TEM mode propagating in the  $+z$  direction are given by (3.77) and are

$$\begin{aligned} \mathbf{E} &= -\mathbf{a}_r \frac{\partial \Phi}{\partial r} e^{-jk_0 z} = -\frac{V_0}{\ln(a/b)} \frac{\mathbf{a}_r}{r} e^{-jk_0 z} \\ &= \frac{V_0}{\ln(b/a)} \frac{\mathbf{a}_r}{r} e^{-jk_0 z} \end{aligned} \quad (3.81a)$$

$$\mathbf{H} = Y_0 \mathbf{a}_z \times \mathbf{e} e^{-jk_0 z} = \frac{Y_0 V_0}{\ln(b/a)} \frac{\mathbf{a}_\phi}{r} e^{-jk_0 z} \quad (3.81b)$$

The potential difference between the two conductors is obviously  $V_0$ ; so the voltage wave associated with the electric field is

$$V = V_0 e^{-jk_0 z} \quad (3.82)$$

The current density on the inner conductor is

$$\mathbf{J}_s = \mathbf{n} \times \mathbf{H} = \mathbf{a}_r \times \mathbf{H} = \frac{Y_0 V_0}{\ln(b/a)} \frac{\mathbf{a}_z}{a} e^{-jk_0 z}$$

The total current, apart from the factor  $e^{-jk_0 z}$ , is

$$I_0 = \frac{Y_0 V_0}{a \ln(b/a)} \int_0^{2\pi} a d\phi = \frac{Y_0 V_0 2\pi}{\ln(b/a)} \quad (3.83)$$

The current on the inner surface of the outer conductor is readily shown to be equal to  $I_0$  also, but directed in the  $-z$  direction. The current wave associated with the magnetic field is therefore

$$I = I_0 e^{-jk_0 z} \quad (3.84)$$

The power, or rate of energy flow, along the line is given by

$$\begin{aligned} P &= \frac{1}{2} \operatorname{Re} \int_a^b \int_0^{2\pi} \mathbf{E} \times \mathbf{H}^* \cdot \mathbf{a}_z r dr d\phi = \frac{1}{2} \frac{Y_0 V_0^2}{[\ln(b/a)]^2} \int_a^b \int_0^{2\pi} \frac{d\phi dr}{r} \\ &= \frac{\pi Y_0 V_0^2}{\ln(b/a)} \end{aligned} \quad (3.85)$$

The power transmitted is seen to be also given, as anticipated, by the expression

$$\frac{1}{2} \operatorname{Re}(VI^*) = \frac{1}{2} V_0 I_0 = \frac{1}{2} V_0^2 \frac{2\pi Y_0}{\ln(b/a)}$$

The characteristic impedance of the line is defined by the ratio

$$\frac{V_0}{I_0} = Z_c \quad (3.86)$$

in terms of which the power may be expressed as  $P = \frac{1}{2} Z_c I_0^2 = \frac{1}{2} Y_c V_0^2$ , where  $Y_c$  is the characteristic admittance of the line and equal to  $Z_c^{-1}$ . The characteristic impedance is a function of the cross-sectional shape of the transmission line.

## Transmission Line with Small Losses

Practical transmission lines always have some loss caused by the finite conductivity of the conductors and also loss that may be present in the dielectric material surrounding the conductors. Consider first the case when the conductors are surrounded by a dielectric with permittivity  $\epsilon = \epsilon' - j\epsilon''$  but the conductors are still considered to be perfect. The presence of a lossy dielectric does not affect the solution for the scalar potential  $\Phi$ . Consequently, the field solution is formally the same as for the ideal line, except that  $k_0$  and  $Y_0$  are replaced by  $k = k_0(\epsilon_r' - j\epsilon_r'')^{1/2}$  and  $Y = Y_0(\epsilon_r' - j\epsilon_r'')^{1/2}$ , where the dielectric constant  $\epsilon_r = \epsilon_r' - j\epsilon_r'' = \epsilon/\epsilon_0$ . For small losses such that  $\epsilon_r'' \ll \epsilon_r'$ , the propagation constant is

$$jk = \alpha + j\beta = j(\epsilon_r')^{1/2} k_0 \left( 1 - j \frac{\epsilon_r''}{\epsilon_r'} \right)^{1/2} \approx j(\epsilon_r')^{1/2} k_0 + \frac{\epsilon_r'' k_0}{2(\epsilon_r')^{1/2}}$$

$$\text{Thus} \quad \alpha = \frac{\epsilon_r'' k_0}{2(\epsilon_r')^{1/2}} \quad (3.87a)$$

$$\beta = (\epsilon_r')^{1/2} k_0 \quad (3.87b)$$

where  $\alpha$  is the attenuation constant and  $\beta$  is the phase constant. The wave consequently attenuates according to  $e^{-\alpha z}$  as it propagates in the  $+z$  direction.

It will be instructive to derive the above expression for  $\alpha$  by means of a perturbation method that is widely used in the evaluation of the attenua-

tion, or damping, factor for a low-loss physical system. This method is based on the assumption that the introduction of a small loss does not substantially perturb the field from its loss-free value. The known field distribution for the loss-free case is then used to evaluate the loss in the system, and from this the attenuation constant can be calculated. In the present case, if  $\epsilon_r'' = 0$ , the loss-free solution is

$$\mathbf{E} = -\nabla_t \Phi e^{-jkz} \quad \mathbf{H} = Y \mathbf{a}_z \times \mathbf{E}$$

where  $k = (\epsilon_r')^{1/2} k_0$  and  $Y = (\epsilon_r')^{1/2} Y_0$ . When  $\epsilon_r''$  is small but not zero, the imaginary part of  $\epsilon$ , that is,  $\epsilon''$ , is equivalent to a conductivity

$$\sigma = \omega \epsilon'' = \omega \epsilon_0 \epsilon_r''$$

A conductivity  $\sigma$  results in a shunt current  $\mathbf{J} = \sigma \mathbf{E}$  between the two conductors. The power loss per unit length of line is

$$P_l = \frac{1}{2\sigma} \int_S \mathbf{J} \cdot \mathbf{J}^* dS = \frac{\omega \epsilon''}{2} \int_S \mathbf{E} \cdot \mathbf{E}^* dS \quad (3.88)$$

where the integration is over the cross section of the line, and the loss-free solution for  $\mathbf{E}$  is used to carry out the evaluation of  $P_l$ . Since loss is present, the power propagated along the line must decrease according to a factor  $e^{-2\alpha z}$ . The rate of decrease of power propagated along the line equals the power loss. If the power at  $z = 0$  is  $P_0$ , then at  $z$  it is  $P = P_0 e^{-2\alpha z}$ . Consequently,

$$-\frac{\partial P}{\partial z} = P_l = 2\alpha P_0 e^{-2\alpha z} = 2\alpha P \quad (3.89)$$

which states that the power loss at any plane  $z$  is directly proportional to the total power  $P$  present at this plane. The power propagated along the line is given by

$$\begin{aligned} P &= \frac{1}{2} \operatorname{Re} \int_S \mathbf{E} \times \mathbf{H}^* \cdot \mathbf{a}_z dS \\ &= \frac{Y}{2} \operatorname{Re} \int_S \mathbf{E} \times (\mathbf{a}_z \times \mathbf{E}^*) \cdot \mathbf{a}_z dS = \frac{Y}{2} \int_S \mathbf{E} \cdot \mathbf{E}^* dS \end{aligned}$$

Hence the attenuation  $\alpha$  is given by

$$\alpha = \frac{P_l}{2P} = \frac{\sigma}{2Y} = \frac{\omega \epsilon''}{2Y_0 (\epsilon_r')^{1/2}} = k_0 \frac{\epsilon_r''}{2(\epsilon_r')^{1/2}}$$

which is the same as the expression (3.87a). For this example the perturbation method does not offer any advantage. However, often the field solution for the lossy case is very difficult to find, in which case the perturbation method is extremely useful and simple to carry out by comparison with other methods. The case of transmission lines with conductors having finite conductivity is an important example of this, and is discussed below.

If the conductors of a transmission line have a finite conductivity, they exhibit a surface impedance

$$Z_m = \frac{1 + j}{\sigma \delta_s} \quad (3.90)$$

where  $\delta_s = (2/\omega\mu\sigma)^{1/2}$  is the skin depth (Sec. 2.9). At the surface the electric field must have a tangential component equal to  $Z_m \mathbf{J}_s$ , where  $\mathbf{J}_s$  is the surface current density. Therefore it is apparent that an axial component of electric field must be present, and consequently the field is no longer that of a TEM wave. The axial component of electric field gives rise to a component of the Poynting vector directed into the conductor, and this accounts for the power loss in the conductor. Generally, it is very difficult to find the exact solution for the fields when the conductors have finite conductivity. However, since  $|Z_m|$  is very small compared with  $Z_0$ , the axial component of electric field is also very small relative to the transverse components. Thus the field is very nearly that of the TEM mode in the loss-free case. The perturbation method outlined earlier may be used to evaluate the attenuation caused by finite conductivity.

The current density  $\mathbf{J}_s$  is taken equal to  $\mathbf{n} \times \mathbf{H}$ , where  $\mathbf{n}$  is the unit outward normal to the conductor surface and  $\mathbf{H}$  is the *loss-free* magnetic field. The power loss in the surface impedance per unit length of line is

$$\begin{aligned} P_l &= \frac{1}{2} \operatorname{Re} Z_m \oint_{S_1+S_2} \mathbf{J}_s \cdot \mathbf{J}_s^* dl \\ &= \frac{R_m}{2} \oint_{S_1+S_2} (\mathbf{n} \times \mathbf{H}) \cdot (\mathbf{n} \times \mathbf{H}^*) dl \\ &= \frac{R_m}{2} \oint_{S_1+S_2} \mathbf{H} \cdot \mathbf{H}^* dl \end{aligned} \quad (3.91)$$

where  $R_m = 1/\sigma\delta_s$  is the high-frequency surface resistance, and

$$\begin{aligned} (\mathbf{n} \times \mathbf{H}) \cdot (\mathbf{n} \times \mathbf{H}^*) &= \mathbf{n} \cdot \mathbf{H} \times (\mathbf{n} \times \mathbf{H}^*) \\ &= \mathbf{n} \cdot [(\mathbf{H} \cdot \mathbf{H}^*)\mathbf{n} - (\mathbf{H} \cdot \mathbf{n})\mathbf{H}^*] = \mathbf{H} \cdot \mathbf{H}^* \end{aligned}$$

since  $\mathbf{n} \cdot \mathbf{H} = 0$  for the infinite-conductivity case. The integration is taken around the periphery  $S_1 + S_2$  of the two conductors. The attenuation constant arising from conductor loss is thus

$$\alpha = \frac{P_l}{2P} = \frac{R_m \oint_{S_1+S_2} \mathbf{H} \cdot \mathbf{H}^* dl}{2Z \int \mathbf{H} \cdot \mathbf{H}^* dS} \quad (3.92)$$

where the power propagated along the line is given by

$$\operatorname{Re} \frac{1}{2} \int \mathbf{E} \times \mathbf{H}^* \cdot \mathbf{a}_z dS = \frac{1}{2} Z \int \mathbf{H} \cdot \mathbf{H}^* dS$$

and  $Z$  is the intrinsic impedance of the medium; that is,  $Z = (\mu/\epsilon)^{1/2}$ .



When both dielectric and conductor losses are present, the attenuation constant is the sum of the attenuation constants arising from each cause, provided both attenuation constants are small.

**Example 3.2 Lossy coaxial line.** Let the coaxial line in Fig. 3.12 be filled with a lossy dielectric ( $\epsilon = \epsilon' - j\epsilon''$ ), and let the conductors have finite conductivity  $\sigma$ . For the loss-free case ( $\epsilon'' = 0$ ,  $\sigma = \infty$ ) the fields are given by (3.81), with  $k_0$  and  $Y_0$  replaced by  $k = (\epsilon'/\epsilon_0)^{1/2}k_0$ ,

$$Y = \left( \frac{\epsilon'}{\epsilon_0} \right)^{1/2} Y_0$$

$$\text{Thus } \mathbf{E} = \frac{V_0}{\ln(b/a)} \frac{\mathbf{a}_r}{r} e^{-jkz} \quad (3.93a)$$

$$\mathbf{H} = \frac{YV_0}{\ln(b/a)} \frac{\mathbf{a}_\phi}{r} e^{-jkz} \quad (3.93b)$$

The power propagated along the line is

$$P = \frac{1}{2} \operatorname{Re} \int_0^{2\pi} \int_a^b \mathbf{E} \times \mathbf{H}^* \cdot \mathbf{a}_z r d\phi dr = \frac{\pi Y V_0^2}{\ln(b/a)} \quad (3.94)$$

The power loss  $P_{l1}$  from the lossy dielectric is, from (3.88),

$$P_{l1} = \frac{\omega \epsilon''}{2} \int_a^b \mathbf{E} \cdot \mathbf{E}^* r d\phi dr = \frac{\omega \epsilon'' V_0^2 \pi}{\ln(b/a)} \quad (3.95a)$$

The power loss from finite conductivity is given by (3.91), and is

$$\begin{aligned} P_{l2} &= \frac{R_m}{2} \frac{Y^2 V_0^2}{[\ln(b/a)]^2} \int_0^{2\pi} \left( \frac{1}{a} + \frac{1}{b} \right) d\phi \\ &= \frac{R_m \pi Y^2 V_0^2}{[\ln(b/a)]^2} \frac{b+a}{ab} \end{aligned} \quad (3.95b)$$

Hence the attenuation constant  $\alpha$  for the coaxial line is given by

$$\begin{aligned} \alpha &= \frac{P_{l1} + P_{l2}}{2P} = \frac{\omega \epsilon''}{2Y} + \frac{R_m Y}{2 \ln(b/a)} \frac{b+a}{ab} \\ &= \frac{k_0 \epsilon_r''}{2(\epsilon_r')^{1/2}} + \frac{R_m}{2Z \ln(b/a)} \frac{b+a}{ab} \end{aligned} \quad (3.96)$$

For the lossy case the propagation constant is consequently taken as

$$\alpha + j\beta = \alpha + jk$$

with  $\alpha$  given by (3.96).

### 3.9 TRANSMISSION-LINE PARAMETERS

In this section the field analysis to determine the circuit parameters  $L$ ,  $R$ ,  $C$ , and  $G$  for a transmission line is examined in greater detail. This will serve further to correlate the field analysis and circuit analysis of transmission lines.

Consider first the case of a loss-free line such as that illustrated in Fig. 3.11. When the scalar potential  $\Phi$  has been determined, the charge density on the conductors may be found from the normal component of electric field at the surface; that is,  $\rho_s = \epsilon \mathbf{n} \cdot \mathbf{e} = -\epsilon \mathbf{n} \cdot \nabla \Phi = -\epsilon \partial \Phi / \partial n$ , where  $\epsilon$  is the permittivity of the medium surrounding the conductors. The total charge  $Q$  per unit length on conductor  $S_2$  is

$$Q = \oint_{S_2} \epsilon \mathbf{n} \cdot \mathbf{e} \, dl$$

The total charge on the conductor  $S_1$  is  $-Q$  per meter. The potential of  $S_2$  is  $V_0$ , and hence the capacitance  $C$  per unit length is

$$C = \frac{Q}{V_0} = \frac{\epsilon \int_{S_2} \mathbf{n} \cdot \mathbf{e} \, dl}{\int_{S_2} \mathbf{e} \cdot d\mathbf{l}} \quad (3.97)$$

The total current on  $S_2$  is

$$I_0 = \oint_{S_2} \mathbf{h} \cdot d\mathbf{l} = \oint_{S_2} Y \mathbf{n} \cdot \mathbf{e} \, dl = \frac{YQ}{\epsilon}$$

since  $|\mathbf{h}| = Y|\mathbf{e}| = Y\mathbf{n} \cdot \mathbf{e}$  at the surface of  $S_2$  because the normal component of  $\mathbf{h}$  and the tangential component of  $\mathbf{e}$  are zero at the perfectly conducting surface  $S_2$ . The characteristic impedance of the line is given by

$$Z_c = \frac{V_0}{I_0} = \frac{V_0 \epsilon}{YQ} = \frac{\epsilon Z}{C} \quad (3.98)$$

A knowledge of the capacitance per unit length suffices to determine the characteristic impedance.

To determine the inductance  $L$  per unit length, refer to Fig. 3.13, which illustrates the magnetic flux lines around the conductors. Since  $\mathbf{h}$  is

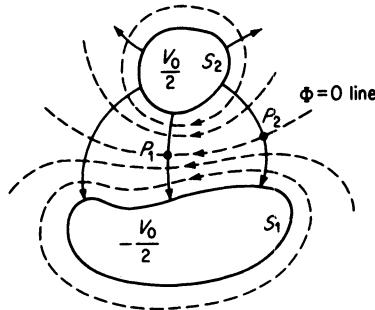


**FIGURE 3.13**  
Magnetic flux lines in a transmission line.

orthogonal to  $\mathbf{e}$ , these coincide with the equipotential lines. All the flux lines from the  $\Phi = 0$  to the  $\Phi = V_0/2$  line link the current on  $S_2$ . The flux linkage is the total flux cutting any path joining the  $\Phi = 0$  line to the surface  $S_2$ . If a path such as  $P_1S_2$  or  $P_2S_2$  is chosen, which is orthogonal to the flux lines, this path coincides with a line of electric force. The flux cutting such a path is

$$\psi = \int_{P_1}^{S_2} \mu h dl = \mu Y \int_{P_1}^{S_2} -\mathbf{e} \cdot d\mathbf{l} = \mu Y \frac{V_0}{2}$$

since  $|\mathbf{h}| = Y|\mathbf{e}|$  for a TEM wave. The inductance of one conductor of the line is

$$L_1 = \frac{\psi}{I_0} = \mu Y \frac{V_0}{2I_0}$$

The inductance of both conductors per unit length is twice this value; so

$$L = \mu Y \frac{V_0}{I_0} = \mu Y Z_c \quad (3.99)$$

From this relation and (3.98) it is seen that  $Z = \mu Z_c/L = CZ_c/\epsilon$ , and hence

$$Z^2 = \frac{\mu}{\epsilon} = \frac{\mu Z_c}{L} \frac{CZ_c}{\epsilon}$$

which gives

$$Z_c = \sqrt{\frac{L}{C}} \quad (3.100)$$

Equations (3.98) and (3.99) also show that

$$\mu\epsilon = LC \quad (3.101)$$

for a transmission line. The above expressions for  $C$  and  $L$  can also be obtained from the definitions based on stored energy. The derivation is left as a problem.

If the dielectric has a complex permittivity  $\epsilon = \epsilon' - j\epsilon''$ , where  $\epsilon''$  includes the conductivity of the dielectric if it is not zero, the total shunt current consists of a displacement current  $I_D$  and a conduction current  $I_S$ . The current leaving conductor  $S_2$  per unit length is

$$I = I_D + I_S = j\omega\epsilon \oint_{S_2} \mathbf{e} \cdot \mathbf{n} dl = j\omega\epsilon' \oint_{S_2} \mathbf{e} \cdot \mathbf{n} dl + \omega\epsilon'' \oint_{S_2} \mathbf{e} \cdot \mathbf{n} dl$$

where the first integral on the right gives the displacement current and the second integral gives the conduction current. The total shunt admittance is given by  $Y = j\omega C + G = (I_S + I_D)/V_0$ , and hence it is seen that

$$G = \frac{I_S}{V_0} = \frac{I_S}{I_D} \frac{I_D}{V_0} = \frac{\omega\epsilon''}{\epsilon'} C \quad (3.102)$$

since  $j\omega C = I_D/V_0$  and  $j\omega C/j\omega\epsilon' = C/\epsilon'$ . This relation shows that  $G$  differs from  $C$  by the factor  $\omega\epsilon''/\epsilon'$  only.

The transmission-line loss from finite conductivity may be accounted for by a series resistance  $R$  per unit length provided  $R$  is chosen so that

$$\frac{1}{2}RI_0^2 = \frac{R_m}{2} \oint_{S_1+S_2} |\mathbf{h}|^2 dl \quad (3.103)$$

The right-hand side gives the total power loss per unit length arising from the high-frequency resistance of the conductors. In terms of this quantity, the resistance  $R$  is thus defined as

$$R = R_m \frac{\oint_{S_1+S_2} |\mathbf{h}|^2 dl}{\left(\oint_{S_2} |\mathbf{h}| dl\right)^2} \quad (3.104)$$

where  $R_m = 1/\sigma\delta_s$  and  $\delta_s$  is the skin depth.

A further effect of the finite conductivity is to increase the series inductance of the line by a small amount because of the penetration of the magnetic field into the conductor. This skin-effect inductance  $L_s$  is readily evaluated on an energy basis. The surface impedance  $Z_m$  has an inductive part  $jX_m = j/\sigma\delta_s$  equal in magnitude to  $R_m$ . The magnetic energy stored in  $X_m$  is (note that  $X_m$  is equivalent to a surface inductance  $X_m/\omega = L_m$ )

$$\begin{aligned} W_m &= \frac{X_m}{4\omega} \oint_{S_1+S_2} |\mathbf{J}_s|^2 dl \\ &= \frac{X_m}{4\omega} \oint_{S_1+S_2} |\mathbf{h}|^2 dl = \frac{X_m}{4\omega} \frac{RI_0^2}{R_m} = \frac{RI_0^2}{4\omega} \end{aligned}$$

by using (3.103) to replace the integral. Defining  $L_s$  by the relation

$$\frac{1}{4}L_s I_0^2 = W_m$$

gives

$$\omega L_s = R \quad (3.105)$$

The series inductive reactance of the line is increased by an amount equal to the series resistance. However, for low-loss lines,  $R \ll \omega L$ , so that  $L_s \ll L$ , and the correction is not significant for most practical lines. The inductance  $L_s$  is called the internal inductance since it arises from flux linkage internal to the conductor surfaces.

It should not come as a surprise to find that  $\omega L_s = R$  since both the inductive reactance and resistance arise from the penetration of the current and fields into the conductor. The effect of this penetration into the conductor by an effective distance equal to the skin depth  $\delta_s$  is correctly accounted for in a simplified manner by introduction of the surface impedance  $Z_m = (1 + j)/\sigma\delta_s$ .

**Example 3.3 Coaxial-line parameters.** For the coaxial line of Fig. 3.12 the potential  $\Phi$  is given by

$$\Phi = V_0 \frac{\ln(r/b)}{\ln(a/b)}$$

The charge on the inner conductor is

$$\begin{aligned} Q &= \epsilon \int_0^{2\pi} \mathbf{a}_r \cdot \mathbf{e} \mathbf{a} d\phi = \epsilon \int_0^{2\pi} -\frac{\partial\Phi}{\partial r} a d\phi \\ &= \frac{-\epsilon V_0}{\ln(a/b)} \int_0^{2\pi} d\phi = \frac{2\pi\epsilon V_0}{\ln(b/a)} \end{aligned}$$

Hence the capacitance per unit length is

$$C = \frac{\epsilon' Q}{\epsilon V_0} = \frac{2\pi\epsilon'}{\ln(b/a)} \quad (3.106)$$

since the capacitance arises only from that part of the charge associated with  $\epsilon'$  whereas  $\epsilon''$  gives rise to the shunt conductance.

The magnetic field is given by (3.93b) as

$$\mathbf{H} = \mathbf{h} e^{-jk_0 z} = \frac{YV_0}{\ln(b/a)} \frac{\mathbf{a}_\phi}{r} e^{-jk_0 z}$$

The current  $I_0$  is

$$I_0 = \int_0^{2\pi} \mathbf{h} \cdot \mathbf{a}_\phi a d\phi = \frac{2\pi YV_0}{\ln(b/a)}$$

Thus the characteristic impedance is

$$Z_c = \frac{V_0}{I_0} = \frac{Z \ln(b/a)}{2\pi} \quad (3.107)$$

The flux linking the center conductor is

$$\psi = \mu \int_a^b \mathbf{h} \cdot \mathbf{a}_\phi dr = \frac{\mu YV_0}{\ln(b/a)} \int_a^b \frac{dr}{r} = \mu YV_0$$

Consequently, the inductance per unit length is

$$L = \frac{\psi}{I_0} = \frac{\mu YV_0}{2\pi YV_0} \ln \frac{b}{a} = \frac{\mu}{2\pi} \ln \frac{b}{a} \quad (3.108)$$

from which it is seen that  $LC = \mu\epsilon'$  and  $Z_c = (L/C)^{1/2}$ .

The shunt conductance  $G$  is given by  $\omega\epsilon''C/\epsilon'$ , and is

$$G = \frac{\omega\epsilon''}{\epsilon'} \frac{2\pi\epsilon'}{\ln(b/a)} = \frac{2\pi\omega\epsilon''}{\ln(b/a)} \quad (3.109)$$

To find the series resistance, the power loss in the inner and outer conductors must be evaluated. This was done in Example 3.2, with the result

[Eq. (3.95b)]

$$\frac{1}{2}RI_0^2 = P_{l2} = \frac{R_m \pi Y^2 V_0^2}{[\ln(b/a)]^2} \frac{b+a}{ab}$$

Solving for  $R$  gives

$$R = \frac{R_m}{2\pi} \frac{b+a}{ab} \quad (3.110)$$

The internal inductance  $L_s$  is equal to  $R/\omega$ ; so the total series line inductance per unit length is

$$L + L_s = \frac{\mu}{2\pi} \ln \frac{b}{a} + \frac{b+a}{2\pi \omega ab \delta_s \sigma} \quad (3.111)$$

The distributed-circuit parameters  $R$ ,  $L$ ,  $C$ , and  $G$  for a transmission line can also be determined from an evaluation of the stored electric and magnetic field energy and the power loss per unit length. Energy storage in the magnetic field is accounted for by the series inductance  $L$  per unit length, whereas energy storage in the electric field is accounted for by the distributed shunt capacitance  $C$  per unit length. Power loss in the conductors is taken into account by a series resistance  $R$  per unit length. Finally, the power loss in the dielectric may be included by introducing a shunt conductance  $G$  per unit length. Suitable definitions for the parameters  $L$ ,  $C$ ,  $R$ , and  $G$  based on the above concepts are

$$L = \frac{\mu}{I_0 I_0^*} \int_S \mathbf{H} \cdot \mathbf{H}^* dS \quad (3.112a)$$

$$C = \frac{\epsilon'}{V_0 V_0^*} \int_S \mathbf{E} \cdot \mathbf{E}^* dS \quad (3.112b)$$

$$R = \frac{R_m}{I_0 I_0^*} \oint_{S_1+S_2} \mathbf{H} \cdot \mathbf{H}^* dl \quad (3.112c)$$

$$G = \frac{\omega \epsilon''}{V_0 V_0^*} \int \mathbf{E} \cdot \mathbf{E}^* dS \quad (3.112d)$$

where  $I_0$  is the total current on the line, and  $V_0$  the potential difference. These expressions are obtained, for example, by equating the magnetic energy  $\frac{1}{4}I_0 I_0^* L = W_m$  stored in the equivalent series inductance  $L$  to the expression for  $W_m$  in terms of the field. The above definitions are readily shown to be equivalent to the other commonly used definitions such as

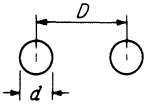
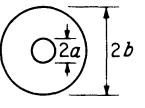
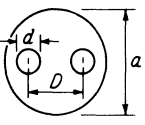
$$L = \frac{\text{magnetic flux linkage}}{\text{total current}} \quad (3.113a)$$

$$C = \frac{\text{total charge per unit length}}{\text{voltage difference between conductors}} \quad (3.113b)$$

$$G = \frac{\text{total shunt current}}{\text{voltage difference between conductors}} \quad (3.113c)$$

Parameters of some common transmission lines are given in Table 3.1.

**TABLE 3.1**  
**Parameters of common transmission lines†**

	$Z_c$	$R$
	$\frac{1}{\pi} \left( \frac{\mu_0}{\epsilon'} \right)^{1/2} \cosh^{-1} \frac{D}{d}$	$\frac{2R_m}{\pi d} \frac{D/d}{[(D/d)^2 - 1]^{1/2}}$
	$\frac{1}{2\pi} \left( \frac{\mu_0}{\epsilon'} \right)^{1/2} \ln \frac{b}{a}$	$\frac{R_m}{2\pi} \left( \frac{1}{a} + \frac{1}{b} \right)$
	$\frac{1}{\pi} \left( \frac{\mu_0}{\epsilon'} \right)^{1/2} \left[ \ln \left( 2p \frac{1 - q^2}{1 + q^2} \right) - \frac{1 + 4p^2}{16p^4} (1 - 4q^2) \right]$	$\frac{2R_m}{\pi d} \left[ 1 + \frac{1 + 2p^2}{4p^4} (1 - 4q^2) \right] + \frac{8R_m}{\pi a} q^2 \left[ (1 + q^2) - \frac{1 + 4p^2}{8p^4} \right]$
$p = \frac{D}{d} \quad q = \frac{D}{a}$		

†For all TEM transmission lines

$$C = \frac{(\mu_0 \epsilon')^{1/2}}{Z_c} \quad L = (\mu_0 \epsilon')^{1/2} Z_c \quad G = \frac{\omega \epsilon'' C}{\epsilon'}$$

$$\alpha_d = \frac{G Z_c}{2} \quad \alpha_c = \frac{R Y_c}{2} \quad R_m = \frac{1}{\sigma \delta_s} = \left( \frac{\omega \mu}{2\sigma} \right)^{1/2}$$

### 3.10 INHOMOGENEOUSLY FILLED PARALLEL-PLATE TRANSMISSION LINE

In Fig. 3.14a we show a parallel-plate transmission line (waveguide) partially filled with dielectric material having a permittivity  $\epsilon = \epsilon_r \epsilon_0$ , where  $\epsilon_r$  is the dielectric constant. The plates are infinitely wide and spaced a distance  $b$  apart. The dielectric sheet has a thickness  $a$  and rests on the bottom plate.

The purpose for studying this particular waveguide is that it exhibits a number of characteristics that are similar to those of the microstrip transmission lines examined in the following section. We will show that the dominant mode of propagation in the waveguide under consideration is an  $E$  mode and that as the frequency approaches zero this mode becomes a TEM mode. Furthermore, in the low-frequency limit, the propagation con-

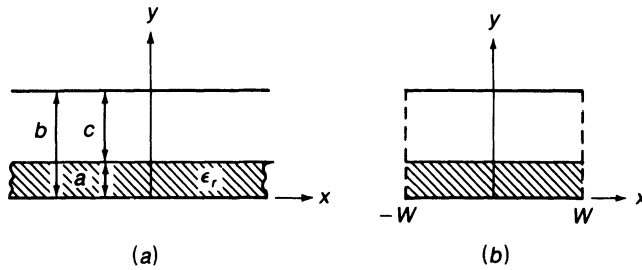


**FIGURE 3.14**

(a) Partially loaded parallel-plate waveguide; (b) parallel-plate waveguide with magnetic walls at  $x = \pm W$ .

stant can be found in terms of the distributed capacitance and inductance per meter by the usual transmission-line formula  $\beta = \omega\sqrt{LC}$ . As the frequency increases  $\beta$  increases faster than  $\omega$ , in which case we say that the transmission line exhibits dispersion.

Another feature that can be easily described for this waveguide is the existence of a surface-wave mode of propagation that consists of a field concentrated near the air-dielectric interface.

Since the analytic solution for the partially filled parallel-plate waveguide is readily constructed, this waveguide serves as a useful example to provide some physical insight into the properties of microstrip transmission lines.

An electric wall is a surface on which the tangential electric field must be zero. A good conductor such as copper provides a surface with a very small skin-effect surface impedance (see Sec. 2.9). When we let the conductivity  $\sigma$  become infinite, we obtain an electric wall on which the boundary condition  $\mathbf{n} \times \mathbf{E} = 0$  holds. The dual of an electric wall is a magnetic wall on which the tangential magnetic field is zero, i.e., the boundary condition  $\mathbf{n} \times \mathbf{H} = 0$  holds. The magnetic wall does not have a physical realization but is, nevertheless, a useful theoretical concept. In practice, a magnetic wall can be inserted into a field region, without disturbing the field, along any surface on which the tangential magnetic field is zero. Such surfaces usually correspond to certain symmetry planes in a given problem. In addition to the above boundary conditions, Maxwell's equations show that on an electric wall the normal component of  $\mathbf{H}$  is zero, that is,  $\mathbf{n} \cdot \mathbf{H} = 0$ . The dual boundary condition  $\mathbf{n} \cdot \mathbf{E} = 0$  holds on a magnetic wall.

For the  $E$  mode that we will consider in the partially filled parallel-plate waveguide, we will assume that the fields do not depend on the  $x$  coordinate but are functions of  $y$  and  $z$  only. A consequence of this assumption is that only the field components  $E_y$ ,  $E_z$  and  $H_x$  are present. Thus we can place a magnetic wall along any  $x = \text{constant}$  surface without disturbing the field. We will now assume that magnetic walls are inserted at  $x = \pm W$  as shown



in Fig. 3.14*b*. By means of this artifice, we are able to talk about a closed waveguide structure, closed by electric walls at  $y = 0, b$  and by magnetic walls at  $x = \pm W$ .

In order to find the solutions for  $E$  modes having the  $z$  dependence  $e^{-j\beta z}$ , we must find solutions for the axial electric field component  $e_z(y)$  first. In an ideal transmission line the propagation constant equals that for plane TEM waves in the surrounding medium. In the structure under investigation we have a nonuniform medium, namely dielectric in the region  $0 \leq y \leq a$  and air in the region  $a \leq y \leq b$ . Consequently, we can anticipate that the propagation phase constant  $\beta$  for the dominant mode will take on an intermediate value, i.e.,

$$k_0 = \omega\sqrt{\mu_0\epsilon_0} < \beta < \sqrt{\epsilon_r}k_0 = k$$

The equation satisfied by  $e_z(y)$  is (3.72*a*) which is repeated below

$$\nabla_t^2 e_z + k_c^2 e_z = 0$$

Since we assume no variation with  $x$ , the transverse laplacian operator becomes simply  $\partial^2/\partial y^2$ . In this equation  $k_c^2 = k_0^2 - \beta^2$  in the air region and equals  $k^2 - \beta^2$  in the dielectric region. The propagation constant  $\beta$  *must be the same* in both regions because the tangential electric and magnetic fields must match at the air-dielectric interface for all values of  $z$ . For convenience, we will let  $k_c = l$  in the dielectric region and let it equal  $p$  in the air region. We thus require that  $p^2 - k_0^2 = l^2 - k^2$  or

$$l^2 - p^2 = (\epsilon_r - 1)k_0^2 \quad (3.114)$$

In the two regions the axial electric field is thus a solution of

$$\frac{d^2 e_z}{dy^2} + l^2 e_z = 0 \quad 0 \leq y \leq a \quad (3.115a)$$

$$\frac{d^2 e_z}{dy^2} + p^2 e_z = 0 \quad a \leq y \leq b \quad (3.115b)$$

along with the boundary conditions

$$e_z(y) = 0 \quad y = 0, b \quad (3.116a)$$

$$e_z(y) \text{ continuous at } y = a \quad (3.116b)$$

$$\left. \frac{\epsilon_r}{l^2} \frac{\partial e_z}{\partial y} \right|_a = \left. \frac{1}{p^2} \frac{\partial e_z}{\partial y} \right|_a \quad (3.116c)$$

The third boundary condition comes from the requirement that  $H_x$  be continuous across the air-dielectric interface. The transverse fields are given

by (3.72b) and (3.72c). The generic form of the equations is

$$E_y = -\frac{j\beta}{k_c^2} \frac{\partial e_z}{\partial y} e^{-j\beta z}$$

$$H_x = Y_e \frac{j\beta}{k_c^2} \frac{\partial e_z}{\partial y} e^{-j\beta z}$$

upon using  $\mathbf{a}_z \times \mathbf{a}_y = -\mathbf{a}_x$ . In the equation for  $H_x$  the wave admittance  $Y_e$  is given by  $kY/\beta$  in the dielectric and by  $(k_0 Y_0)/\beta$  in the air region where  $kY = \omega\sqrt{\mu_0\epsilon}\sqrt{\epsilon/\mu_0} = \epsilon_r k_0 Y_0$ . Thus we have

$$e_y(y) = \begin{cases} -\frac{j\beta}{l^2} \frac{\partial e_z}{\partial y} & \text{dielectric region} \\ -\frac{j\beta}{p^2} \frac{\partial e_z}{\partial y} & \text{air region} \end{cases} \quad (3.117a)$$

$$h_x(y) = \begin{cases} \frac{j\epsilon_r k_0 Y_0}{l^2} \frac{\partial e_z}{\partial y} & \text{dielectric region} \\ \frac{jk_0 Y_0}{p^2} \frac{\partial e_z}{\partial y} & \text{air region} \end{cases} \quad (3.117b)$$

An examination of the expression for  $h_x(y)$  shows that continuity of  $h_x$  at  $y = a$  gives the boundary condition specified by (3.116c). We also find that in an inhomogeneously filled waveguide, the wave impedance, defined by the ratio  $-E_y/H_x$ , is not constant since it has a different value in the air region from that in the dielectric region.

The reader can readily verify that the solutions of (3.115a) and (3.115b) that satisfy the boundary conditions at  $y = 0$  and  $b$  are

$$e_z(y) = C_1 \sin ly \quad 0 \leq y \leq a$$

$$e_z(y) = C_2 \sin p(b - y) \quad a \leq y \leq b$$

where  $C_1$  and  $C_2$  are unknown amplitude constants. The boundary condition (3.116b) requires that

$$C_1 \sin la = C_2 \sin pc$$

where  $c = b - a$ . The last boundary condition (3.116c) requires

$$\frac{\epsilon_r}{l} C_1 \cos la = -\frac{1}{p} C_2 \cos pc$$

When we divide the first equation by the second one, we obtain

$$l \tan la = -\epsilon_r p \tan pc \quad (3.118)$$

This transcendental equation must be solved simultaneously with (3.114) to determine the allowed values of  $l$  and  $p$ . There will be an infinite number of solutions; consequently an infinite number of  $E$  modes are possible. Since  $\beta$  is given by

$$\beta = \sqrt{k_0^2 - p^2} = \sqrt{k^2 - l^2} \quad (3.119)$$

most of the modes will be nonpropagating since increasing values of  $p$  and  $l$  give  $p > k_0$  which makes  $\beta$  imaginary. When  $\beta$  is imaginary the  $z$  dependence is of the form  $e^{-|\beta|z}$  and the field decays exponentially from the point at which it is excited. These nonpropagating modes are called evanescent modes.

We note from (3.119) that a value of  $\beta$  between  $k_0$  and  $k$  can occur only if  $p$  is imaginary. Thus we must consider the possibility that an imaginary  $p$ , say  $p = jp_0$ , is a possible solution to (3.118). If we let  $l_0$  be the corresponding value of  $l$ , then our relevant equations become

$$l_0 \tan l_0 a = \epsilon_r p_0 \tanh p_0 c \quad (3.120a)$$

$$l_0^2 + p_0^2 = (\epsilon_r - 1)k_0^2 \quad (3.120b)$$

We consider solutions of these equations and the corresponding fields in the low- and high-frequency limits in the next two subsections.

### Low-Frequency Solution

When the frequency is very low,  $k_0^2$  is a very small number (at 1 MHz,  $k_0$  equals 0.02094 rad/m); hence  $l_0$  and  $p_0$  are then also small. We will assume that  $b$  is at most a few centimeters, then  $l_0 a$  and  $p_0 c$  are also small and we can replace the tangent function and the hyperbolic tangent function by their arguments. Thus (3.120a) becomes

$$l_0^2 a = \epsilon_r p_0^2 c$$

Upon using (3.120b) we readily find that

$$(\epsilon_r - 1)k_0^2 - p_0^2 = \frac{\epsilon_r p_0^2 c}{a}$$

or

$$p_0^2 = \frac{(\epsilon_r - 1)k_0^2 a}{a + \epsilon_r c}$$

The solution for  $\beta$  in the low-frequency limit is thus

$$\beta = \sqrt{k_0^2 + p_0^2} = \sqrt{\frac{\epsilon_r b}{a + \epsilon_r c}} k_0 = \sqrt{\epsilon_e} k_0 \quad (3.121)$$

where  $\epsilon_e$ , given by this equation, is called the effective dielectric constant.

We will now show that this equals  $\omega\sqrt{LC}$ , where  $L$  and  $C$  are the static distributed inductance and capacitance per meter for the given structure.

If we have a uniform current density  $J_z$  on the inner surface of the upper plate and  $-J_z$  on the inner surface of the lower plate, the magnetic field between the plates will be given by  $H_x = J_z$ . The time-average stored magnetic energy per unit length is given by

$$W_m = \frac{\mu_0}{4} \int_0^b \int_{-W}^W H_x^2 dx dy = \frac{\mu_0}{2} WbJ_z^2$$

We equate this to  $\frac{1}{4}LI_z^2$  where the total current  $I_z = 2WJ_z$  and then find that

$$L = \frac{\mu_0 b}{2W} \quad (3.122)$$

The distributed capacitance  $C$  per meter is found by considering the capacitance of the dielectric and air regions as represented by two equivalent parallel-plate capacitances  $C_d$  and  $C_a$  in series where

$$C_d = \frac{\epsilon_r \epsilon_0 2W}{a} \quad C_a = \frac{\epsilon_0 2W}{c}$$

The capacitance  $C_d$  is that of a parallel-plate capacitor of width  $2W$ , unit length, plate spacing  $a$ , and filled with dielectric.  $C_a$  is the capacitance of the air-filled section which has a spacing  $c$ .

The series capacitance is given by

$$C = \frac{C_a C_d}{C_a + C_d} = \frac{2W\epsilon_r \epsilon_0}{\epsilon_r c + a} \quad (3.123)$$

The product  $LC = \epsilon_r \epsilon_0 \mu_0 b / (\epsilon_r c + a)$  which gives the solution for  $\beta = \omega\sqrt{LC}$  equal to that in (3.121).

The expressions for the fields can be written down in simplified form using the small argument approximations and the relationship  $C_2 = C_1 \sin l_0 a / j \sinh p_0 c \approx -jC_1 l_0 a / p_0 c$  obtained from the boundary condition requiring continuity of  $e_z$  at  $y = a$ . We readily find that in the region  $0 \leq y \leq a$ ,

$$e_z = C_1 l_0 y \quad (3.124a)$$

$$e_y = -\frac{j\beta}{l_0} C_1 = -jC_1 \sqrt{\frac{b}{(\epsilon_r - 1)c}} \quad (3.124b)$$

$$h_x = \frac{j\epsilon_r k_0 Y_0}{l_0} C_1 = jY_0 C_1 \sqrt{\frac{\epsilon_r(\epsilon_r c + a)}{(\epsilon_r - 1)c}} \quad (3.124c)$$

and in the air region

$$e_z = C_1 \frac{l_0 a}{c} (b - y) \quad (3.124d)$$

$$e_y = -\frac{j\beta l_0 a}{p_0^2 c} C_1 = -\frac{j\beta}{l_0} \epsilon_r C_1 = -jC_1 \epsilon_r \sqrt{\frac{b}{(\epsilon_r - 1)c}} \quad (3.124e)$$

$$h_x = \frac{jk_0 Y_0}{l_0} C_1 = jY_0 C_1 \sqrt{\frac{\epsilon_r(\epsilon_r c + a)}{(\epsilon_r - 1)c}} \quad (3.124f)$$

We note that in the low-frequency limit  $e_z$  vanishes as  $k_0$ , and hence  $l_0$ , approach zero, while  $e_y$  and  $h_x$  remain constant. If we define the voltage  $V$  between the upper and lower plates by the line integral of  $e_y$ , then

$$V = -\int_0^b e_y dy = jC_1 \sqrt{\frac{b}{(\epsilon_r - 1)c}} (a + \epsilon_r c)$$

The total  $z$ -directed current on the upper plate is  $I_z = 2WJ_z = 2WH_x$ , and hence the characteristic impedance is given by

$$Z_c = \frac{V}{I_z} = \frac{Z_0}{2W} \sqrt{\frac{(\epsilon_r c + a)b}{\epsilon_r}} = \sqrt{\frac{L}{C}} \quad (3.125)$$

Thus we find that in the low-frequency limit the dominant mode of propagation in the partially filled parallel-plate waveguide becomes a TEM mode and the waveguide may be analyzed as a transmission line. The propagation constant and characteristic impedance are determined by the static distributed inductance and capacitance. In general, at low frequencies the mode of propagation would be called a quasi-TEM mode since the axial electric field  $e_z$ , even though it is small, is not zero. At high frequencies the mode of propagation is an  $E$  mode and departs significantly from a TEM mode in its field distribution.

## High-Frequency Solution

At high frequencies  $k_0$ , and hence  $l_0$  and  $p_0$ , are large. In this case  $p_0 c$  is large so we can replace  $\tanh p_0 c$  by unity and (3.120a) gives

$$l_0 \tan l_0 a = \epsilon_r p_0 = \epsilon_r \sqrt{(\epsilon_r - 1)k_0^2 - l_0^2} \quad (3.126)$$

upon using (3.120b) to eliminate  $p_0$ . This equation is independent of the

plate separation  $b$ . The solution for  $e_z$  can be approximated as follows:

$$e_z(y) = C_1 \sin l_0 y \quad 0 \leq y \leq a \quad (3.127a)$$

$$e_z(y) = C_2 j \sinh p_0(b - y)$$

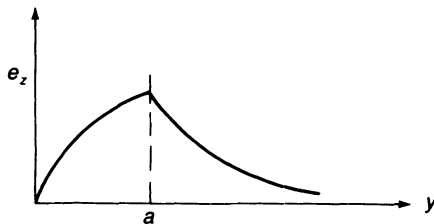
$$= C_1 \sin l_0 a \frac{\sinh p_0(b - y)}{\sinh p_0(b - a)}$$

$$\approx C_1 \sin l_0 a \frac{e^{p_0(b-y)}}{e^{p_0(b-a)}}$$

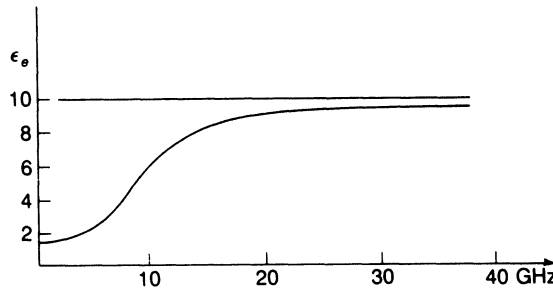
$$= C_1 \sin(l_0 a) e^{-p_0(y-a)} \quad a \leq y \leq b \quad (3.127b)$$

This is a field that decays exponentially away from the air-dielectric surface and does not depend on  $b$  as long as  $p_0 c = p_0(b - a)$  is large. This field is guided by the dielectric sheet on the ground plane (lower conductor) even if the upper plate is removed to infinity. This type of mode is called a surface-wave mode because its field is confined close to the guiding surface. The axial electric field for this surface-wave mode is illustrated in Fig. 3.15.

The first root for  $l_0$  in the eigenvalue equation (3.126) occurs for  $l_0 a < \pi/2$  or  $l_0 < \pi/2a$ . Thus, as  $k_0$  approaches infinity,  $l_0$  remains bounded but  $p_0$  will become large because  $p_0^2 = (\epsilon_r - 1)k_0^2 - l_0^2$ . Consequently, for large enough  $k_0$  we will have  $l_0^2 \ll k^2$  and then  $\beta \approx k$ . As we go from zero frequency to very high frequencies, the propagation constant varies from a low value of  $\sqrt{\epsilon_e} k_0$  given by (3.121) to an asymptotic value of  $\sqrt{\epsilon_r} k_0$ . We see that  $\beta$  is not a linear function of  $\omega$  or  $k_0$  and for this reason is said to exhibit dispersion. The term *dispersion* arises from a consideration of signal propagation. In our discussion of waveguides later on in this chapter, we will show that a signal consisting of a band of frequencies will have its frequency components dispersed whenever  $\beta$  is not a linear function of  $\omega$ . This is caused by the phase velocity  $v_p$ , given by the relation  $\beta = \omega/v_p$  and thus  $v_p = \omega/\beta = 1/\sqrt{\epsilon_e \mu_0 \epsilon_0}$ , being a function of  $\omega$ . The ratio  $\beta^2/k_0^2$  gives the effective dielectric constant at any frequency. In Fig. 3.16 we show a plot of  $\epsilon_e$  versus frequency for the case when  $\epsilon_r = 10$ ,  $a = 0.4$  cm, and  $b = 1$  cm. This curve is derived by solving the pair of equations (3.120). Microstrip transmission lines exhibit similar dispersion characteristics.



**FIGURE 3.15**  
Axial electric field for surface-wave mode.

**FIGURE 3.16**

Effective dielectric constant as a function of frequency for  $\epsilon_r = 10$ ,  $a = 0.4$  cm, and  $b = 1$  cm.

A second surface-wave mode solution can be found from (3.120a) with  $l_0 a$  in the range  $\pi < l_0 a < 3\pi/2$  provided  $\sqrt{\epsilon_r - 1} k_0$  is larger than  $\pi$  so that (3.120b) can also be satisfied. For large  $k_0 a$  many surface-wave modes can propagate. In addition to the surface-wave modes, there are also an infinite number of solutions to (3.118) for real values of  $p$ . The higher-order solutions have values of  $p$  on the order of  $n\pi/b$  in value, where  $n$  is an integer. Provided  $\pi/b$  is greater than  $k_0$ , these values of  $p$  will give imaginary values of  $\beta$  and hence nonpropagating modes. The cutoff occurs when  $p = k_0$  giving  $\beta = 0$ . Thus at cutoff

$$l \tan la = -\epsilon_r k_0 \tan k_0 c = \sqrt{\epsilon_r} k_0 \tan \sqrt{\epsilon_r} k_0 a$$

since  $l = k$  for  $\beta = 0$ . This equation reduces to

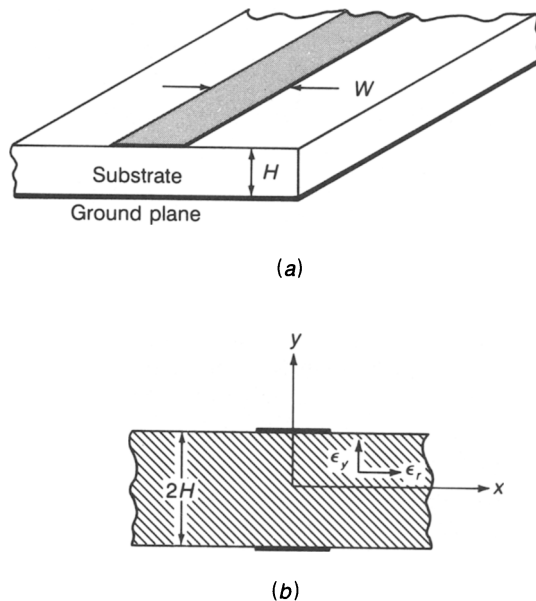
$$\tan \sqrt{\epsilon_r} k_0 a = -\sqrt{\epsilon_r} \tan k_0 c$$

which can be solved for the values of  $k_0$  at which the various modes cease to propagate.

We will not consider the partially filled parallel-plate waveguide any further even though a good deal more could be said about its mode spectrum. The purpose of our discussion is to highlight those features that will be displayed by microstrip transmission lines, which is the next topic taken up.

### 3.11 PLANAR TRANSMISSION LINES

A planar transmission line is a transmission line with conducting metal strips that lie entirely in parallel planes. The most common structure is one or more parallel metal strips placed on a dielectric substrate material adjacent to a conducting ground plane. A planar transmission line that is widely used is the microstrip line shown in Fig. 3.17. It consists of a single conducting strip of width  $W$  placed on a dielectric substrate of thickness  $H$  and located on a ground plane. By image theory this transmission line is equivalent to a line consisting of two parallel conducting strips placed opposite each other on a dielectric sheet of thickness  $2H$  as also shown in

**FIGURE 3.17**

(a) The microstrip transmission line; (b) equivalent parallel strip line obtained by using image theory.

Fig. 3.17. Typical dimensions for a microstrip line are substrate thickness of 0.25 to 1 mm and strip widths of 0.1 to 5 mm.

The microstrip transmission line can be fabricated using conventional printed-circuit-board techniques which result in good mechanical tolerances and a low cost.

In addition to the microstrip line, there are many other planar-transmission-line structures that are used for various purposes. A number of these other transmission-line configurations are shown in Figs. 3.18 to 3.20. The coupled microstrip line shown in Fig. 3.18a is used in directional couplers. The coupled microstrip line supports two modes of propagation. The even mode of propagation has the same voltage and current on the two strips, while the odd mode of propagation has opposite voltages and currents on the two strips.

The coplanar transmission line shown in Fig. 3.18b consists of a single strip mounted between two ground planes on the same side of the dielectric substrate. The coplanar line has an advantage over the microstrip line in that shunt connection of components to the ground plane can be made on the same side of the substrate. In addition, it allows the series connection of components to be made with equal facility to that for microstrip lines. The coplanar strip line shown in Fig. 3.18c is similar to the coplanar line in that all conducting strips are in the same plane (coplanar). It is less desirable than the coplanar line because it is not balanced relative to a ground plane and thus wave propagation on this line is more strongly influenced by nearby conductors such as a shielding enclosure. In practice, a shielding



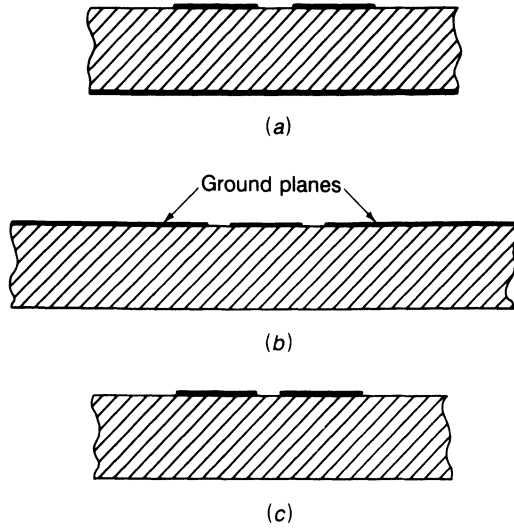


**FIGURE 3.18**

(a) Coupled microstrip lines; (b) coplanar transmission line; (c) coplanar strip transmission line.

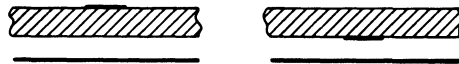


**FIGURE 3.19**

Suspended and inverted suspended microstrip line.

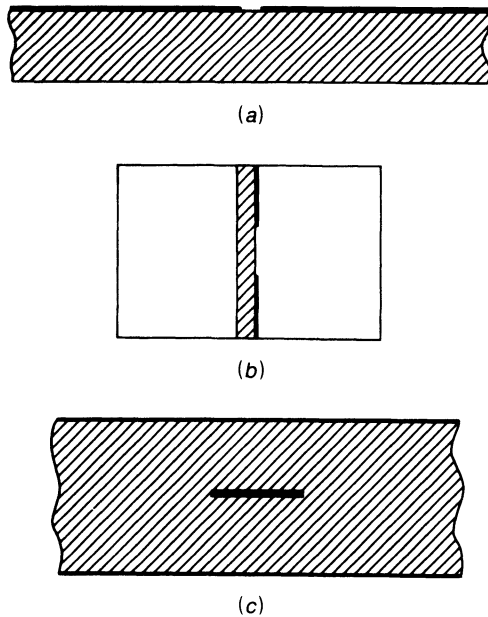


**FIGURE 3.20**

(a) Slot line; (b) shielded slot line or fin line; (c) strip line.

enclosure for a microwave circuit is needed to reduce spurious radiation from the circuit, eliminate electromagnetic coupling with nearby circuits, and for environmental protection.

In Fig. 3.19 are illustrated the suspended and inverted suspended microstrip lines which are quite similar to the conventional microstrip line but involve less dielectric substrate material. Figure 3.20*a* shows a slot line. The open slot line is not as widely used as the microstrip and coplanar lines are. The shielded slot line, which is typically a slot line placed inside a rectangular waveguide as shown in Fig. 3.20*b*, is called a fin line and has found to be useful for many circuit applications. Only shunt-connected components can be used with a slot line.

The final transmission-line structure illustrated here is the strip line shown in Fig. 3.20*c*. This line consists of a strip placed between two parallel plates that function as ground planes. The strip may be rigid enough to be suspended in air or it may be sandwiched between two dielectric sheets as shown in the figure. The strip line was often used in microwave filters and couplers before the other forms of planar transmission lines became popular. The strip line is somewhat more difficult to fabricate but has certain advantages for special applications to filters and couplers. Many directional coupler, power divider, and filter designs using strip lines were developed in the period from 1955 to 1975. An excellent reference source for design data for strip-line circuits is the book by Howe listed in the references at the end of this chapter.

The methods used to fabricate planar-transmission-line structures and related circuit elements are compatible with integrated circuit fabrication and have allowed the development of microwave integrated circuits (MIC circuits). In integrated microwave circuits the active devices and all interconnecting transmission lines, impedance-matching elements, needed capacitors and resistors, etc., are fabricated on the same chip. In these applications the microstrip and coplanar transmission lines are the ones most easily adapted for on-chip fabrication. In MIC circuits the substrate thickness and line widths are generally much smaller than in hybrid circuits. The term *hybrid* is used to describe integrated microwave circuits where the discrete components such as transistors, capacitors, and resistors are soldered in place.

The dielectric substrate material used in a planar transmission line must have low loss, i.e., a small loss tangent. A large dielectric constant results in a shorter propagation wavelength and hence a more compact circuit. The substrate material should have good mechanical strength, be easy to machine, and have good thermal conduction. When active devices are mounted into a planar-transmission-line circuit, the heat generated by the active device is in part conducted away to the ground plane through the substrate material. It is difficult to use metal heat sinks in a microwave circuit because these large metal structures would interact with the electro-

magnetic field in an undesirable, and often unpredictable, manner. Consequently, in power amplifier circuits substrate materials with good thermal conductivity are required. Dielectric materials used in low-frequency circuit boards are generally too lossy to be used for microwave transmission lines. The dielectric constant and thickness must be maintained to a high level of uniformity in the manufacturing of substrates because otherwise the fabricated transmission lines will not perform according to the specified design since the propagation phase constant and characteristic impedance both depend on these parameters. Uniform thickness and dielectric constant is particularly important in the design of filters and impedance-matching elements whose dimensions are critical. Once a printed microwave structure such as a filter has been constructed, it is not very easy to add external tuning elements to bring the constructed filter performance into specifications.

A commonly used substrate material is polytetrafluoroethylene (PTFE)<sup>†</sup> which has a dielectric constant of 2.1 and a loss tangent of 0.0002 at 1 MHz and around 0.0005 at microwave frequencies. This material has excellent resistance to chemicals used in the photoetching process. In order to increase the mechanical strength, it can be loaded with woven fiberglass mat or glass microparticles. This increases the dielectric constant to the range 2.2 to 3. The use of glass fiber results in some anisotropy in the dielectric constant. In the manufacturing process the glass fibers are generally aligned parallel with the substrate so the dielectric constant along the substrate is typically 5 to 10 percent larger than that normal to the substrate. By using ceramic powders as fillers, notably titanium oxide, much larger dielectric constants can be obtained. Typical values are in the range 5 to 15.

Ceramic materials such as aluminum oxide (alumina) and boron nitride, as well as the glasslike material sapphire, are also used for substrates. These materials are very difficult to machine. Alumina is perhaps the most commonly used material. It has excellent thermal conductivity. For integrated microwave circuits the usual semiconductor materials germanium, silicon, and gallium arsenide are used. These substrate materials have a high dielectric constant and may exhibit some conductivity depending on the doping level.

In Table 3.2 we have summarized the important properties of a number of substrate materials. In this table  $\epsilon_x$  is the dielectric constant along the substrate and  $\epsilon_y$  is the dielectric constant normal to the substrate.<sup>‡</sup>

---

<sup>†</sup>This material is commonly known as Teflon, which is a registered trade name of Du Pont.

<sup>‡</sup>In order to keep the notation as simple as possible, we use  $\epsilon_y$  instead of  $\epsilon_{,y}$  for the relative permittivity (dielectric constant) in the  $y$  direction.

**TABLE 3.2**  
**Properties of substrate materials**

Material	$\epsilon_r$	$\epsilon_y$	Loss tangent	Thermal conductivity	Machinability
PTFE/woven glass	2.84	2.45	0.001–0.002	Fair	Good
PTFE/microfiberglass	2.26	2.2	0.0005–0.001	Fair	Good
*CuFlon	2.1	2.1	0.0004	Fair	Good
*RT/Duroid 5880	2.26	2.2	0.001	Fair	Good
*RT/Duroid 6006	6.36	6		Medium	Good
*Epsilam 10	13	10.3		Medium	Good
Boron nitride	5.12	3.4		Good	Poor
Silicon	11.7–12.9	11.7–12.9	0.001–0.003	Medium	Poor
Germanium	16	16		Medium	Poor
Gallium arsenide	12.9	12.9	0.0005–0.001	Medium	Poor
Alumina	9.6–10.1	9.6–10.1	0.0005–0.002	Good	Poor
Sapphire	9.4	11.6	0.0002	Good	Poor
Beryllium oxide	6.7	6.7	0.001–0.002	Good	Poor

\*CuFlon is a registered trademark of Polyflon Company. It is a Teflon material electroplated with copper. RT/Duroid is a registered trademark of Rogers Corporation. Rogers Corporation also manufactures substrates with dielectric constants around 10. Epsilam 10 is a registered trademark of the 3M Company. It is a ceramic-filled Teflon material.

The data in Table 3.2 have been compiled from a variety of sources.† Since the dielectric constant and loss tangent are frequency dependent and also influenced by the material processing, the listed data should be viewed as representative values at microwave frequencies.

Substrate materials are usually plated with copper in 0.5-, 1-, or 2-oz weights (amount of copper per square foot). The use of 1-oz copper weight gives a plating thickness of 0.0014 in. Gold plating is sometimes used on top of the copper to prevent oxidation of the metal. In integrated microwave circuit construction a metalization thickness of a few microns is typical. One-half oz copper-clad board has a metalization thickness of 18  $\mu\text{m}$ .

### 3.12 MICROSTRIP TRANSMISSION LINE

In a microstrip transmission line the dielectric material does not completely surround the conducting strip and consequently the fundamental mode of propagation is not a pure TEM mode. At low frequencies, typically below a

†H. Howe, "Stripline Circuit Design," Artech. House Books, Dedham, Mass., 1974.

T. Laverghetta, Microwave Materials: The Choice is Critical, *Microwave J.*, vol. 28, p. 163, 1985.

M. N. Afsar and K. J. Button, Precise Millimeter-Wave Measurements of Complex Refractive Index, Complex Dielectric Permittivity and Loss Tangent of GaAs, Si, SiO<sub>2</sub>, Al<sub>2</sub>O<sub>3</sub>, BeO, Macor, and Glass, *IEEE Trans.*, vol. MTT-31, pp. 217–223, 1983.

Some data were also obtained from manufacturers' literature.

few gigahertz for practical microstrip lines, the mode is a quasi-TEM mode. In the frequency range up to a gigahertz or somewhat higher, the microstrip transmission line can be characterized in terms of its distributed capacitance and inductance per meter in a manner similar to what was found for the partially loaded parallel-plate transmission line in the previous section. Unfortunately, there are no simple closed-form analytic expressions that can be derived for describing the field distribution or the characteristics of planar transmission lines. Formal solutions can be derived and evaluated on a computer and have been used to compile data on the characteristics of these transmission-line structures. Static field analysis has also been extensively used to obtain the low-frequency characteristics. However, even the static field analysis is quite complex.

The analysis of planar transmission lines can be based directly on a solution for the electric and magnetic fields in the structure. An alternative approach is to first solve for the scalar and vector potential functions and from these find the corresponding electromagnetic field. In actual fact the propagation constant and characteristic impedance can be found from the potentials without a detailed consideration of the fields. The advantage of using the scalar and vector potentials in the analysis is that this approach provides a direct link to the quasistatic solutions in terms of more familiar low-frequency concepts.

In this section we will develop the essential equations to be satisfied by the scalar and vector potentials for a microstrip transmission line. From these equations we then obtain simplified ones that will describe the quasi-TEM mode of propagation at low frequencies. The term low frequency is a relative one. It is the ratio of line dimensions to wavelength that determines whether a microstrip line can be adequately described in terms of the quasi-TEM mode of propagation. In MIC circuits with line widths as small as  $100\ \mu\text{m}$ , the low-frequency region can extend as high as 20 to 30 GHz. Even though space does not permit a full development of analytic methods suitable for solving planar-transmission-line problems, some insight into the properties of these structures is obtained from the basic formulation of the relevant equations.

After we have presented the theoretical foundations, typical dispersion curves and graphical results for characteristic impedances are given for a number of important substrate materials and a range of microstrip conductor widths.

The vector and scalar potential functions are solutions of Helmholtz equations as described in Sec. 2.10 when the sources are located in vacuum (air). For the microstrip line shown in Fig. 3.17, two added complications enter due to the presence of the dielectric in only part of the region of interest and the anisotropic nature of some substrate materials. For this reason we need to derive new equations to be satisfied by the potential functions. The substrate material will be characterized by a dielectric constant  $\epsilon_y$  in the  $y$  direction which is normal to the interface and by a

dielectric constant  $\epsilon_r$  in the  $x$  and  $z$  directions. The unknown charge and current densities on the conducting microstrip will be denoted by  $\rho$  and  $\mathbf{J}$ . These source densities are concentrated along  $y$  since they exist only on the microstrip which is assumed to have negligible thickness. The source concentration can be described by introducing the delta function  $\delta(y - H)$  to localize the sources at  $y = H$ . Thus we can write

$$\rho(x, y, z) = \rho_s(x, z)\delta(y - H) \quad (3.128a)$$

$$\mathbf{J}(x, y, z) = \mathbf{J}_s(x, z)\delta(y - H) \quad (3.128b)$$

where  $\mathbf{J}_s$  and  $\rho_s$  now describe surface densities rather than volume densities.

We will assume that the dielectric constants  $\epsilon_y(y)$  and  $\epsilon_r(y)$  are functions of  $y$  that are constant in the substrate and undergo a rapid change in value to unity as the interface is crossed into the air region. The reason for doing this is that the equations we then obtain for the potentials will automatically give us the boundary conditions needed to properly join the solutions for the potentials in the substrate region to those in the air region.

We begin the derivation by letting

$$\mathbf{B} = \nabla \times \mathbf{A}$$

From Maxwell's equation

$$\nabla \times \mathbf{E} = -j\omega\mathbf{B} = -j\omega\nabla \times \mathbf{A}$$

we get  $\nabla \times (\mathbf{E} + j\omega\mathbf{A}) = 0$  which has the general solution

$$\mathbf{E} = -j\omega\mathbf{A} - \nabla\Phi$$

where  $\Phi$  is a scalar potential function. Up to this point we have followed the same steps as in Sec. 2.10. Maxwell's curl equation for the magnetic field is

$$\nabla \times \mathbf{H} = j\omega\mathbf{D} + \mathbf{J}$$

For an anisotropic dielectric we have

$$\mathbf{D} = \epsilon_0\epsilon_r(E_x\mathbf{a}_x + E_z\mathbf{a}_z) + \epsilon_0\epsilon_y E_y\mathbf{a}_y$$

We can replace  $\mathbf{H}$  by  $\mu_0^{-1}\nabla \times \mathbf{A}$  to obtain

$$\nabla \times \nabla \times \mathbf{A} = \nabla\nabla \cdot \mathbf{A} - \nabla^2\mathbf{A} = j\omega\mu_0\mathbf{D} + \mu_0\mathbf{J}$$

and express  $\mathbf{D}$  in terms of the potentials as follows:

$$\begin{aligned} \mathbf{D} = & -\epsilon_0\epsilon_r \left[ j\omega(A_x\mathbf{a}_x + A_z\mathbf{a}_z) + \mathbf{a}_x \frac{\partial\Phi}{\partial x} + \mathbf{a}_z \frac{\partial\Phi}{\partial z} \right] \\ & - \epsilon_0\epsilon_y \left( jA_y\mathbf{a}_y + \mathbf{a}_y \frac{\partial\Phi}{\partial y} \right) \end{aligned}$$

By adding and subtracting a term to the  $y$  component that includes the factor  $\epsilon_r$ , we can reexpress  $\mathbf{D}$  in the form

$$\mathbf{D} = -\epsilon_r \epsilon_0 (j\omega \mathbf{A} + \nabla \Phi) - \epsilon_0 (\epsilon_y - \epsilon_r) \left( j\omega A_y \mathbf{a}_y + \mathbf{a}_y \frac{\partial \Phi}{\partial y} \right)$$

We wish to eliminate the  $\nabla \nabla \cdot \mathbf{A}$  term in the equation for  $\mathbf{A}$  by setting it equal to the gradient of another function. For this purpose we now express  $\epsilon_r \nabla \Phi$  in the form  $\nabla(\epsilon_r \Phi) - \Phi \nabla \epsilon_r$ , where  $\nabla \epsilon_r$  has only a  $y$  component since  $\epsilon_r$  is a function of  $y$  only. We can set  $\nabla \nabla \cdot \mathbf{A}$  equal to  $-j\omega \epsilon_0 \mu_0 \nabla(\epsilon_r \Phi)$  which gives the Lorentz condition

$$\nabla \cdot \mathbf{A} = -j\omega \epsilon_0 \epsilon_r \mu_0 \Phi \quad (3.129)$$

The equation for the vector potential now becomes

$$-\nabla^2 \mathbf{A} = j\omega \mu_0 \left[ -j\omega \epsilon_0 \epsilon_r \mathbf{A} + \epsilon_0 \Phi \nabla \epsilon_r - \epsilon_0 (\epsilon_y - \epsilon_r) \left( j\omega \mathbf{a}_y A_y + \mathbf{a}_y \frac{\partial \Phi}{\partial y} \right) \right] + \mu_0 \mathbf{J}$$

The current  $\mathbf{J}$  does not have a  $y$  component so the  $x$  and  $z$  components of this equation are

$$\nabla^2 A_x + \epsilon_r(y) k_0^2 A_x = -\mu_0 J_x \quad (3.130a)$$

$$\nabla^2 A_z + \epsilon_r(y) k_0^2 A_z = -\mu_0 J_z \quad (3.130b)$$

while the  $y$  component becomes

$$\begin{aligned} \nabla^2 A_y + \epsilon_y(y) k_0^2 A_y &= -j\omega \mu_0 \epsilon_0 \left[ \Phi \frac{\partial \epsilon_r}{\partial y} - (\epsilon_y - \epsilon_r) \frac{\partial \Phi}{\partial y} \right] \\ &= j\omega \mu_0 \epsilon_0 \left[ (\epsilon_y - \epsilon_r) \frac{\partial \Phi}{\partial y} + \Phi(H) (\epsilon_r - 1) \delta(y - H) \right] \end{aligned} \quad (3.131)$$

where  $-(\epsilon_r - 1)\delta(y - H)$  expresses the derivative of the step change that occurs in  $\epsilon_r$  as  $y$  crosses the interface at  $H$ , that is,  $\epsilon_r(y)$  changes from  $\epsilon_r$  to unity.

The equations for  $A_x$  and  $A_z$  are of the same form as derived in Sec 2.10, but the equation for  $A_y$  is new. The equation for  $A_y$  is coupled to the scalar potential  $\Phi(H)$  at the boundary even if we have an isotropic substrate. Thus boundary conditions require the presence of an  $A_y$  component even though there is no  $y$  component of current.

A separate equation for the scalar potential is obtained by using Gauss' law  $\nabla \cdot \mathbf{D} = \rho$  and the Lorentz condition (3.129). Thus we find that

$$\begin{aligned}\nabla \cdot \mathbf{D} &= \nabla \cdot \left[ -\epsilon_r \epsilon_0 (j\omega \mathbf{A} + \nabla \Phi) - \epsilon_0 (\epsilon_y - \epsilon_r) \left( j\omega \mathbf{a}_y A_y + \mathbf{a}_y \frac{\partial \Phi}{\partial y} \right) \right] \\ &= -\epsilon_0 \left[ j\omega \nabla \cdot (\epsilon_r \mathbf{A}) + \nabla \cdot (\epsilon_r \nabla \Phi) + j\omega \frac{\partial}{\partial y} (\epsilon_y - \epsilon_r) A_y \right. \\ &\quad \left. + \frac{\partial}{\partial y} (\epsilon_y - \epsilon_r) \frac{\partial \Phi}{\partial y} \right] \\ &= -\epsilon_0 \left[ j\omega (\epsilon_r \nabla \cdot \mathbf{A} + \mathbf{A} \cdot \nabla \epsilon_r) + \nabla \cdot (\epsilon_r \nabla \Phi) + j\omega \frac{\partial}{\partial y} (\epsilon_y - \epsilon_r) A_y \right. \\ &\quad \left. + \frac{\partial}{\partial y} (\epsilon_y - \epsilon_r) \frac{\partial \Phi}{\partial y} \right] = \rho\end{aligned}$$

By replacing  $\nabla \cdot \mathbf{A}$  with  $-j\omega \epsilon_0 \mu_0 \epsilon_r \Phi$  from the Lorentz condition, we obtain

$$\begin{aligned}\nabla \cdot (\epsilon_r \nabla \Phi) + \frac{\partial}{\partial y} (\epsilon_y - \epsilon_r) \frac{\partial \Phi}{\partial y} + \epsilon_r^2 k_0^2 \Phi \\ = -j\omega A_y \frac{\partial \epsilon_r}{\partial y} - j\omega \frac{\partial}{\partial y} (\epsilon_y - \epsilon_r) A_y - \frac{\rho}{\epsilon_0}\end{aligned}$$

The last step is to simplify this equation using

$$\frac{\partial}{\partial y} (\epsilon_y - \epsilon_r) A_y = (\epsilon_y - \epsilon_r) \frac{\partial A_y}{\partial y} + A_y \left( \frac{\partial \epsilon_y}{\partial y} - \frac{\partial \epsilon_r}{\partial y} \right)$$

and 
$$\nabla \cdot \epsilon_r \nabla \Phi = \epsilon_r \nabla^2 \Phi + \frac{\partial \epsilon_r}{\partial y} \frac{\partial \Phi}{\partial y}$$

$$\frac{\partial}{\partial y} (\epsilon_y - \epsilon_r) \frac{\partial \Phi}{\partial y} = (\epsilon_y - \epsilon_r) \frac{\partial^2 \Phi}{\partial y^2} + \frac{\partial \Phi}{\partial y} \left( \frac{\partial \epsilon_y}{\partial y} - \frac{\partial \epsilon_r}{\partial y} \right)$$

By using these expressions a number of terms cancel and we obtain the final form

$$\begin{aligned}\epsilon_r \left( \frac{\partial^2 \Phi}{\partial x^2} + \frac{\partial^2 \Phi}{\partial z^2} \right) + \frac{\partial}{\partial y} \left( \epsilon_y \frac{\partial \Phi}{\partial y} \right) + \epsilon_r^2 k_0^2 \Phi \\ = -\frac{\rho}{\epsilon_0} + j\omega (\epsilon_y - 1) A_y (H) \delta(y - H) - j\omega (\epsilon_y - \epsilon_r) \frac{\partial A_y}{\partial y}\end{aligned}\quad (3.132)$$

where we have also used

$$A_y \frac{\partial \epsilon_y(y)}{\partial y} = -(\epsilon_y - 1) A_y (H) \delta(y - H)$$



This equation also displays a coupling between the scalar potential and  $A_y(H)$  at the interface as well as coupling within the substrate whenever  $\epsilon_y$  does not equal  $\epsilon_r$ , that is, for anisotropic substrates. In the air region  $y > H$ , both  $\epsilon_r$  and  $\epsilon_y$  are replaced by unity in (3.130) to (3.132).

After the above lengthy derivation we can now obtain simpler equations to be solved in each separate region along with boundary conditions to use in joining the solutions at the interface  $y = H$ . The source terms  $\rho$  and  $\mathbf{J}$  when expressed in the form (3.128) contain the  $\delta(y - H)$  factor. In order for the left-hand sides of (3.130) to (3.132) to equal the corresponding right-hand sides, we must obtain a delta function  $\delta(y - H)$  from the derivative of the potentials with respect to  $y$ . In (3.130a) and (3.130b) this requires that  $\partial A_x/\partial y$  and  $\partial A_z/\partial y$  have a step change at the interface so that the second derivative with respect to  $y$  will produce a delta function. The required step change can be found by integrating both sides of the equation over a vanishingly small interval centered on  $y = H$ . The integral of terms not involving a derivative with respect to  $y$  will vanish since these terms must be continuous at  $y = H$  and the interval length vanishes. For example, if  $A_x$  were not continuous at  $y = H$ , the second derivative with respect to  $y$  would generate a singular term corresponding to the derivative of the delta function and no such term exists on the right-hand side of the equation. Thus from (3.130a) we obtain

$$\begin{aligned} \lim_{\tau \rightarrow 0} \int_{H-\tau}^{H+\tau} \frac{\partial^2 A_x}{\partial y^2} dy &= \left. \frac{\partial A_x}{\partial y} \right|_{H^-}^{H^+} \\ &= \lim_{\tau \rightarrow 0} \int_{H-\tau}^{H+\tau} -\mu_0 \mathbf{J}_{sx}(x, z) \delta(y - H) dy = -\mu_0 \mathbf{J}_{sx} \end{aligned}$$

$$\text{or} \quad \left. \frac{\partial A_x}{\partial y} \right|_{H^-}^{H^+} = -\mu_0 \mathbf{J}_{sx} \quad (3.133a)$$

In a similar way we obtain

$$\left. \frac{\partial A_z}{\partial y} \right|_{H^-}^{H^+} = -\mu_0 \mathbf{J}_{sz} \quad (3.133b)$$

The notation  $H^+$  and  $H^-$  means evaluating the derivative on adjacent sides of the interface at  $y = H$ . These two equations state that the tangential components of the magnetic field must be discontinuous across the current sheet  $\mathbf{J}_s$  since from the equation  $\mathbf{B} = \nabla \times \mathbf{A}$ :

$$\frac{\partial A_z}{\partial y} = \mu_0 H_x \quad \frac{\partial A_x}{\partial y} = -\mu_0 H_z$$

In a similar way we obtain the following boundary conditions by integrating

(3.131) and (3.132) about a small interval centered on  $y = H$ :

$$\left. \frac{\partial A_y}{\partial y} \right|_{H^-}^{H^+} = j\omega\mu_0\epsilon_0(\epsilon_r - 1)\Phi(H) \quad (3.133c)$$

$$\left. \frac{\partial \Phi}{\partial y} \right|_{H^+} - \epsilon_y \left. \frac{\partial \Phi}{\partial y} \right|_{H^-} = -\frac{\rho_s}{\epsilon_0} + j\omega(\epsilon_y - 1)A_y(H) \quad (3.133d)$$

A term such as  $(\epsilon_y - \epsilon_r)\partial\Phi/\partial y$  that occurs in (3.131), and a similar term occurring in (3.132), does not contribute because

$$\lim_{\tau \rightarrow 0} \int_{H-\tau}^{H+\tau} (\epsilon_y - \epsilon_r) \frac{\partial \Phi}{\partial y} dy = \lim_{\tau \rightarrow 0} (\epsilon_y - \epsilon_r) \int_{H-\tau}^H \frac{\partial \Phi}{\partial y} dy = 0$$

since  $\partial\Phi/\partial y$  is continuous in the interval  $H - \tau \leq y < H$  and for  $y > H$  we have  $\epsilon_y = \epsilon_r = 1$ . The boundary conditions on  $\Phi$  reflect the fact that the total  $y$ -directed electric field has a contribution from  $A_y$  so that the discontinuity in  $D_y$  across the charge layer is given by

$$-\epsilon_0 \left( \frac{\partial \Phi}{\partial y} + j\omega A_y \right) \Big|_{H^+} + \epsilon_y \epsilon_0 \left( \frac{\partial \Phi}{\partial y} + j\omega A_y \right) \Big|_{H^-} = \rho_s$$

which is (3.133d).

By using the above boundary conditions, we can solve (3.130) to (3.132) in each respective region away from the interface. Thus we need only to solve the following homogeneous equations, subject to the specified boundary conditions, in the substrate region:

$$(\nabla^2 + \epsilon_r k_0^2)A_x = 0 \quad (3.134a)$$

$$(\nabla^2 + \epsilon_r k_0^2)A_z = 0 \quad (3.134b)$$

$$\nabla^2 A_y + \epsilon_y k_0^2 A_y = j\omega\mu_0\epsilon_0(\epsilon_y - \epsilon_r) \frac{\partial \Phi}{\partial y} \quad (3.134c)$$

$$\frac{\partial^2 \Phi}{\partial x^2} + \frac{\partial^2 \Phi}{\partial z^2} + \frac{\epsilon_y}{\epsilon_r} \frac{\partial^2 \Phi}{\partial y^2} + \epsilon_r k_0^2 \Phi = -j\omega(\epsilon_y - \epsilon_r) \frac{\partial A_y}{\partial y} \quad (3.134d)$$

In the air region the equations to be solved are obtained by setting  $\epsilon_r = \epsilon_y = 1$ . There is no volume coupling between  $\Phi$  and  $A_y$  in the air region or in an isotropic substrate region. Since we are interested in wave solutions representing waves propagating in the  $z$  direction, we can assume that the  $z$  dependence is  $e^{-j\beta z}$ . The second derivative with respect to  $z$  can then be replaced by  $-\beta^2$ . The common factor  $e^{-j\beta z}$  can be deleted from the equations just as  $e^{j\omega t}$  was dropped for convenience.

## Low-Frequency Solutions

We can obtain the equations to be solved in the zero-frequency limit by assuming that the potentials and the source terms can be expanded as

power series in  $\omega$ . Thus we let

$$\mathbf{A} = \mathbf{A}^0 + \omega\mathbf{A}^1 + \omega^2\mathbf{A}^2 + \cdots \quad (3.135a)$$

$$\Phi = \Phi^0 + \omega\Phi^1 + \omega^2\Phi^2 + \cdots \quad (3.135b)$$

$$\mathbf{J} = \mathbf{J}^0 + \omega\mathbf{J}^1 + \omega^2\mathbf{J}^2 + \cdots \quad (3.135c)$$

$$\rho = \rho^0 + \omega\rho^1 + \omega^2\rho^2 + \cdots \quad (3.135d)$$

The parameter  $k_0^2 = \omega^2\mu_0\epsilon_0$  is of second order in  $\omega$ . The propagation constant  $\beta$  can be expressed in the form  $\beta = \sqrt{\epsilon_e}k_0$ , where  $\epsilon_e$  is a frequency-dependent effective dielectric constant. Consequently,  $\beta^2$  is also of second order in  $\omega$ .

We now substitute these power-series expansions into (3.130) to (3.132) and equate all zero-order terms to obtain the following lowest-order equations:

$$\left( \frac{\partial^2}{\partial x^2} + \frac{\partial^2}{\partial y^2} \right) A_x^0 = -\mu_0 J_x^0 \quad (3.136a)$$

$$\left( \frac{\partial^2}{\partial x^2} + \frac{\partial^2}{\partial y^2} \right) A_z^0 = -\mu_0 J_z^0 \quad (3.136b)$$

$$\left( \frac{\partial^2}{\partial x^2} + \frac{\partial^2}{\partial y^2} \right) A_y^0 = 0 \quad (3.136c)$$

$$\left( \epsilon_r \frac{\partial^2}{\partial x^2} + \frac{\partial}{\partial y} \epsilon_y \frac{\partial}{\partial y} \right) \Phi^0 = -\frac{\rho^0}{\epsilon_0} \quad (3.136d)$$

Further information is obtained from the Lorentz condition (3.129) which gives

$$\frac{\partial A_x^0}{\partial x} + \frac{\partial A_y^0}{\partial y} = 0 \quad (3.137a)$$

$$-j\beta A_z^0 = -j\omega\epsilon_0\epsilon_r\Phi^0 \quad (3.137b)$$

In the air region  $\epsilon_r$  and  $\epsilon_y$  are set equal to unity. From the continuity equation relating current and charge, namely,

$$\nabla \cdot \mathbf{J} = -j\omega\rho$$

we obtain

$$\frac{\partial J_x^0}{\partial x} = 0 \quad (3.138a)$$

$$-j\beta J_z^0 = -j\omega\rho^0 \quad (3.138b)$$

In the above equations the  $e^{-j\beta z}$  factor is not included but any derivative with respect to  $z$  was replaced by  $-j\beta$ .

Since  $J_x^0$  must be zero at the edges  $x = \pm W/2$  of the microstrip, we conclude that  $J_x^0$  is zero because the integral of  $\partial J_x^0 / \partial x$  is at most a constant. Hence, to lowest order, there is no  $x$ -directed current on the microstrip and  $A_x^0$  is zero. The Lorentz condition then requires that  $\partial A_y^0 / \partial y = 0$  and hence  $A_y^0 = 0$  also since a constant  $A_y^0$  is a trivial solution and would not produce any magnetic field contribution. Thus, to lowest order, we only have to solve for an  $A_z^0$  and a scalar potential  $\Phi^0$ . If we assume the microstrip to be at a potential  $V$ , then the boundary condition on  $\Phi^0$  is that it equals  $V$  on the microstrip and equals zero on the ground plane.

We can integrate the continuity equation (3.138b) across the microstrip line to get

$$\beta I_z^0 = \omega Q^0 \quad (3.139)$$

where  $I_z^0$  is the total  $z$ -directed current on the microstrip and  $Q^0$  is the total charge. On the microstrip the axial electric field must be zero. To lowest order this boundary condition is

$$E_z^1 = -j\omega A_z^0 - \frac{\partial \Phi^0}{\partial z} = -j\omega A_z^0 + j\beta \Phi^0 = 0$$

$$\text{or} \quad \omega A_z^0 = \beta V \quad (3.140)$$

Hence  $A_z^0$  is also constant on the microstrip.

We will show shortly that the inductance  $L$  per unit length of the microstrip line is given by the equation

$$I_z^0 L = A_z^0 \quad (3.141)$$

The capacitance per unit length is given by

$$C = \frac{Q^0}{V} \quad (3.142)$$

By using these expressions to eliminate  $Q^0$  in (3.139) and  $A_z^0$  in (3.140), we obtain the pair of equations

$$\beta I_z^0 = \omega CV \quad (3.143a)$$

$$\omega L I_z^0 = \beta V \quad (3.143b)$$

from which we find that

$$\beta^2 = \omega^2 LC \quad (3.144a)$$

$$\frac{V}{I_z^0} = \sqrt{\frac{L}{C}} \quad (3.144b)$$

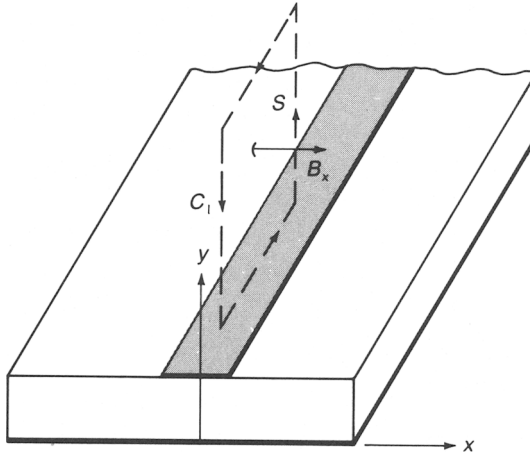


**FIGURE 3.21**  
Surface used to find the magnetic flux linkage in a microstrip line.

We have thus been able to show in a rigorous way that in the low-frequency limit the microstrip line can be analyzed as a static field problem and that its propagation constant and characteristic impedance are determined by the low-frequency distributed capacitance and inductance. The analysis leading up to (3.144) is quite general and applies to other planar transmission lines as well.

At this point we return to the promised derivation of (3.141) giving the line inductance. With reference to Fig. 3.21 we note that the magnetic flux  $\psi$  linking the microstrip per unit length is given by the integral of  $B_x$  over the area extending from the microstrip to infinity. Thus

$$\psi = \int_0^1 \int_H^\infty \mathbf{B} \cdot \mathbf{a}_x \, dy \, dz$$

By using  $\mathbf{B} = \nabla \times \mathbf{A}$  and Stokes' law, we can write

$$\begin{aligned} \psi &= \int_0^1 \int_H^\infty \nabla \times \mathbf{A} \cdot \mathbf{a}_x \, dy \, dz \\ &= \oint_{C_l} \mathbf{A} \cdot d\mathbf{l} \end{aligned}$$

where  $C_l$  is the boundary of the area. Since  $A_y^0$  is zero and  $A_z^0$  is zero at infinity and is constant on the microstrip, we obtain  $\psi = A_z^0$  for the flux linkage. The inductance is given by  $\psi/I_z^0$  and this gives (3.141).

We can also derive equations for the next level of approximation. However, the solution of these equations is not much easier than the solution of the original equations; so it is not worthwhile to develop the power-series solutions beyond the lowest order. Thus the equations to be

solved are

$$\left( \frac{\partial^2}{\partial x^2} + \frac{\partial^2}{\partial y^2} \right) A_z^0 = 0 \quad y < H, y > H \quad (3.145a)$$

$$\left( \frac{\partial^2}{\partial x^2} + \frac{\epsilon_y}{\epsilon_r} \frac{\partial^2}{\partial y^2} \right) \Phi^0 = 0 \quad y < H \quad (3.145b)$$

$$\left( \frac{\partial^2}{\partial x^2} + \frac{\partial^2}{\partial y^2} \right) \Phi^0 = 0 \quad y > H \quad (3.145c)$$

with the boundary conditions

$$\left. \frac{\partial A_z^0}{\partial y} \right|_{H^-}^{H^+} = -\mu_0 J_{sz}^0 \quad (3.145d)$$

$$\left. \frac{\partial \Phi^0}{\partial y} \right|_{H^+} - \epsilon_y \left. \frac{\partial \Phi^0}{\partial y} \right|_{H^-} = -\frac{\rho_s}{\epsilon_0} \quad (3.145e)$$

$$\Phi^0 = V \quad \text{on microstrip}$$

$$A_z^0 = \text{constant} \quad \text{on microstrip}$$

Along the interface and away from the microstrip, the right-hand sides of (3.145d) and (3.145e) are zero. In addition,  $\Phi^0$  and  $A_z^0$  must be zero on the ground plane in order to make the tangential electric field vanish on this surface.

The equations for  $A_z^0$  do not depend on the dielectric constants of the substrate material. Hence the line inductance is the same as for an air-filled line. But for an air-filled transmission line with distributed capacitance  $C_a$ , we have

$$\sqrt{LC_a} = \sqrt{\mu_0 \epsilon_0} \quad \text{and hence} \quad L = \frac{\mu_0 \epsilon_0}{C_a}$$

so we can find  $L$  by finding the distributed capacitance of an air-filled microstrip line. By introducing  $C_a$  in place of  $L$ , the solutions for  $\beta$  and  $Z_c$  can be expressed in the form

$$\beta = \omega \sqrt{LC} = \sqrt{\frac{C}{C_a}} k_0 = \sqrt{\epsilon_e} k_0 \quad (3.146a)$$

$$Z_c = \sqrt{\frac{L}{C}} = \frac{\sqrt{\mu_0 \epsilon_0}}{\sqrt{CC_a}} = \sqrt{\frac{L}{C_a}} \sqrt{\frac{C_a}{C}} = \frac{Z_{c0}}{\sqrt{\epsilon_e}} \quad (3.146b)$$

where  $Z_{c0}$  is the characteristic impedance of the air-filled line and the ratio  $C/C_a$  gives the low-frequency equivalent (effective) dielectric constant  $\epsilon_e$ .

The effect of having an anisotropic dielectric substrate does not add any additional complication. If we introduce a new variable  $u = (\epsilon_r/\epsilon_y)^{1/2}y$ , then upon using

$$\frac{\partial}{\partial y} = \frac{\partial}{\partial u} \frac{\partial u}{\partial y} = \sqrt{\frac{\epsilon_r}{\epsilon_y}} \frac{\partial}{\partial u}$$

we find that (3.145b) reduces to

$$\left( \frac{\partial^2}{\partial x^2} + \frac{\partial^2}{\partial u^2} \right) \Phi^0 = 0 \quad (3.147)$$

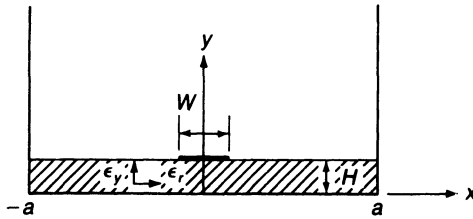
When  $y = H$  the corresponding value of  $u$  is  $(\epsilon_r/\epsilon_y)^{1/2}H$ ; so the solution of (3.147) is that for a microstrip with an equivalent substrate thickness  $H_e$  given by  $(\epsilon_r/\epsilon_y)^{1/2}H = H_e$ . The boundary condition (3.145e) becomes

$$\left. \frac{\partial \Phi^0}{\partial y} \right|_{H^+} - \epsilon_y \sqrt{\frac{\epsilon_r}{\epsilon_y}} \left. \frac{\partial \Phi^0}{\partial u} \right|_{H_e^-} = \left. \frac{\partial \Phi^0}{\partial y} \right|_{H^+} - \sqrt{\epsilon_r \epsilon_y} \left. \frac{\partial \Phi^0}{\partial u} \right|_{H_e^-} = -\frac{\rho_s}{\epsilon_0} \quad (3.148)$$

which shows that the equivalent dielectric constant of the substrate should be taken as the geometric mean  $\epsilon_g = \sqrt{\epsilon_r \epsilon_y}$ . Thus, by modifying the substrate thickness and introducing the equivalent dielectric constant, the solution for the distributed capacitance  $C$  for the case of an anisotropic substrate can be reduced to that for an isotropic substrate. The distributed capacitance  $C_a$  is that for the unscaled microstrip line.

The unit of length does not enter directly into the differential equations for the potentials. Thus  $x$  and  $y$  can be in units of meters, centimeters, inches, or any other convenient unit. What this means is that the distributed capacitance and inductance per unit length is dependent only on the ratio of strip width to substrate thickness, i.e., on  $W/H$ . If we have found  $C$  and  $L$  for a given set of values for  $W$  and  $H$  on a per-meter basis, then if we change  $W$  to  $sW$  and  $H$  to  $sH$ , where  $s$  is a scaling factor, both  $C$  and  $L$  on a per-meter basis do not change. Hence the characteristic impedance, effective dielectric constant, and propagation constant  $\beta$  for any planar transmission line is invariant to a scaling of the cross-sectional dimensions. However, the attenuation caused by conductor loss does not scale since the series resistance is inversely proportional to the conductor widths. The attenuation due to conductor losses will double if the conductor size is reduced by a factor of 2. The scaling law is clearly illustrated for an ideal parallel-plate capacitor with a plate dimension of  $Wl$  and separation  $H$  and having a capacitance  $\epsilon_0 Wl/H$ . Clearly keeping the ratio  $W/H$  fixed keeps the capacitance unchanged.

A variety of methods exist for solving the two-dimensional Laplace equation (3.147). For planar transmission lines the conformal mapping method is widely used, generally along with some approximations that are necessary because of not having a dielectric medium filling all of the space


**FIGURE 3.22**

A microstrip line with perfectly conducting side walls inserted at  $x = \pm a$  with  $a \gg W$ .

around the conductors. A number of useful solutions obtained by conformal mapping methods are described in App. III. We will refer to some of these solutions as needed.

In order to illustrate the general method of solution, we will develop a Fourier series solution to (3.145) which will turn out to provide an efficient method to obtain the parameters of a microstrip transmission line. In order to use the Fourier series method, we place perfectly conducting (electric) walls at  $x = \pm a$  as shown in Fig. 3.22. Provided  $a$  is chosen equal to  $10W$  or  $10H$ , whichever is larger, the sidewalls have a negligible effect on the field which is concentrated near the microstrip.

We can expand the unknown charge density  $\rho_s$  into a Fourier series of the form

$$\rho_s(x) = \sum_{n=1,3,\dots}^{\infty} \rho_n \cos \frac{n\pi x}{2a} \quad (3.149a)$$

The charge coefficients  $\rho_n$  are given by

$$\rho_n = \frac{1}{a} \int_{-W/2}^{W/2} \rho_s(x') \cos \frac{n\pi x'}{2a} dx' \quad (3.149b)$$

The charge density is an even function of  $x$  because of the symmetry involved; so only a cosine series is needed. The functions are chosen so that they vanish at  $x = \pm a$ , a required boundary condition for the potential; so only odd integers  $n$  are used.

The potential  $\Phi(x, y)$  can also be expanded into Fourier series; so we let

$$\begin{aligned} \Phi(x, y) &= \sum_{n=1,3,\dots}^{\infty} f_n(y) \cos \frac{n\pi x}{2a} & y \geq H \\ &= \sum_{n=1,3,\dots}^{\infty} g_n(y) \cos \frac{n\pi x}{2a} & 0 \leq y \leq H_e \end{aligned} \quad (3.150)$$

where  $f_n(y)$  and  $g_n(y)$  are to be found. We are using an effective substrate thickness  $H_e$ , so that an anisotropic substrate can be accommodated. We have dropped the superscript 0 since it is understood from the context that we are solving for a static potential field.



Each Fourier term in the expansion of  $\Phi$  must be a solution of Laplace's equation. Hence we require that

$$\left( \frac{\partial^2}{\partial x^2} + \frac{\partial^2}{\partial y^2} \right) \begin{pmatrix} f_n(y) \\ g_n(y) \end{pmatrix} \cos \frac{n\pi x}{2a} = 0$$

which gives

$$\frac{d^2 f_n(y)}{dy^2} - w_n^2 f_n(y) = 0$$

$$\frac{d^2 g_n(y)}{dy^2} - w_n^2 g_n(y) = 0$$

where  $w_n^2 = (n\pi/2a)^2$ . In the region  $y \leq H_e$ , a suitable solution for  $g_n(y)$  that vanishes on the ground plane is

$$g_n(y) = C_n \sinh w_n y$$

where  $C_n$  is an unknown constant. In the region  $y \geq H$ , we need a solution that will vanish as  $y$  approaches infinity; so we choose

$$f_n(y) = D_n e^{-w_n y}$$

where  $D_n$  is another unknown constant. At  $y = H_e$ ,  $H$  the two potential functions must match; so we have

$$C_n \sinh w_n H_e = D_n e^{-w_n H}$$

The Fourier series expansion of the charge density  $\rho_s$  represents this charge density as sheets of charge  $\rho_n \cos n\pi x/2a$  that extend from  $x = -a$  to  $x = a$ . By superimposing an infinite number of such charge sheets, we obtain a charge density  $\rho_s$  that is nonzero only on the microstrip  $-W/2 \leq x \leq W/2$ . The boundary condition (3.148) is applied to each Fourier term to obtain

$$\left( \left. \frac{df_n}{dy} \right|_H - \epsilon_g \left. \frac{dg_n}{dy} \right|_{H_e} \right) = -\frac{\rho_n}{\epsilon_0}$$

$$\text{or} \quad -w_n D_n e^{-w_n H} - \epsilon_g w_n C_n \cosh w_n H_e = -\frac{\rho_n}{\epsilon_0}$$

We now have two equations which we can solve to find  $C_n$  and  $D_n$ . The solutions are

$$C_n = \frac{\rho_n}{\epsilon_0 w_n (\sinh w_n H_e + \epsilon_g \cosh w_n H_e)}$$

$$D_n = \frac{\rho_n e^{w_n H} \sinh w_n H_e}{\epsilon_0 w_n (\sinh w_n H_e + \epsilon_g \cosh w_n H_e)}$$

where  $\epsilon_g = \sqrt{\epsilon_r \epsilon_y}$ .

We now substitute our solutions for  $f_n$  and  $g_n$  into (3.150) and use (3.149b) for  $\rho_n$ . Thus we obtain

$$\Phi(x, y) = \sum_{n=1, 3, \dots}^{\infty} \int_{-W/2}^{W/2} \frac{\cos w_n x \cos w_n x'}{-W/2 \epsilon_0 w_n a (\sinh w_n H_e + \epsilon_g \cosh w_n H_e)} \times \left\{ \begin{array}{l} \sinh w_n y \\ \sinh w_n H_e e^{-w_n(y-H)} \end{array} \right\} \rho_s(x') dx' \quad (3.151)$$

where the upper term is for  $y \leq H_e$  and the lower one is for  $y \geq H$ . The factor multiplying  $\rho_s(x')$  under the integral sign represents the Green's function for this problem. It is designated by the symbol  $G(x, y; x', y')$ ; so in abbreviated form we express (3.151) as

$$\Phi(x, y) = \int_{-W/2}^{W/2} G(x, y; x', H_e) \rho_s(x') dx' \quad (3.152)$$

The last boundary condition to be imposed is the requirement that  $\Phi = V$  on the microstrip; thus

$$V = \int_{-W/2}^{W/2} G(x, H_e; x', H_e) \rho_s(x') dx' \quad -\frac{W}{2} \leq x \leq \frac{W}{2} \quad (3.153)$$

This is an integral equation whose solution would determine the unknown charge density  $\rho_s(x')$ . Once we know the charge density, we can calculate the total charge on the microstrip using

$$Q = \int_{-W/2}^{W/2} \rho_s(x') dx'$$

and find  $C = Q/V$ .

Integral equations are most often not solvable by analytic means. However, various numerical schemes exist for obtaining good approximate solutions. The most popular method is the *Method of Moments*.<sup>†</sup> In this method the first step is to choose a finite number of basis functions and to expand  $\rho_s(x')$  in terms of these in the form

$$\rho_s(x') = \sum_{n=1}^N Q_n \psi_n(x') \quad -\frac{W}{2} \leq x' \leq \frac{W}{2}$$

where  $Q_n$  are unknown coefficients. The basis functions could be the unit height pulse functions shown in Fig. 3.23, the cosine functions  $\cos 2n\pi x/W$ , or any other reasonable set that would give a good approximation to  $\rho_s(x')$ .

<sup>†</sup>R. F. Harrington, "Field Computation by Moment Methods," Krieger Publishing Company, Inc., Malabar, Fla., 1968.

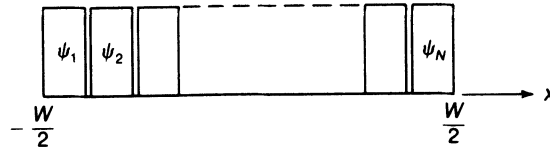


FIGURE 3.23

Unit height pulse functions for expanding the charge density.

When this substitution is made in (3.153), we obtain

$$V = \sum_{n=1}^N Q_n G_n(x) \quad -\frac{W}{2} \leq x \leq \frac{W}{2} \quad (3.154)$$

where

$$G_n(x) = \int_{-W/2}^{W/2} G(x, H_e; x', H_e) \psi_n(x') dx'$$

The next step is to convert (3.154) into a matrix equation for the unknowns either by making both sides of the equation equal at  $N$  points in  $x$  along the microstrip, or by using weighting functions to make  $N$  weighted averages of both sides equal. We can choose the  $\psi_m(x)$  as weighting functions, in which case the method is called Galerkin's method. Other choices for the weighting functions can also be made. If we use Galerkin's method, we obtain

$$\sum_{n=1}^N G_{nm} Q_n = V_m \quad m = 1, 2, \dots, N \quad (3.155)$$

where the matrix elements are given by

$$\begin{aligned} G_{nm} &= \int_{-W/2}^{W/2} G_n(x) \psi_m(x) dx \\ &= \iint_{-W/2}^{W/2} G(x, x') \psi_n(x) \psi_m(x') dx dx' \end{aligned}$$

and the components  $V_m$  of the source vector are given by

$$V_m = \int_{-W/2}^{W/2} V \psi_m(x) dx \quad m = 1, 2, \dots, N$$

The system of linear equations given in (3.155) can be solved for the unknown charge amplitude coefficients  $Q_n$ . If  $N$  is chosen sufficiently large, we will obtain a good approximation for the charge density.

If we know a priori how  $\rho_s(x')$  is distributed on the strip, or a close approximation to it, we could get an excellent approximate solution using very few basis functions. From conformal mapping solutions we know that on an isolated infinitely long conducting strip of width  $W$  and with total

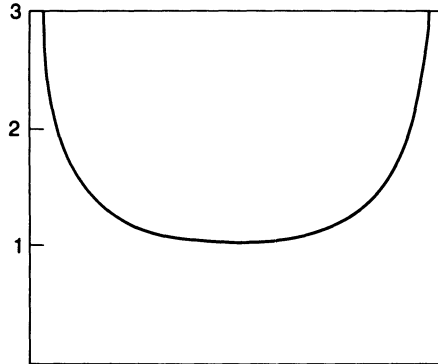


**FIGURE 3.24**  
Charge density on an ideal isolated strip of width  $W$ .

charge  $Q$  per meter that the charge density is given by

$$\rho_s(x) = \frac{2Q}{\pi W \sqrt{1 - x^2/(W/2)^2}} \quad (3.156)$$

This charge distribution is illustrated in Fig. 3.24. At sharp corners and edges the charge density always exhibits an infinite behavior. However, the density is never so singular that it cannot be integrated. The reader can readily verify that if the substitution  $x = (W/2)\sin \theta$ ,  $dx = (W/2)\cos \theta d\theta$  is made, then

$$\int_{-W/2}^{W/2} \rho_s(x) dx' = \frac{Q}{\pi} \int_{-\pi/2}^{\pi/2} d\theta = Q$$

In a microstrip line the charge density is influenced by the dielectric substrate and the ground plane but surprisingly (3.156) remains a good approximation. By using a two- or three-term polynomial along with (3.156), i.e., choosing

$$\rho_s(x) = \frac{Q_0 + Q_1x^2 + Q_2x^4}{\sqrt{1 - x^2/(W/2)^2}} \quad (3.157)$$

an excellent approximate solution for  $\rho_s(x)$  will be obtained.

We do not plan to solve the integral equation (3.153) numerically using the Method of Moments. It does require considerable numerical computation to evaluate the matrix elements because we only have the Green's function expressed as an infinite Fourier series. What we are going to do is to express the integral equation in a form that we can interpret as representing the capacitances between a conducting strip *in air* above a ground plane with spacings  $H_e$ ,  $2H_e$ ,  $3H_e$ , etc. We can then make use of the conformal mapping solution for a pair of strips in air to evaluate the distributed capacitance  $C$  for the microstrip line.

Let us choose  $\epsilon_g = 1$  but still retain the strip spacing above the ground plane as  $H_e$ . By using (3.151) in the integral equation (3.153) for this case, we obtain (note that  $\sinh w_n H_e + \cosh w_n H_e = e^{w_n H_e}$ )

$$Q \int_{-W/2}^{W/2} \sum_{n=1,3,\dots}^{\infty} \frac{\cos w_n x \cos w_n x'}{4\epsilon_0 w_n a} (1 - e^{-2w_n H_e}) \frac{\rho_s(x')}{Q} dx' = V \quad (3.158)$$

where we have set  $y = H_e$  and multiplied and divided by the total charge  $Q$ . The part multiplied by  $-e^{-2w_n H_e}$  represents the effect of the ground plane which is equivalent to that of the image strip at  $y = -H_e$  and having a charge density  $-\rho_s$ . A solution of (3.158) provides the solution for the problem of a strip above a ground plane, as well as the solution to the problem of two parallel strips in air and separated by a distance  $2H_e$ . The capacitance per meter for a strip above a ground plane is given by

$$C_a(H_e) = \frac{Q}{V}$$

while that between two strips separated by a distance  $2H_e$  is

$$\frac{Q}{2V} = \frac{C_a(H_e)}{2} = C_a(2H_e)$$

We see that the integral, involving the normalized charge density, represents  $1/C_a(H_e)$ .

Consider now the factor

$$\frac{\sinh w_n H_e}{\sinh w_n H_e + \epsilon_g \cosh w_n H_e}$$

that occurs in the Green's function in (3.151) at  $y = H_e$ . We can express this term in the form

$$\begin{aligned} \frac{e^{w_n H_e} - e^{-w_n H_e}}{(1 + \epsilon_g)e^{w_n H_e} - (1 - \epsilon_g)e^{-w_n H_e}} &= \frac{1 - e^{-2w_n H_e}}{(1 + \epsilon_g) \left( 1 - \frac{1 - \epsilon_g}{1 + \epsilon_g} e^{-2w_n H_e} \right)} \\ &= \frac{1}{1 + \epsilon_g} (1 - e^{-2w_n H_e}) (1 - \eta e^{-2w_n H_e})^{-1} \end{aligned}$$

where  $\eta = (1 - \epsilon_g)/(1 + \epsilon_g)$ . The last factor is now expanded into a power

series to obtain

$$\begin{aligned} & \frac{1}{1 + \epsilon_g} (1 - e^{-2w_n H_e}) \sum_{m=0}^{\infty} \eta^m e^{-2m w_n H_e} \\ &= \frac{1}{1 + \epsilon_g} \left( \sum_{m=0}^{\infty} \eta^m e^{-2m w_n H_e} - \sum_{m=0}^{\infty} \eta^m e^{-2(m+1)w_n H_e} \right) \end{aligned}$$

We now add  $-\eta^m$  to both series which has no net effect because of the minus sign in front of the second series. This gives

$$\frac{1}{1 + \epsilon_g} \left[ - \sum_{m=0}^{\infty} \eta^m (1 - e^{-2m w_n H_e}) + \sum_{m=0}^{\infty} \eta^m (1 - e^{-2(m+1)w_n H_e}) \right]$$

The  $m = 0$  term is zero in the first series so we can change  $m$  to  $m + 1$  and still sum this for  $m = 0, 1, 2, 3, \dots$  without changing its value; thus we get

$$\begin{aligned} & \frac{1}{1 + \epsilon_g} \left[ - \sum_{m=0}^{\infty} \eta^{m+1} (1 - e^{-2(m+1)w_n H_e}) + \sum_{m=0}^{\infty} \eta^m (1 - e^{-2(m+1)w_n H_e}) \right] \\ &= - \frac{1}{1 + \epsilon_g} (\eta - 1) \sum_{m=0}^{\infty} \eta^m (1 - e^{-2(m+1)w_n H_e}) \\ &= \frac{2\epsilon_g}{(1 + \epsilon_g)^2} \sum_{m=0}^{\infty} \eta^m (1 - e^{-2(m+1)w_n H_e}) \end{aligned} \quad (3.159)$$

Upon using this expansion in the Green's function, the integral equation (3.153) can be expressed in the form

$$\begin{aligned} & \sum_{m=0}^{\infty} \frac{4\epsilon_g}{(1 + \epsilon_g)^2} \eta^m Q \int_{-W/2}^{W/2} \sum_{n=1,3,\dots} \frac{\cos w_n x \cos w_n x'}{4\epsilon_0 w_n a} \\ & (1 - e^{-2(m+1)w_n H_e}) \frac{\rho_s(x')}{Q} dx' = V \end{aligned} \quad (3.160)$$

We note that the  $m$ th term considered by itself is an integral equation of the same form as that in (3.158) apart from the multiplying factor  $4\epsilon_g \eta^m / (1 + \epsilon_g)^2$ . This integral equation would provide a solution for the capacitance of a strip in air spaced a distance  $(m + 1)H_e$  above the ground plane. If we assumed that the normalized charge density  $\rho_s(x')/Q$  was the same for any strip, independent of the spacing above the ground plane, each integral would produce a constant voltage  $V_m$  but different from  $V$ . With increased strip spacing and constant total charge on each strip, the integral has to give a larger voltage since  $Q = C_a[(m + 1)H_e]V_m$  and  $C_a[(m + 1)H_e]$ , the capacitance between the strip and the ground plane, decreases with increasing  $m$ . The approximation that the charge density is the same independent of strip-ground-plane spacing is a necessary one to make since there is only one charge density expression in the integral equation. The

approximation is a good one and by using it we can express (3.160) in the form

$$\sum_{m=0}^{\infty} \frac{4\epsilon_g}{(1 + \epsilon_g)^2} \eta^m \frac{Q}{C_a[(m+1)H_e]} = V \quad (3.161)$$

since by our assumption

$$\begin{aligned} Q \int_{-W/2}^{W/2} \sum_{n=1,3,\dots}^{\infty} \frac{\cos w_n x \cos w_n x'}{4\epsilon_0 w_n a} (1 - e^{-2(m+1)H_e}) \\ \frac{\rho_s(x')}{Q} dx' = V_m = \frac{Q}{C_a[(m+1)H_e]} \end{aligned}$$

From (3.161) we now obtain the following solution for the distributed capacitance  $C = Q/V$ :

$$C = \frac{\left[ (1 + \epsilon_g)^2 / 4\epsilon_g \right] C_a(H_e)}{1 + C_a(H_e) \sum_{m=1}^M \eta^m \frac{1}{C_a[(m+1)H_e]}} \quad (3.162)$$

where  $M$  is the number of terms that are kept. Since  $\eta$  is negative the series is an alternating one. Typically, from 10 to 40 terms are needed for good accuracy. The evaluation can be done on a computer very quickly and requires only a simple program to implement. However, we do require an expression for the capacitance between a strip in air as a function of the spacing above the ground plane, which is given below.

The exact solution for the capacitance between a strip of width  $2W$  and a distance  $H$  above a ground plane is given in App. III, along with tabulated values as a function of  $2W/H$ . For practical applications it is desirable to have simple formulas that will enable the capacitance to be evaluated with an accuracy of 1 percent or better. A number of investigators have proposed such formulas which are based on approximate analytic solutions, along with empirical adjustment of various numerical constants so as to achieve the desired accuracy.† The following formulas give excellent results for the

†H. A. Wheeler, Transmission Line Properties of a Strip on a Dielectric Sheet on a Plane, *IEEE Trans.*, vol. MTT-25, pp. 631–647, August, 1977.

E. O. Hammerstad, Accurate Models for Microstrip Computer-Aided Design, *IEEE MTT-S Int. Microwave Symp. Dig.*, pp. 407–409, 1980.

E. O. Hammerstad, Equations for Microstrip Circuit Design, *Proc. European Micro. Conf., Hamburg, W. Germany*, pp. 268–272, September, 1975. Equations (3.163) and (3.166) come from this publication.

S. Y. Poh, W. C. Chew, and J. A. Kong, Approximate Formulas for Line Capacitance and Characteristic Impedance of Microstrip Line, *IEEE Trans.*, vol. MTT-29, pp. 135–142, February, 1981.

capacitance per meter of a strip of width  $W$  at a height  $H$  above a ground plane and with air dielectric:

$$C_a = \frac{2\pi\epsilon_0}{\ln\left(\frac{8H}{W} + \frac{W}{4H}\right)} \quad \frac{W}{H} \leq 1 \quad (3.163a)$$

$$C_a = \epsilon_0 \left[ \frac{W}{H} + 1.393 + 0.667 \ln\left(\frac{W}{H} + 1.444\right) \right] \quad \frac{W}{H} > 1 \quad (3.163b)$$

These formulas give results that agree with those tabulated in App. III to within 1/4 percent.

The effect of finite thickness  $T$  for the microstrip on the distributed capacitance is normally negligible. If necessary the effect of finite thickness can be included by using an effective width  $W_e$ , where  $W_e$  is given by the following expressions due to Gunston and Weale:†

$$\begin{aligned} W_e &= W + 0.398T \left( 1 + \ln \frac{4\pi W}{T} \right) & \frac{W}{H} &\leq \frac{1}{2\pi} \\ &= W + 0.398T \left( 1 + \ln \frac{2H}{T} \right) & \frac{W}{H} &> \frac{1}{2\pi} \end{aligned}$$

The above expressions can be used in (3.162) to evaluate the capacitance  $C$  for a microstrip line with an isotropic or anisotropic dielectric substrate. The effective dielectric constant  $\epsilon_e$  for a microstrip line is given by

$$\epsilon_e = \frac{C}{C_a} \quad (3.164)$$

where  $C_a$  is the capacitance of the unscaled air-filled line. The characteristic impedance is given by

$$Z_c = \sqrt{\frac{L}{C}} = \frac{\sqrt{\epsilon_e} \sqrt{\mu_0 \epsilon_0}}{C} = \sqrt{\frac{\mu_0 \epsilon_0}{\epsilon_e}} \frac{1}{C_a} \quad (3.165)$$

Even though computations based on (3.162) are straightforward, there is an easier way to find  $\epsilon_e$ . Schneider has presented a remarkably simple formula for the effective dielectric constant of a microstrip line with an isotropic substrate.‡ This formula was modified by Hammerstad to improve

†M. A. R. Gunston and J. R. Weale, Variation of Microstrip Impedance with Strip Thickness, *Electron. Lett.*, vol. 5, p. 697, 1969.

‡M. V. Schneider, Microstrip Lines for Microwave Integrated Circuits, *Bell System Tech. J.*, vol. 48, pp. 1422–1444, 1969. Schneider's formula has a numerical coefficient of 10 instead of 12 multiplying the  $H/W$  term.



the accuracy.† The modified formula, which we will refer to as the S-H formula, is

$$\epsilon_e = \frac{\epsilon_r + 1}{2} + \frac{\epsilon_r - 1}{2} \left( 1 + \frac{12H}{W} \right)^{-1/2} + F(\epsilon_r, H) - 0.217(\epsilon_r - 1) \frac{T}{\sqrt{WH}} \quad (3.166)$$

where  $F(\epsilon_r, H) = 0.02(\epsilon_r - 1)(1 - W/H)^2$  for  $W/H < 1$  and equals zero for  $W/H > 1$ . The last term accounts for the reduction in  $\epsilon_e$  caused by the finite thickness of the microstrip. We have checked the accuracy of this formula against the results obtained by solving the integral equation and found the agreement to be better than 1 percent for  $0.25 \leq W/H \leq 6$  and  $1 < \epsilon_r \leq 16$ . We can also adapt the S-H formula to treat the case of an anisotropic substrate as follows: For an anisotropic substrate we replace the spacing parameter  $H$  by the effective spacing  $H_e$  given by

$$H_e = \sqrt{\frac{\epsilon_r}{\epsilon_y}} H$$

and use the geometric mean  $\epsilon_g = \sqrt{\epsilon_r \epsilon_y}$  for the dielectric constant  $\epsilon_r$ . The S-H formula gives the capacitance of a microstrip line with spacing  $H_e$  and dielectric constant  $\epsilon_g$  relative to an air-filled line with the same spacing  $H_e$ ; thus

$$\frac{C(\epsilon_g, H_e)}{C_a(H_e)} = \frac{\epsilon_g + 1}{2} + \frac{\epsilon_g - 1}{2} \left( 1 + 12 \frac{H_e}{W} \right)^{-1/2} + F(\epsilon_g, H_e)$$

The effective dielectric constant is, however, given by the ratio of  $C(\epsilon_g, H_e)$  to the capacitance of the air-filled line according to (3.164). Hence, for the case of an anisotropic substrate, we have

$$\epsilon_e = \left[ \frac{\epsilon_g + 1}{2} + \frac{\epsilon_g - 1}{2} \left( 1 + 12 \frac{H_e}{W} \right)^{-1/2} + F(\epsilon_g, H_e) \right] \frac{C_a(H_e)}{C_a(H)} \quad (3.167)$$

The capacitances for the air-filled lines are readily computed using (3.163).

For comparison purposes, typical results obtained for  $\epsilon_e$  using (3.162), formulas (3.166) or (3.167), and those obtained by solving the integral equation are given in Table 3.3. Also listed are the number of terms needed in the formula (3.162) to give a numerical convergence of 0.3 percent. Overall, all three methods give values for  $\epsilon_e$  that are in close agreement. Equation (3.162) gives values that are on the high side for wide strips and substrates with large dielectric constants. This is caused by the variation in charge density with strip spacing above the ground plane, which is more

---

†E. O. Hammerstad, *loc. cit.* (1975 paper).

**TABLE 3.3**  
**Comparison of values for effective dielectric constant using**  
**different formulas**

$W/H$	Integral equation		Integral equation			
	Eq. (3.162)	Eq. (3.166)	Eq. (3.162)	Eq. (3.162)	Eq. (3.166)	Eq. (3.166)
	$\epsilon_r = 2$		$\epsilon_r = 5.12, \epsilon_y = 3.4\dagger$			
0.25	1.588	1.589 (7)‡	1.583	2.671	2.675 (15)	2.69
0.5	1.61	1.612 (7)	1.605	2.694	2.698 (15)	2.721
1	1.645	1.649 (7)	1.639	2.731	2.734 (15)	2.731
2	1.696	1.699 (7)	1.689	2.797	2.802 (16)	2.794
4	1.762	1.761 (8)	1.75	2.906	2.929 (16)	2.890
6	1.801	1.799 (8)	1.789	2.979	2.944 (16)	2.963
	$\epsilon_r = 6$		$\epsilon_r = 10$			
0.25	3.896	3.896 (22)	3.913	6.195	6.192 (36)	6.244
0.5	4.003	4.004 (22)	4.025	6.387	6.40 (37)	6.445
1	4.173	4.169 (22)	4.193	6.69	6.70 (37)	6.748
2	4.428	4.447 (23)	4.444	7.15	7.16 (38)	7.201
4	4.763	4.837 (23)	4.75	7.757	7.946 (39)	7.750
6	4.966	5.012 (23)	4.943	8.127	8.303 (40)	8.098

†Boron nitride.

‡The numbers in parentheses are the number of terms used in the numerical solution.

pronounced for wide strips. From the tabulated results it can be inferred that the modified Schneider's formula will be acceptable for most applications since even the dielectric constant of the substrate is often not known to an accuracy much better than 1 percent. The following two examples will illustrate the application of the above formulas to microstrip lines.

**Example 3.4.** A microstrip line uses a substrate with dielectric constant  $\epsilon_r = 9.7$  (alumina) and thickness 0.5 mm. The strip width is also 0.5 mm. We wish to find the effective dielectric constant, the characteristic impedance, and the microstrip wavelength at a frequency of 2 GHz.

Since the substrate is isotropic, we use (3.166) to find  $\epsilon_e$ . Thus since  $W/H = 1$ ,

$$\epsilon_e = \frac{10.7}{2} + \frac{8.7}{2} (1 + 12)^{-1/2} = 6.556$$

In order to evaluate  $Z_c$  using (3.165), we first find  $C_a$  using (3.163). Thus

$$\frac{C_a}{\epsilon_0} = \frac{2\pi}{\ln(8 + \frac{1}{4})} = 2.978$$

From (3.165) we get

$$Z_c = \frac{Z_0}{2.978\sqrt{\epsilon_e}} = \frac{120\pi}{2.978\sqrt{6.556}} = 49.44 \Omega$$

At 2 GHz the propagation constant is  $\beta = \sqrt{\epsilon_e} 2\pi/\lambda_0 = 1.0725 \text{ rad/cm}$ . Hence  $\lambda = 2\pi/\beta = 5.858 \text{ cm}$ . The wavelength can also be found using  $\lambda = \lambda_0/\sqrt{\epsilon_e}$ .

**Example 3.5.** A microstrip line uses a sapphire substrate 1 mm thick and having  $\epsilon_r = 9.4$ ,  $\epsilon_y = 11.6$ . We want to find the effective dielectric constant and characteristic impedance for the case when the strip is 0.5 mm wide.

Since this substrate is anisotropic, we first find  $\epsilon_g = \sqrt{\epsilon_r \epsilon_y} = 10.44$  and  $H_e = \sqrt{\epsilon_r/\epsilon_y} H = 0.9 \text{ mm}$ . We now use (3.167) to find  $\epsilon_e$ . By using (3.163a) we get the ratio

$$\frac{C_a(H_e)}{C_a(H)} = \frac{2.347}{2.26} = 1.0385$$

From (3.167)

$$\begin{aligned} \epsilon_e &= 1.0385 \left[ \frac{11.44}{2} + \frac{9.44}{2} \left( 1 + 12 \frac{0.9}{0.5} \right)^{-1/2} + 0.02 \times 9.44 \times \frac{1}{4} \right] \\ &= 7.02 \end{aligned}$$

From (3.163a) we get  $C_a(H) = 2.26\epsilon_0$  and using (3.165) gives

$$Z_c = \frac{120\pi}{2.26\sqrt{7.02}} = 62.96 \Omega$$

## Microstrip Attenuation

Dielectric losses and conductor losses will introduce attenuation. The attenuation caused by the finite conductivity of the conductors is accounted for by the series resistance  $R$ , while attenuation caused by dielectric loss is modeled by the shunt conductance  $G$  in the distributed circuit model of the microstrip line. The separate attenuation constants are given by

$$\alpha_c = \frac{R}{2Z_c} \quad (3.168a)$$

$$\alpha_d = \frac{G}{2Y_c} \quad (3.168b)$$

and the total attenuation is given by

$$\alpha = \alpha_c + \alpha_d \quad (3.168c)$$

The attenuation in decibels per unit length is obtained by multiplying  $\alpha$  by 8.686.

We will first examine the attenuation caused by dielectric loss. The dielectric loss arises when the permittivity  $\epsilon$  is complex, that is,  $\epsilon = \epsilon' - j\epsilon''$ . The loss tangent

$$\tan \delta_l = \frac{\epsilon''}{\epsilon'} \approx \delta_l$$

is the usual given parameter for a dielectric material. Maxwell's equation

$$\nabla \times \mathbf{H} = j\omega\epsilon\mathbf{E} + \sigma\mathbf{E} = j\omega\epsilon'\mathbf{E} + (\omega\epsilon'' + \sigma)\mathbf{E}$$

shows that  $\omega\epsilon''$  can be viewed as the effective conductivity of a lossy dielectric when the ohmic conductivity  $\sigma$  is zero. Normally we can assume that  $\sigma = 0$  except for a semiconductor substrate, in which case  $\sigma$  will depend on the doping level.

The electric energy stored in the substrate region of the microstrip line is given by

$$W_{e1} = \frac{\epsilon'}{4} \int_{V_1} \mathbf{E} \cdot \mathbf{E}^* dV$$

where  $V_1$  is the volume of the substrate region per unit length of line. The power loss due to dielectric loss is given by

$$P_l = \frac{\omega\epsilon''}{2} \int_{V_1} \mathbf{E} \cdot \mathbf{E}^* dV$$

Thus we see that

$$\frac{P_l}{W_{e1}} = \frac{2\omega\epsilon''}{\epsilon'}$$

If the dielectric filled all of the space around the microstrip, we could equate  $W_{e1}$  to  $CV^2/4$  and  $P_l$  to  $GV^2/2$  and thereby obtain

$$G = \frac{\omega\epsilon''}{\epsilon'} C$$

However, for a partially filled line some of the electric energy is located in the air region that occupies a volume we will call  $V_2$ . Consequently, we have

$$W_{e1} + W_{e2} = \frac{\epsilon'}{4} \int_{V_1} \mathbf{E} \cdot \mathbf{E}^* dV + \frac{\epsilon_0}{4} \int_{V_2} \mathbf{E} \cdot \mathbf{E}^* dV = \frac{CV^2}{4}$$

If we had an air-filled line, we could write

$$W_{e1} + W_{e2} = \frac{\epsilon_0}{4} \int_{V_1} \mathbf{E} \cdot \mathbf{E}^* dV + \frac{\epsilon_0}{4} \int_{V_2} \mathbf{E} \cdot \mathbf{E}^* dV = \frac{C_a V^2}{4}$$

with the understanding that the electric field in the two cases will not be the same. There is no simple exact way to determine how the electric energy is split between the two regions. There is, however, an approximate method to find the division of the total energy between the two regions and this is based on the assumption that the volume integrals of  $\mathbf{E} \cdot \mathbf{E}^*$  in the two cases are approximately the same. By making this assumption we can write

$$\epsilon' I_1 + \epsilon_0 I_2 = CV^2$$

$$\epsilon_0 I_1 + \epsilon_0 I_2 = C_a V^2$$

where  $I_1$  and  $I_2$  represent the values of the integrals over  $V_1$  and  $V_2$ , respectively. The above two equations can be solved for  $I_1$  and  $I_2$  to give

$$I_1 = \frac{C - C_a}{\epsilon' - \epsilon_0} V^2 \quad I_2 = \frac{\epsilon'_r C_a - C}{\epsilon' - \epsilon_0} V^2$$

where  $\epsilon'_r = \epsilon'/\epsilon_0$ . The fraction of the total energy in the dielectric region is

$$\frac{\epsilon'_r I_1}{\epsilon'_r I_1 + I_2} = \frac{\epsilon'_r (C - C_a)}{(\epsilon'_r - 1)C} = \frac{\epsilon'_r \epsilon_e - 1}{\epsilon_e \epsilon'_r - 1} = q \frac{\epsilon'_r}{\epsilon_e} \quad (3.169)$$

where we have used  $C = \epsilon_e C_a$ . The parameter  $q$  is called the filling factor. If  $q$  was found independently, then we could solve for  $\epsilon_e$  to get  $\epsilon_e = \epsilon'_r q + (1 - q)$ . The parameter  $q$  is the ratio of the integral of  $\mathbf{E} \cdot \mathbf{E}^*$  over the volume  $V_1$  to the integral over the total volume  $V_1 + V_2$ , that is,  $q = I_1/(I_1 + I_2)$  and clearly represents a filling factor.

With the above assumption regarding no change in the volume integrals for the two cases, we see that  $G$ , as given earlier, should be reduced by the same fraction by which the total electric energy was split since there is essentially no loss in the air region. Hence an estimate for  $G$  is

$$G = \frac{\epsilon'_r \epsilon_e - 1}{\epsilon_e \epsilon'_r - 1} \frac{\omega \epsilon''_r}{\epsilon'_r} C \quad (3.170)$$

By using  $Z_c = \sqrt{\epsilon_e} \sqrt{\mu_0 \epsilon_0} / C$  we obtain

$$\alpha_d = \frac{G Z_c}{2} = \frac{\pi}{\lambda_0} \frac{\epsilon'_r}{\sqrt{\epsilon_e}} \frac{\epsilon_e - 1}{\epsilon'_r - 1} \tan \delta_l \quad (3.171)$$

for the attenuation constant due to dielectric loss. In the derivation we used  $\omega \sqrt{\mu_0 \epsilon_0} = k_0 = 2\pi/\lambda_0$ . As an example if  $\epsilon'_r = 9.7$ ,  $\epsilon_e = 6.55$ , and  $\tan \delta_l = 2 \times 10^{-4}$  we get  $\alpha_d = 1.52 \times 10^{-3}$  Np/wavelength. In decibel units this equals 0.013 dB/wavelength, which is a relatively small value. The attenuation caused by conductor losses will be significantly larger. Equation (3.171) is valid for isotropic substrates only.

We now turn our attention to evaluating the attenuation caused by finite conductivity of the microstrip and the ground plane. The continuity equation (3.138b) shows that the current density  $J_z$  along the conductors varies the same way as the charge density. Thus on a conducting strip of width  $W$  the current density will be similar to the charge density given by (3.156). At the edge of an infinitely thin strip, the current density will increase inversely proportional to the square root of the distance from the edge and becomes infinite at the edge. However, the density can be integrated to give a finite value for the total current. But since power-loss calculations require integrating the square of the current density, we would find that for the current density on an infinitely thin strip we would obtain infinite power loss. In practice, the conductors have a finite thickness and the current density is less singular at the edge and the power loss is finite.

Consequently, it is necessary to take into account the finite thickness of the conductors. In addition, it is necessary to determine how the total current divides between the two faces of the microstrip since the presence of a ground plane results in an unequal division of the current for strip widths greater than one-half of the spacing above the ground plane.

The current distribution, current division, and power loss can be evaluated using conformal mapping techniques. In order to obtain useful formulas, some approximations are necessary. The analysis for a microstrip line is carried out in App. III and the results obtained are repeated here (note that in App. III the strip width is  $2w$  and the thickness is  $2t$ , whereas here we use  $W$  for the width and  $T$  for the thickness). The normalized series distributed resistance for the microstrip is  $R_1$  where

$$\frac{R_1 W}{R_m} = \text{LR} \left( \frac{1}{\pi} + \frac{1}{\pi^2} \ln \frac{4\pi W}{T} \right) \quad (3.172)$$

The loss ratio LR is given by

$$\begin{aligned} \text{LR} &= 1 & \frac{W}{H} &\leq 0.5 \\ \text{LR} &= 0.94 + 0.132 \frac{W}{H} - 0.0062 \left( \frac{W}{H} \right)^2 & 0.5 < \frac{W}{H} \leq 10 \end{aligned} \quad (3.173)$$

The loss ratio gives the increase in resistance that results from an unequal division of the current. The normalized series resistance  $R_2$  of the ground plane is given by

$$W \frac{R_2}{R_m} = \frac{W/H}{W/H + 5.8 + 0.03H/W} \quad 0.1 \leq \frac{W}{H} \leq 10 \quad (3.174)$$

This formula states that the effective width of the ground plane is  $W + 5.8H$  and having uniform current density. The skin-effect resistance  $R_m$  is given by  $R_m = (\omega\mu/\sigma)^{1/2}$ . For copper with a conductivity of  $5.8 \times 10^7$  S/m, we have  $R_m = 8.22 \times 10^{-3} \sqrt{f}$   $\Omega$  where  $f$  is in gigahertz. The total series resistance is  $R_1 + R_2$  and thus upon using (3.34b) we get

$$\alpha_c = \frac{R_1 + R_2}{2Z_c} \quad (3.175)$$

for the attenuation caused by conductor losses. For the quasi-TEM mode the magnetic field, and hence the conductor losses, do not depend on the substrate material.

The equations presented above predict somewhat higher theoretical attenuation than that obtained from a formula developed by Pucel, Masse, and Hartwig using Wheeler's incremental inductance rule.† Our formulas

†R. A. Pucel, D. J. Masse, and C. P. Hartwig, Losses in Microstrip, *IEEE Trans.*, vol. MTT-16, pp. 342-350, June, 1966.

appear to be in better agreement with experimental results. For practical microstrip lines surface roughness can increase the attenuation by as much as 50 percent or more depending on the scale of surface roughness relative to the skin depth. The etching process does not produce a perfectly flat end face at the sides of the strip. Some undercutting of the edge occurs along with some roughness, which will also result in an increase of the attenuation above the theoretical values.

**Example 3.6.** We wish to find the attenuation for a microstrip line using a copper strip of width 0.5 mm, a spacing of 0.5 mm above the ground plane, an alumina substrate with  $\epsilon_r = 9.7$ , and a loss tangent of  $2 \times 10^{-4}$ . The strip thickness  $T$  is 0.02 mm. The frequency of operation is 4 GHz.

The effective dielectric constant and characteristic impedance were found in Example 3.4 and are  $\epsilon_e = 6.556$ ,  $Z_c = 49.44 \Omega$ . The wavelength of operation is 7.5 cm. The attenuation caused by dielectric loss was calculated after (3.171) was presented and is  $1.52 \times 10^{-3}$  Np/wavelength or  $2.02 \times 10^{-4}$  Np/cm.

For this microstrip line  $W/H = 1$  and  $W/T = 25$ . From (3.173) we find that the loss ratio is 1.0658 and (3.172) gives

$$\begin{aligned} R_1 &= \frac{1.0658 \times 8.22 \times 10^{-3} \sqrt{4}}{0.05} \left( \frac{1}{\pi} + \frac{1}{\pi^2} \ln 100\pi \right) \\ &= 3.157 \times 10^{-1} \Omega/\text{cm} \end{aligned}$$

By using (3.174) we obtain

$$R_2 = \frac{8.22 \times 10^{-3} \sqrt{4}}{0.05} \left[ \frac{1}{1 + 5.8 + 0.03} \right] = 4.81 \times 10^{-2} \Omega/\text{cm}$$

For this case the loss in the microstrip is a factor of 6.5 greater than that in the ground plane. The reason for this is the high current density near the edges in the microstrip as compared with a more uniform current distribution over a wider area on the ground plane. By using (3.175) we find that the attenuation due to conductor loss is

$$\alpha_c = \frac{3.157 \times 10^{-1} + 4.81 \times 10^{-2}}{2 \times 49.44} = 3.68 \times 10^{-3} \text{ Np/cm}$$

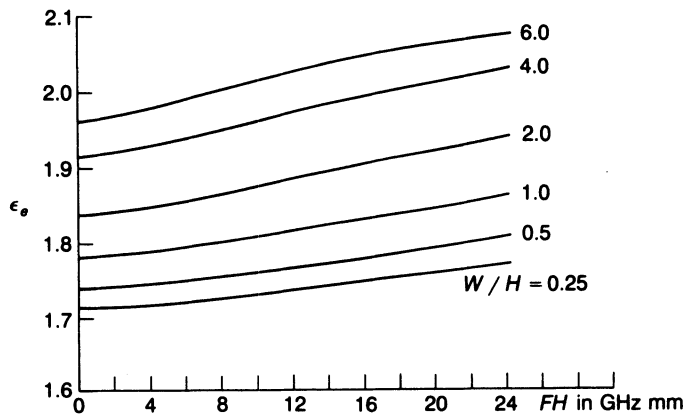
This attenuation is 18.4 times greater than that caused by dielectric loss. The total attenuation is

$$\alpha = \alpha_c + \alpha_d = 3.88 \times 10^{-3} \text{ Np/cm}$$

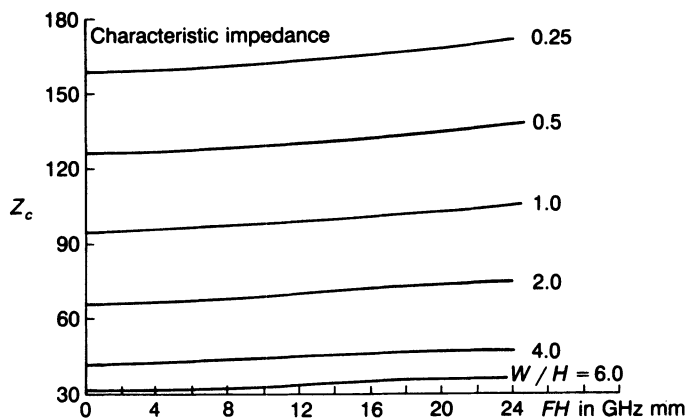
which equals 0.0337 dB/cm. Surface roughness could result in a real attenuation 15 to 25 percent higher than this at 4 GHz. In this example we neglected the correction to  $\epsilon_e$  and  $Z_c$  due to the finite thickness  $T$  since it is small.

## High-Frequency Properties of Microstrip Lines

The equations describing the quasi-TEM mode can be used with acceptable accuracy for frequencies up to 2 to 4 GHz for a substrate thickness of 1 mm. For a substrate 0.5 mm thick, the upper frequency limit would be 4 to 8 GHz. When these limits are exceeded, it is necessary to take into account the frequency dispersion of the effective dielectric constant and the change in characteristic impedance with frequency. At the higher frequencies the electric field becomes more confined to the region between the microstrip and ground plane. The greater concentration of the field in this region results in an increase in the effective dielectric constant as well as increased



(a)

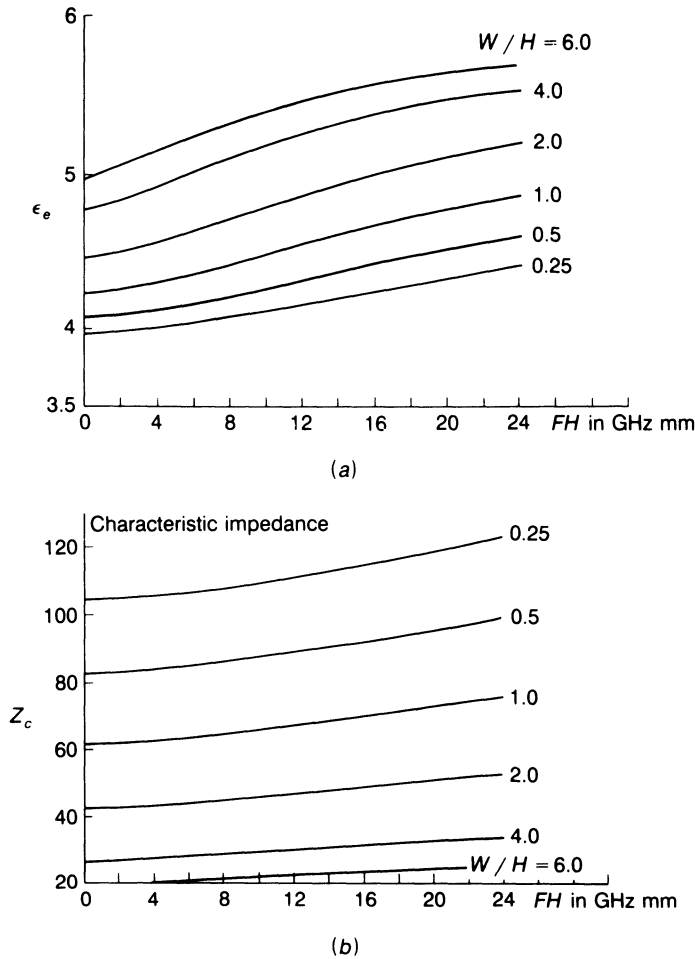


(b)

**FIGURE 3.25**

(a) Effective dielectric constant for a PTFE/microfiber glass substrate with  $\epsilon_r = 2.26$ ,  $\epsilon_y = 2.2$ ;  
 (b) characteristic impedance.

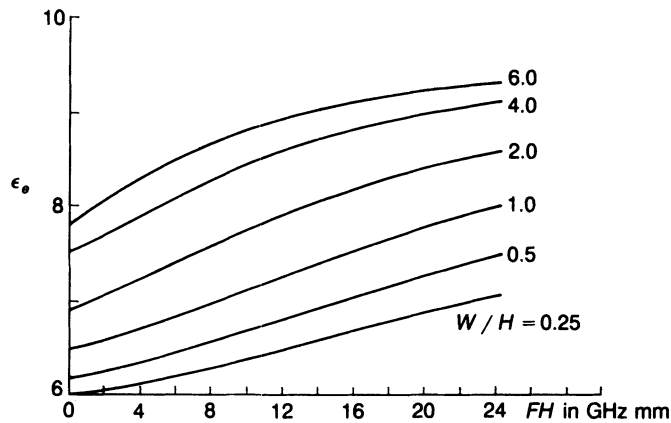


**FIGURE 3.26**

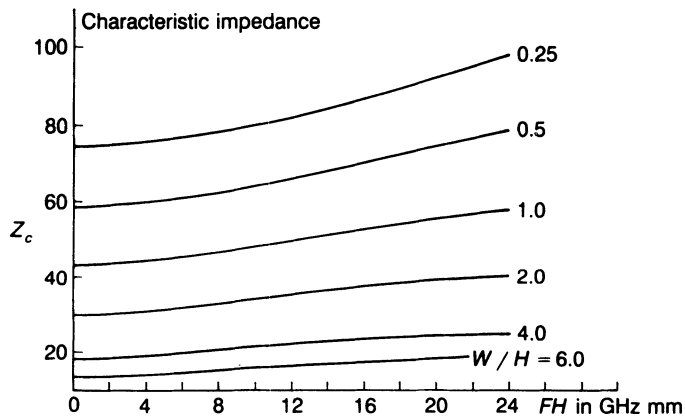
(a) Effective dielectric constant for an RT/Duroid 6006 substrate having  $\epsilon_r = 6.36$ ,  $\epsilon_y = 6$ ; (b) characteristic impedance.

attenuation because of a greater concentration of the electric field in the substrate which has some loss. The conductor loss also increases because the skin-effect resistance  $R_m$  increases and more of the current flows on the inner face of the microstrip.

In order to determine the effective dielectric constant at high frequencies, it is necessary to carry out a full wave analysis, i.e., the complete set of equations given earlier for the potentials must be solved. In Figs. 3.25 to 3.28 we show the dispersive properties for four common substrate materials, a PTFE/microfiber glass substrate with  $\epsilon_r = 2.26$ ,  $\epsilon_y = 2.2$ , RT/Duroid 6006 with  $\epsilon_r = 6.36$ ,  $\epsilon_y = 6$ , alumina with  $\epsilon_r = 9.7$ , and gallium arsenide



(a)



(b)

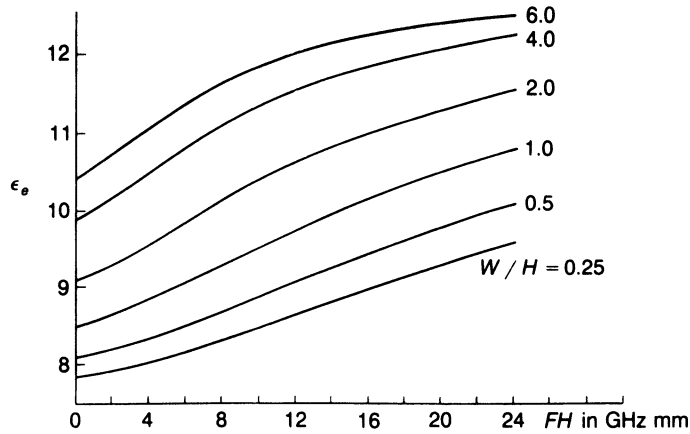
**FIGURE 3.27**

(a) Effective dielectric constant for an alumina substrate with  $\epsilon_r = 9.7$ ; (b) characteristic impedance.

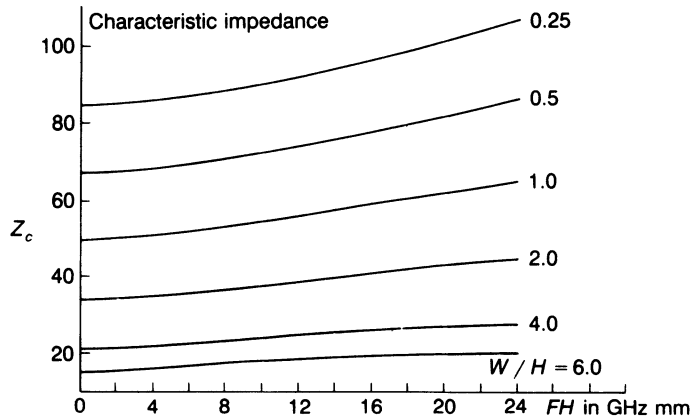
with  $\epsilon_r = 12.9$ . An examination of these figures shows that dispersion effects are more pronounced for wider strips and large dielectric constants.

Along with each figure giving the effective dielectric constant as a function of normalized frequency is a figure showing the characteristic impedance as a function of normalized frequency. The normalized frequency is the actual frequency in gigahertz multiplied by the substrate thickness in millimeters. Thus, for substrates 0.5 mm thick, the frequency range covered is 0 to 48 GHz.

When the propagating mode is not a TEM or quasi-TEM mode, there is no unique value for the characteristic impedance because it is not possible to define a unique value for the voltage as given by the line integral of the electric field between the ground plane and the microstrip. The characteris-



(a)



(b)

**FIGURE 3.28**

(a) Effective dielectric constant for gallium-arsenide substrate with  $\epsilon_r = 12.9$ ; (b) characteristic impedance.

tic impedances given in Figs. 3.25 to 3.28 are based on using the following definition for the equivalent voltage:

$$V = - \int_0^H E_y dy = \int_0^H \left( j\omega A_y + \frac{\partial \Phi}{\partial y} \right) dy$$

where the path of integration is along a straight line from the ground plane to the center of the microstrip. The current  $I$  is chosen as the total  $z$ -directed current on the microstrip and  $Z_c$  was calculated from the ratio  $V/I$ . In general, the power flow along the microstrip transmission line will not equal  $\frac{1}{2}VI$ . The characteristic impedance can be defined in terms of the power flow  $P$  by choosing either the current  $I$  or voltage  $V$  according to the

above definitions and using

$$P = \frac{I^2 Z_c}{2}$$

$$= \frac{V^2}{2Z_c}$$

to find  $Z_c$ . These two equations will give different values for the characteristic impedance with neither one being equal to  $V/I$ .

The lack of a unique value for the characteristic impedance is not a great disadvantage since microstrip junctions and discontinuities can be described by equivalent circuits using any convenient definition for the characteristic impedance. In Chap. 4 we will find that an equivalent transmission-line circuit theory can be formulated for any waveguiding system and does not require that there be a unique characteristic impedance associated with the propagating modes.

For computer-aided design (CAD) of microstrip circuits, it is important to have simple formulas that can be used to find the effective dielectric constant. Many different formulas have been proposed. The most accurate one that covers the full range of parameter values likely to be encountered was developed empirically by Kobayashi and is given below:†

$$\epsilon_e(f) = \epsilon_r - \frac{\epsilon_r - \epsilon_e(0)}{1 + (f/f_a)^m} \quad (3.176)$$

where

$$f_a = \frac{f_b}{0.75 + (0.75 - 0.332\epsilon_r^{-1.73})W/H}$$

$$f_b = \frac{47.746}{H\sqrt{\epsilon_r - \epsilon_e(0)}} \tan^{-1} \epsilon_r \sqrt{\frac{\epsilon_e(0) - 1}{\epsilon_r - \epsilon_e(0)}}$$

$$m = m_0 m_c \leq 2.32$$

$$m_0 = 1 + \frac{1}{1 + \sqrt{W/H}} + 0.32(1 + \sqrt{W/H})^{-3}$$

$$m_c = \begin{cases} 1 + \frac{1.4}{1 + W/H} (0.15 - 0.235e^{-0.45f/f_a}) & \frac{W}{H} \leq 0.7 \\ 1 & \frac{W}{H} > 0.7 \end{cases}$$

†M. Kobayashi, A Dispersion Formula Satisfying Recent Requirements in Microstrip CAD, *IEEE Trans.*, vol. MTT-36, pp. 1246–1250, August, 1988.

In these formulas  $H$  is in millimeters, the frequency  $f$  is in gigahertz, and whenever the product  $m_0 m_c$  is greater than 2.32 the parameter  $m$  is chosen equal to 2.32. The effective dielectric constant at the frequency  $f$  is  $\epsilon_e(f)$  and  $\epsilon_e(0)$  is the quasistatic value which can be found using (3.166). It requires only a simple computer program to evaluate  $\epsilon_e(f)$  using Kobayshi's formula. The accuracy is estimated to be within 0.6 percent for  $0.1 \leq W/H \leq 10$ ,  $1 \leq \epsilon_r \leq 128$  and for any value of  $H/\lambda_0$ .†

In microstrip circuit design where junctions of microstrip lines with different widths are involved, it is necessary to characterize the junction in terms of an equivalent circuit. The parameters of this equivalent circuit will depend on frequency. The equivalent characteristic impedances that are assigned to the microstrip lines are arbitrary and often are simply chosen to have normalized values of unity. Any impedance level change that occurs at the junction is incorporated as part of the equivalent circuit of the junction. For these reasons we will not quote any of the formulas that have been proposed for evaluating characteristic impedance as a function of frequency because they are of limited use in practice.

## Attenuation

Simple formulas giving the attenuation of microstrip lines at high frequencies do not exist. Equation (3.171) can be expected to give a good estimate for the attenuation due to dielectric loss provided  $\epsilon_e$  is replaced by the effective dielectric constant that applies at the frequency of interest.

A realistic evaluation of the attenuation caused by the finite conductivity of the conductors requires evaluation of the current density on the microstrip and the ground plane at the frequency of interest. In general, the current tends to be more uniform across the microstrip at high frequencies, particularly for wide strips. In Fig. 3.29 we show several computed current distributions at frequencies of 10 and 20 GHz for an alumina substrate 1 mm thick. The quasistatic current distribution is also shown. The current density has been normalized so that the total current on the microstrip equals  $W$ . In view of the tendency for the current density to become nearly uniform at high frequencies for wide strips, the attenuation constant can be estimated with fair accuracy by assuming uniform current density over a width  $W$  on both the microstrip and the ground plane. In this limit the attenuation caused by the conductor loss for wide strips that are not too thin is given by

$$\alpha_c = \frac{R_m}{WZ_c} \quad (3.177)$$

---

†The author has verified the accuracy of Kobayshi's formula by comparison with calculated numerical results for  $0.25 \leq W/H \leq 6$  and  $2 \leq \epsilon_r \leq 12$ .

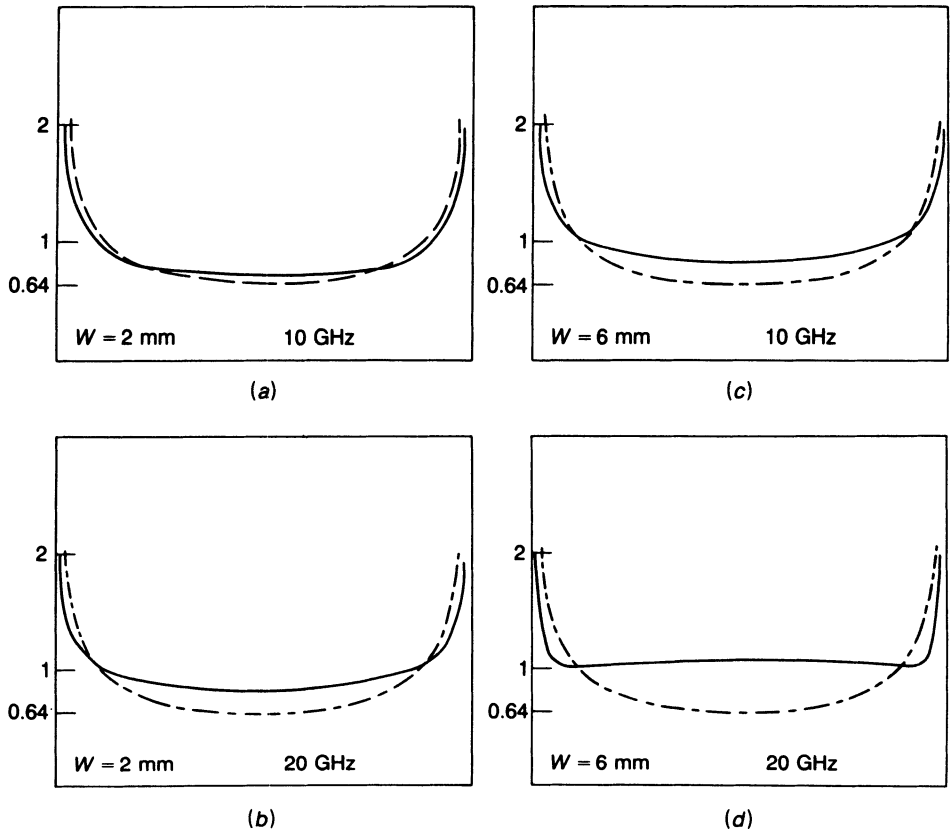


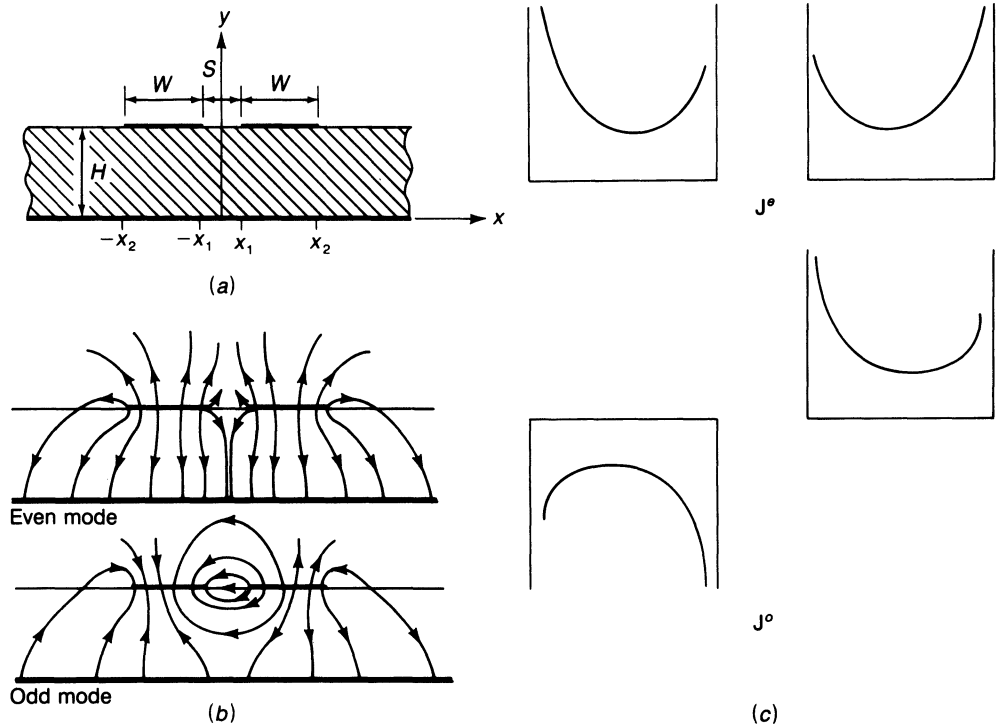
**FIGURE 3.29**

Current distribution on the microstrip for an alumina substrate with  $H = 1$  mm and two different widths. The broken curves give the quasistatic distribution. (a)  $W = 2$  mm,  $f = 10$  GHz; (b)  $W = 2$  mm,  $f = 20$  GHz; (c)  $W = 6$  mm,  $f = 10$  GHz; (d)  $W = 6$  mm,  $f = 20$  GHz.

For narrow strips and high frequencies, no simple formulas for attenuation appear to be available. For narrow strips, say  $W/H < 1$ , the quasistatic formula (3.175) is probably a reasonably good estimate since the current density does not depart significantly from the quasistatic distribution for narrow strips.

### 3.13 COUPLED MICROSTRIP LINES

When two conducting strips of width  $W$  are placed side by side on a dielectric substrate above a ground plane as shown in Fig. 3.30a, we obtain a coupled microstrip line. Since this is a three-conductor transmission line, there are two fundamental quasi-TEM modes of propagation. The even mode is the mode corresponding to both strips being at the same potential  $V$


**FIGURE 3.30**

(a) Coupled microstrip line; (b) the electric field distribution for the even and odd modes; (c) the current distribution for the even and odd modes.

and on which the same currents exist. The odd mode corresponds to the strips being at opposite potentials,  $-V$  and  $V$ , relative to the ground plane. For the odd mode the currents on the two strips are also equal in amplitude but of opposite sign. A sketch of the electric field lines for the two modes is shown in Fig. 3.30*b*. For isolated strips in air, i.e., with no ground plane and substrate present, the theoretical current distributions for the two modes are:<sup>†</sup>

$$J^e(x) = \frac{x}{\sqrt{(x^2 - x_1^2)(x_2^2 - x^2)}} \quad (3.178a)$$

$$J^o(x) = \frac{x_2}{\sqrt{(x^2 - x_1^2)(x_2^2 - x^2)}} \quad (3.178b)$$

<sup>†</sup>R. E. Collin, "Field Theory of Guided Waves," 2nd ed., chap. 4, IEEE Press, Piscataway, N.J., 1991.

For the even mode the factor  $x$  in the numerator reduces the amplitude of the singular behavior near the inner edges at  $x = \pm x_1$ . When  $x_1$  equals zero the current singularity at  $\pm x_1$  vanishes and  $J^e(x)$  becomes the expected current density on a single strip  $2x_2$  units wide. For the odd mode the current singularity at the inner edges  $\pm x_1$  is more like a  $1/x$  singularity when  $x_1$  is very small. This is caused by the strong electric field across a very narrow slit with the adjacent conductors at opposite potential. The current distribution for the two modes is shown in Fig. 3.30c.

The coupled microstrip line is used in various directional coupler designs and these applications will be discussed in Chap. 6. The important parameters describing the quasi-TEM mode properties of the coupled microstrip line are the even- and odd-mode effective dielectric constants  $\epsilon_e^e, \epsilon_e^o$  that determine the two propagation constants, and the even- and odd-mode characteristic impedances  $Z_c^e, Z_c^o$ . An important parameter in directional coupler design is the coupling coefficient, which is given in terms of the characteristic impedances of the two modes by

$$C = \frac{Z_c^e - Z_c^o}{Z_c^e + Z_c^o} \quad (3.179)$$

The coupling coefficient is commonly expressed in decibel units, that is,  $20 \log C$ . In a coupled microstrip line it is not practical to achieve much more than a 2.5:1 impedance ratio; so strong coupling cannot be realized in a simple coupled microstrip directional coupler. However, other designs are available, so this is not a problem for the microwave circuit engineer.

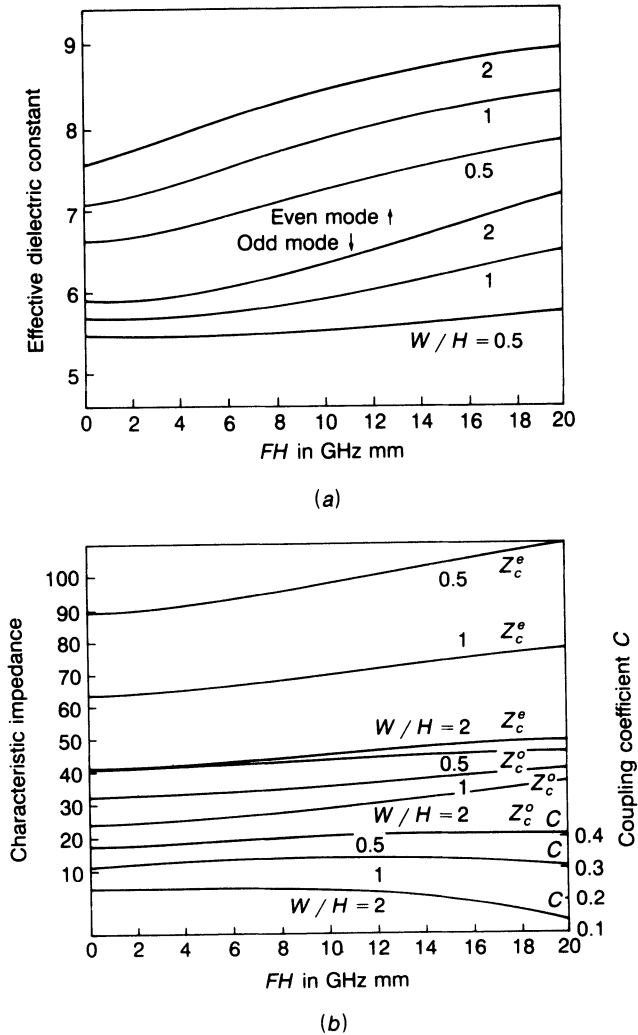
There are no simple formulas giving the quasi-TEM properties of coupled microstrip lines that have an accuracy comparable to that for microstrip lines. Bahl and Bhartia list formulas characterizing coupled microstrip lines that give results which are acceptable for noncritical applications.† The computer program CMST implements these formulas. We have checked the accuracy against numerical results obtained from a full wave solution for an alumina substrate. The effective dielectric constants were found to be accurate to within 3 percent. The characteristic impedance for the even mode was also found to be accurate to within 3 percent. For the odd-mode characteristic impedance, the error was as large as 8 percent for  $W/H = 1$ ,  $S/H = 0.25$ , but considerably less for larger values of  $W/H$  and  $S/H$ .

The dispersion properties for coupled microstrip lines on a variety of different substrates have been computed by Morich.‡ In Figs. 3.31 to 3.33

†J. Bahl and P. Bhartia, "Microwave Solid State Circuit Design," p. 28, John Wiley & Sons, Inc., New York, 1988.

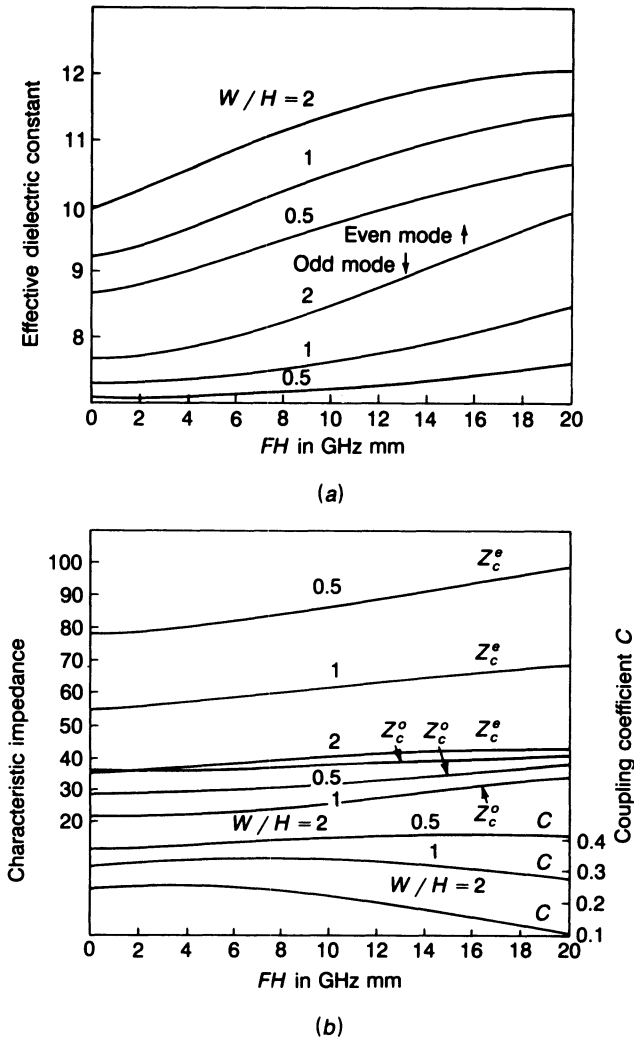
‡M. Morich, Broadband Dispersion Analysis of Coupled Microstrip on Anisotropic Substrates by Perturbation-Iteration Theory, M.S. Thesis, Case Western Reserve University, Cleveland, Ohio, May, 1987.



**FIGURE 3.31**

Dispersion characteristics of a coupled microstrip line on an alumina substrate.  $S/H = 0.25$ ,  $\epsilon_r = 9.7$ . (a) Even- and odd-mode effective dielectric constant; (b) even- and odd-mode characteristic impedance and coupling coefficient  $C$ .

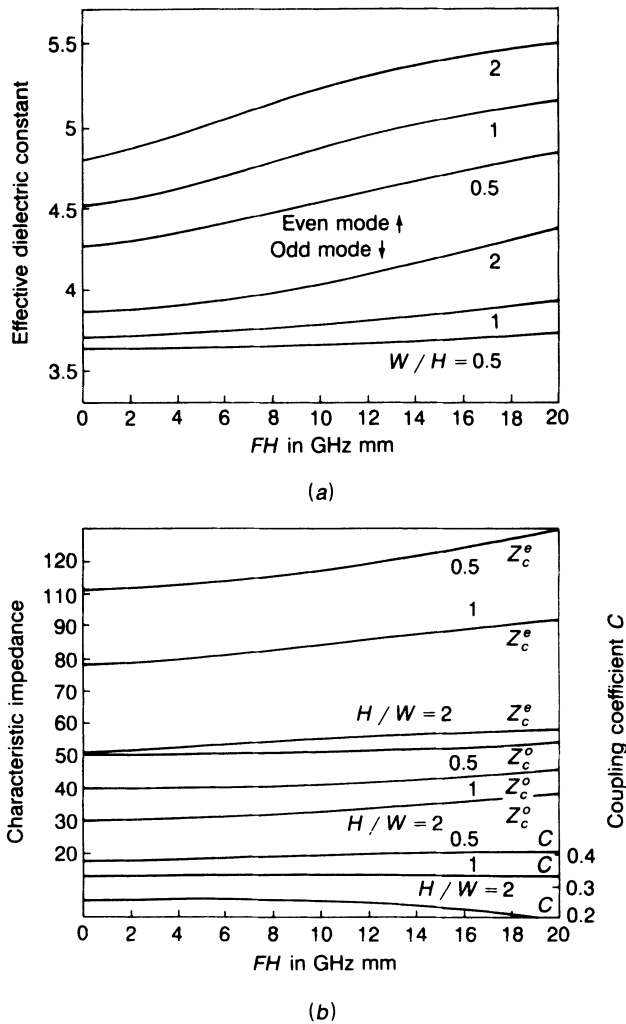
we show graphical results for coupled microstrip lines on alumina, gallium-arsenide, and RT/Duroid 6006 substrates. The horizontal axis scale is the product of frequency  $F$  and substrate thickness  $H$ . Thus, for a substrate with  $H = 0.5$  mm, the frequency range covered is 0 to 40 GHz. The coupling coefficient  $C$  given by (3.179) is also shown. For  $W/H = 0.5$  and  $S/H = 0.25$ , there is little change in the coupling coefficient with frequency. If the spacing is reduced to make  $S/H = 0.1$ , the coupling coefficient (not shown) for an alumina substrate increases to 0.483 at low frequencies and



**FIGURE 3.32**

Dispersion characteristics of coupled microstrip line on a gallium-arsenide substrate.  $S/H = 0.25$ ,  $\epsilon_r = 12.9$ . (a) Even- and odd-mode effective dielectric constant; (b) even- and odd-mode characteristic impedance and coupling coefficient  $C$ .

rises to a value of 0.524 at  $FH = 20$  GHz mm. A coupling coefficient of 0.5 is needed for a 6-dB directional coupler. The effective dielectric constant for the odd mode is smaller than that for the even mode because a larger percentage of the electric field energy is located in the air region. The capacitance between closely spaced parallel strips at opposite potentials is large so the characteristic impedance of the odd mode is smaller than that for the even mode for the normal range of parameters involved. For wide strips with large spacing, there is very little coupling and the two mode impedances will be almost the same.

**FIGURE 3.33**

Dispersion characteristics of coupled microstrip line on an RT/Duroid 6006 substrate.  $S/H = 0.25$ ,  $\epsilon_r = 6.36$ . (a) Even- and odd-mode effective dielectric constant; (b) even- and odd-mode characteristic impedance and coupling coefficient  $C$ .

The attenuation constant for coupled microstrip lines is comparable to that for the microstrip line. For closely spaced strips the increased concentration of the current near the two inner edges for the odd mode, along with the smaller characteristic impedance, increases the attenuation of this mode relative to that for the even mode. For the odd mode the attenuation caused by dielectric loss will be less than that for the even mode since the electric field energy is more evenly distributed between the air region and the substrate region for this mode.

### 3.14 STRIP TRANSMISSION LINES

The basic strip transmission line consists of a conducting strip embedded in a dielectric medium between two ground planes as shown in Fig. 3.34*a*. Figures 3.34*b* and *c* illustrate coupled strip lines. For broadside coupled strips as shown in Fig. 3.34*c*, the coupling coefficient is significantly greater than for coplanar strips. Thus the strip line with broadside coupled strips is suitable for directional couplers where a coupling of 3 dB is required. Since the dielectric completely surrounds the strips, the strip line and the coupled strip line support pure TEM modes of propagation. There is no frequency dispersion or change in effective dielectric constant with frequency. Consequently, for the coupled strip line the even and odd modes of propagation have the same phase velocity, which is also a desirable feature for directional coupler design.

For the symmetrical strip line and coupled strip line, the TEM-mode characteristic impedance is readily found from the distributed capacitance with the latter determined by conformal mapping techniques. The distributed capacitance for the symmetrical strip line is found in App. III.

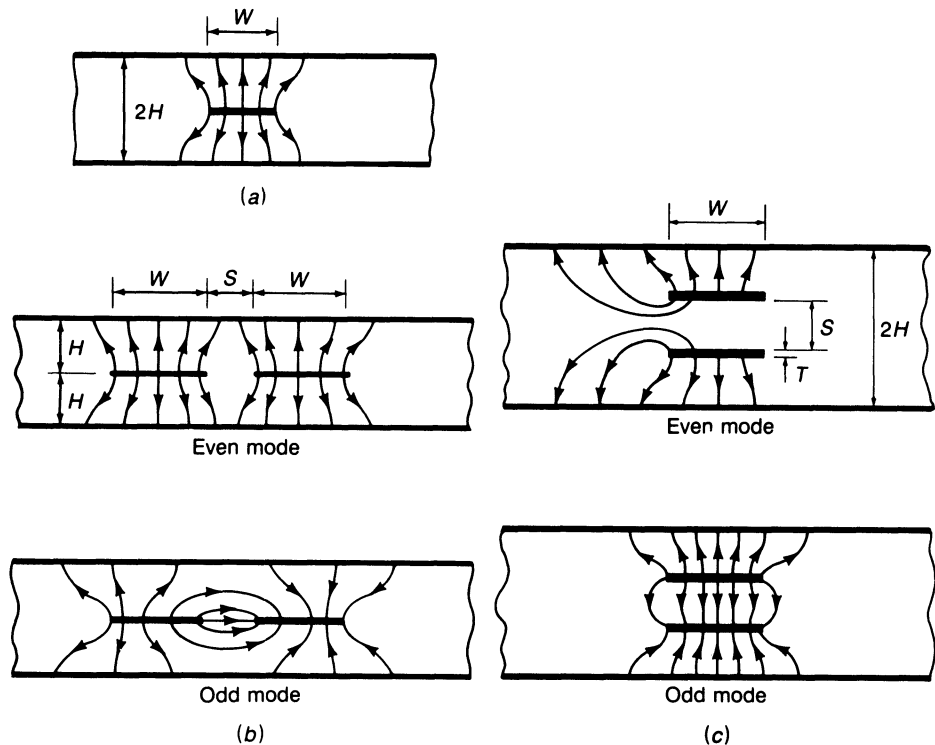


**FIGURE 3.34**

(*a*) The basic strip-line configuration; (*b*) coupled strip line using coplanar strips; (*c*) coupled strip line using broadside coupled strips. The electric field lines for the TEM modes are also shown.

From the given expression (III.27) and using (III.13c), we have

$$Z_c = \frac{Z_0}{4\sqrt{\epsilon'_r}} \frac{K(k)}{K(k')} = \frac{Z_0 K}{4\sqrt{\epsilon'_r} K'} \quad (3.180a)$$

where

$$k = \frac{1}{\cosh \pi W/4H} \quad k' = \tanh \pi \frac{W}{4H}$$

$$\frac{K}{K'} = \frac{1}{\pi} \ln \left( 2 \frac{1 + \sqrt{k}}{1 - \sqrt{k}} \right) \quad 0.7 \leq k < 1$$

$$\frac{K}{K'} = \left[ \frac{1}{\pi} \ln \left( 2 \frac{1 + \sqrt{k'}}{1 - \sqrt{k'}} \right) \right]^{-1} \quad 0 < k \leq 0.7$$

and  $\epsilon_r$  is the dielectric constant of the dielectric material that completely surrounds the center strip. For  $W \geq 2H$  the formula for  $Z_c$  reduces to the simple form

$$Z_c = \frac{\pi Z_0}{8\sqrt{\epsilon'_r} (\ln 2 + \pi W/4H)} \quad W \geq 2H \quad (3.180b)$$

For a very narrow strip

$$Z_c = \frac{Z_0}{2\pi\sqrt{\epsilon'_r}} \ln \frac{16H}{\pi W} \quad W \leq 0.4H \quad (3.180c)$$

## Attenuation

Since the dielectric material completely fills the strip line, the attenuation due to dielectric loss is given by (3.87a) and is

$$\alpha_d = \frac{\pi \epsilon''_r}{\lambda_0 \sqrt{\epsilon'_r}} = \frac{\pi \sqrt{\epsilon'_r} \tan \delta_l}{\lambda_0} \quad (3.181)$$

Formulas for the attenuation in a strip line due to conductor losses and assuming an inner conductor of elliptical cross section have been derived using conformal mapping techniques.† In App. III it is shown that the series resistance of an isolated conductor of elliptical cross section is greater than that for a conductor with a rectangular cross section. By using an equivalent center thickness  $T_e$  for the conductor with elliptical cross section, the two series resistances will be equal provided  $T_e$  is chosen to be

$$T_e = e^{-\pi/2} \sqrt{\frac{4WT}{\pi}} \quad (3.182)$$

†R. E. Collin, *loc. cit.*, chap. 4, eqs. (73), (74), and (76).

We will assume that this equivalence is also a good approximation for a conductor placed between two ground planes. On this basis the attenuation by the center conductor is

$$\alpha_{c1} = \frac{\pi R_m}{16Z_c HK'^2 k'} \ln \frac{16Hk'}{k\pi T_e} \quad (3.183a)$$

and that due to the ground planes is

$$\alpha_{c2} = \frac{\pi^2 R_m W}{64Z_c H^2 K'^2 k'} \quad (3.183b)$$

For wide and narrow strips these formulas reduce to the following simplified forms:

$$\alpha_{c1} = \frac{R_m \sqrt{\epsilon'_r}}{2Z_0 H} \frac{\ln \frac{8H}{\pi T_e} + \frac{\pi W}{4H}}{\ln 2 + \frac{\pi W}{4H}} \quad W \geq 2H \quad (3.184a)$$

$$\alpha_{c2} = \frac{\pi R_m \sqrt{\epsilon'_r} W}{8Z_0 H^2 \left( \ln 2 + \frac{\pi W}{4H} \right)} \quad W \geq 2H \quad (3.184b)$$

$$\alpha_{c1} = \frac{2R_m \sqrt{\epsilon'_r} \ln \frac{4W}{T_e}}{\pi Z_0 W \ln \frac{16H}{\pi W}} \quad W \leq 0.4H \quad (3.184c)$$

$$\alpha_{c2} = \frac{R_m \sqrt{\epsilon'_r}}{2Z_0 H \ln \frac{16H}{\pi W}} \quad W \leq 0.4H$$

Suitable formulas for evaluating  $K$  and  $K'$  are given by (III.13) in App. III. The total attenuation for a strip line is given by

$$\alpha = \alpha_d + \alpha_{c1} + \alpha_{c2} \quad (3.185)$$

**Example 3.7.** A strip line has a ground-plane spacing  $2H = 1$  cm and uses a centered copper conducting strip of width  $W = 1$  cm and thickness  $T = 0.002$  cm. The dielectric filling material has a dielectric constant  $\epsilon'_r = 2.2$  and a loss tangent equal to  $10^{-3}$ . We want to find the characteristic impedance and attenuation at a frequency of 10 GHz. For this line  $W/H = 2$ , so (3.180b) can be used. Thus

$$Z_c = \frac{120\pi^2}{8\sqrt{2.2}(\ln 2 + \pi/2)} = 44.09 \Omega$$

The wavelength of operation is 3 cm; so by using (3.181) we find the attenuation due to dielectric loss to be

$$\begin{aligned}\alpha_d &= \frac{\pi\sqrt{2.2} \times 10^{-3}}{3} \\ &= 1.55 \times 10^{-3} \text{ Np/cm} \quad \text{or} \quad 1.35 \times 10^{-2} \text{ dB/cm}\end{aligned}$$

From (3.182) we obtain  $T_e = 0.00742$  cm for the equivalent thickness. We can use (3.184a) to find

$$\begin{aligned}\alpha_{c1} &= \frac{8.22 \times 10^{-3} \sqrt{10} \sqrt{2.2}}{240\pi \times 0.5} \frac{\ln \frac{4}{\pi \times 0.00724} + \frac{\pi}{2}}{\ln 2 + \frac{\pi}{2}} \\ &= 3.034 \times 10^{-4} \text{ Np/cm} \quad \text{or} \quad 2.635 \times 10^{-3} \text{ dB/cm}\end{aligned}$$

From (3.184b) we obtain

$$\begin{aligned}\alpha_{c2} &= \frac{8.22 \times 10^{-3} \sqrt{10} \sqrt{2.2} \pi}{8 \times 120\pi \times 0.5^2 (\ln 2 + \pi/2)} \\ &= 7.096 \times 10^{-5} \text{ Np/cm} \quad \text{or} \quad 6.163 \times 10^{-4} \text{ dB/cm}\end{aligned}$$

The total attenuation is 0.0167 dB/cm. For this transmission line the dielectric loss is greater than the conductor loss.

According to a formula for strip-line conductor attenuation developed by Cohn, we would get  $\alpha_c = 3.236 \times 10^{-3}$  dB/cm, which agrees very closely with  $3.25 \times 10^{-3}$  dB/cm obtained with our formulas.†

### 3.15 COUPLED STRIP LINES

For coplanar strips of width  $W$  and spacing  $S$ , the even- and odd-mode characteristic impedances are given by‡

$$Z_c^e = \frac{Z_0}{4\sqrt{\epsilon_r}} \frac{K(k'_e)}{K(k_e)} \quad (3.186a)$$

$$Z_c^o = \frac{Z_0}{4\sqrt{\epsilon_r}} \frac{K(k'_o)}{K(k_o)} \quad (3.186b)$$

†See H. Howe, "Strip Line Circuit Design," eq. (1.5), Artech House Books, Dedham, Mass. 1974.

‡S. B. Cohn, Shielded Coupled Strip Transmission Line, *IRE Trans.*, vol. MTT-5, pp. 29–37, October, 1955.

S. B. Cohn, Characteristic Impedances of Broadside-Coupled Strip Transmission Lines, *IRE Trans.*, vol. MTT-8, pp. 633–637, November, 1960.

S. B. Cohn, Thickness Corrections for Capacitive Obstacles and Strip Conductors, *IRE Trans.*, vol. MTT-8, pp. 638–644, November, 1960.

where

$$k_e = \tanh\left(\frac{\pi W}{4H}\right) \tanh\left(\frac{\pi(W+S)}{4H}\right)$$

$$k_o = \tanh\left(\frac{\pi W}{4H}\right) \coth\left(\frac{\pi(W+S)}{4H}\right)$$

and

$$k'_e = \sqrt{1 - k_e^2} \quad k'_o = \sqrt{1 - k_o^2}.$$

Note that  $K(k') = K'(k)$ . For the evaluation of  $K$  and  $K'$  see (III.13).

For coplanar strips with a thickness  $T$ ,

$$Z_c^i = \frac{Z_0(2H - T)}{4\sqrt{\epsilon_r}(W + (H/\pi)C_f A_i)} \quad i = e, o \quad W \geq 0.7H \quad (3.187)$$

$$A_e = 1 + \frac{\ln[1 + \tanh(\pi S/4H)]}{\ln 2}$$

$$A_o = 1 + \frac{\ln[1 + \coth(\pi S/4H)]}{\ln 2}$$

$$C_f = 2 \ln\left(\frac{4H - T}{2H - T}\right) - \frac{T}{2H} \ln\left[\frac{T(4H - T)}{(2H - T)^2}\right]$$

For broadside coupled strips as shown in Fig. 3.34c, the even- and odd-mode characteristic impedances are given by [valid for  $W \geq 0.35S$ ,  $W \geq 0.7H(1 - S/2H)$ ]

$$Z_c^e = \frac{Z_0}{2\sqrt{\epsilon_r} \left\{ \frac{W}{2H - S - 2T} + 0.4413 + \frac{1}{\pi} \left[ \ln \frac{2H}{2H - S - 2T} + \frac{S + 2T}{2H - S - 2T} \ln \frac{2H}{S + 2T} \right] \right\}} \quad (3.188a)$$

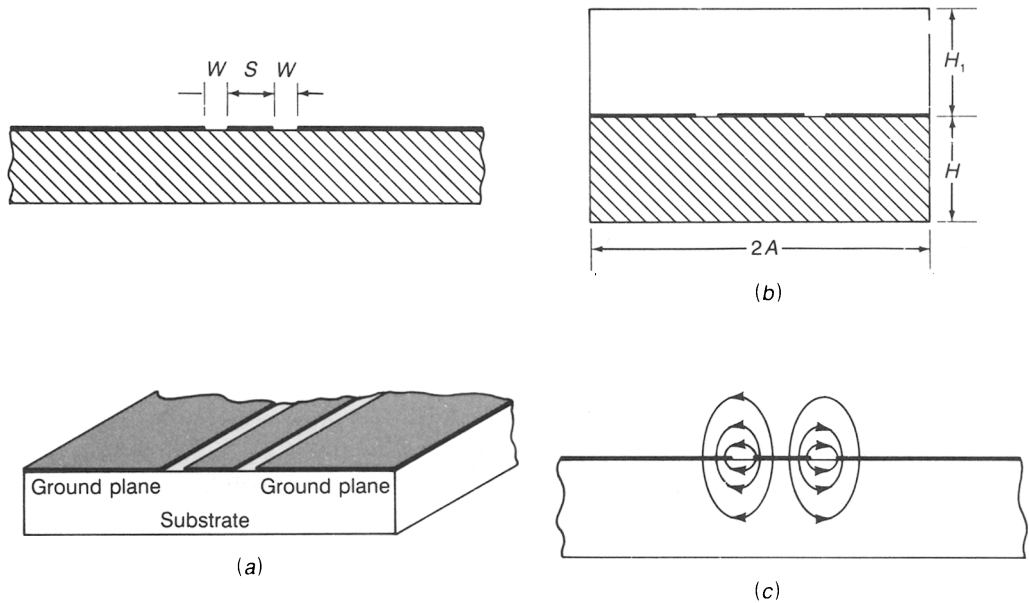
$$Z_c^o = \frac{Z_0}{2\sqrt{\epsilon_r} \left\{ \frac{W}{2H - S - 2T} + \frac{W}{S} + C_f^o + \frac{2}{\pi} \left[ \left(1 + \frac{T}{S}\right) \ln\left(1 + \frac{T}{S}\right) - \frac{T}{S} \ln \frac{T}{S} \right] \right\}} \quad (3.188b)$$

where

$$C_f^o = \frac{2H - 2T}{\pi S} \left[ \ln \frac{2H - 2T}{2H - S - 2T} + \frac{S}{2H - S - 2T} \ln \frac{2H - 2T}{S} \right]$$

All of the characteristic impedances given above refer to the impedance from one strip to the ground planes.



**FIGURE 3.35**

(a) Basic coplanar transmission line; (b) a shielded coplanar transmission line; (c) electric field distribution.

### 3.16 COPLANAR TRANSMISSION LINES

An illustration of a coplanar transmission line is shown in Fig. 3.35a. A shielded coplanar line is shown in Fig. 3.35b. The strip width is  $S$  and the strip to ground-plane spacing is  $W$ . The coplanar line is often called a coplanar waveguide (CPW). The most significant advantage that a coplanar line has over a microstrip line is the ability to connect active and passive circuit components in shunt from the conducting strip to the ground plane on the same side of the substrate. In a microstrip line a connection to the ground plane requires drilling a hole through the substrate which is somewhat difficult for ceramic materials such as alumina. Figure 3.35c shows the electric field distribution in a coplanar line.

The characteristics of a coplanar line at low frequencies can be determined by conformal mapping techniques. A solution for the coplanar line is given in App. III. For the ideal case when the ground planes are very wide relative to the slot width  $W$  and the dielectric substrate is very thick, the electric field has the same distribution as for a coplanar line in air. The reason for this is that the mapping of the air-dielectric boundary, shown as the intervals  $BC$  and  $EF$  in Fig. III.4, is the two parallel sides in the ideal parallel-plate capacitor shown in Fig. III.3. Thus the solution for the potential is not affected by the presence of the dielectric. The distributed

capacitance of the coplanar line is thus the capacitance of one-half of the air-filled line plus one-half of that for a line completely surrounded by dielectric. This capacitance is given by III.14 and for the line with dielectric on one side only we have

$$C = 2\epsilon_0 \frac{K}{K'} + 2\epsilon_r \epsilon_0 \frac{K}{K'} = 4\epsilon_0 \frac{(\epsilon_r + 1) K}{2 K'} \quad (3.189)$$

where  $K(k)$  and  $K' = K(k')$  are again the complete elliptical integrals of the first kind. The modulus  $k$  is given by the ratio

$$k = \frac{1}{1/k} = \frac{S/2}{W + S/2} = \frac{S}{S + 2W} \quad (3.190)$$

since in Fig. III.4 the center conductor extends from  $-1$  to  $1$  and the ground planes begin at  $u = \pm(1/k)$ . From (3.189) it is clear that the effective dielectric constant for the coplanar line is given by

$$\epsilon_e = \frac{\epsilon_r + 1}{2} \quad (3.191)$$

Consequently, the characteristic impedance is given by

$$Z_c = \frac{Z_0 K'}{4\sqrt{\epsilon_e} K} \quad (3.192)$$

When the substrate material is anisotropic with a dielectric constant  $\epsilon_y$  in the direction perpendicular to the air-dielectric interface and  $\epsilon_r$  in the direction parallel to the conductors, then  $\epsilon_r$  should be replaced by  $\epsilon_g = \sqrt{\epsilon_r \epsilon_y}$  in (3.189) and (3.191).

In most applications it is necessary to provide shielding of a microwave circuit. If the shield dimensions are large, the shield will not produce a significant effect on the line characteristics. In monolithic microwave integrated circuits, the substrate is very thin and fragile; so it is desirable to use another ground plane below the substrate to mechanically strengthen the overall circuit and to also provide a better heat sink to help dissipate the power generated by active devices. Ghione and Naldi have considered a number of different shield arrangements as well as coupled coplanar lines.† We will present results only for the shielded coplanar line shown in Fig. 3.35b. For this structure the effect of the sidewalls, spaced by amount  $2A$ , is negligible provided  $2A > 10(S + 2W)$ . We will assume that this is the case. Ghione and Naldi make the assumption that the air-dielectric interface in the slot regions can be replaced by magnetic walls in order to simplify the

†G. Ghione and C. U. Naldi, Coplanar Waveguides for MMIC Applications: Effect of Upper Shielding, Conductor Backing, Finite Extent Ground Planes, and Line-to-Line Coupling, *IEEE Trans.*, vol. MTT-35, pp. 260–267, March, 1987.

conformal mapping solution. The assumption is a correct one only for the case when the upper and lower shields are spaced the same distance from the coplanar line, that is,  $H = H_1$  in Fig. 3.35*b*. For the line dimensions encountered in most practical applications of coplanar lines, the assumption does not introduce significant error. The advantage of this assumption is that it decouples the air and dielectric regions; so it is only necessary to find the capacitance of the air- and dielectric-filled sections separately.

It was found that the effective dielectric constant is given by

$$\epsilon_e = 1 + q(\epsilon_r - 1) \quad (3.193a)$$

where the filling factor  $q$  is given by

$$q = \frac{K(k_1)/K(k'_1)}{K(k_2)/K(k'_2) + K(k)/K(k')} \quad (3.193b)$$

$K$  is the complete elliptic integral of the first kind,  $k'_1$  and  $k'_2$  are the complementary moduli given by  $\sqrt{1 - k_1^2}$  and  $\sqrt{1 - k_2^2}$ , and

$$k_1 = \frac{\tanh(\pi S/4H)}{\tanh[\pi(S + 2W)/H]} \quad (3.193c)$$

$$k_2 = \frac{\tanh(\pi S/4H_1)}{\tanh[\pi(S + 2W)/4H_1]} \quad (3.193d)$$

The characteristic impedance is given by

$$Z_c = \frac{Z_0}{2\sqrt{\epsilon_e} [K(k_1)/K(k'_1) + K(k_2)/K(k'_2)]} \quad (3.194)$$

The ratios  $K/K'$  are easily evaluated using III.13*c*. For an anisotropic substrate  $\epsilon_r$  should be replaced by  $\epsilon_g = \sqrt{\epsilon_r \epsilon_y}$  and  $H$  should be replaced by the effective thickness  $H_e = \sqrt{\epsilon_r/\epsilon_y} H$ . When  $H$  and  $H_1$  are very large,  $k_1$  and  $k_2$  become equal to  $k$  given by (3.190) and the filling factor  $q$  equals 0.5.

If the lower shield plate is replaced by a magnetic wall, we obtain an approximate model of a coplanar line with a substrate of finite thickness  $H$  and with an upper shield at a spacing  $H_1$  above the coplanar conductors. For this case Ghione and Naldi give

$$q = \frac{K(k_3)/K(k'_3)}{K(k_2)/K(k'_2) + K(k)/K(k')} \quad (3.195a)$$

$$Z_c = \frac{Z_0}{2\sqrt{\epsilon_e} [K(k_2)/K(k'_2) + K(k)/K(k')]} \quad (3.195b)$$

where

$$k_3 = \frac{\sinh(\pi S/4H)}{\sinh[\pi(S + 2W)/4H]}$$

and  $k_2$  is given by (3.193d),  $k$  is given by (3.190), and  $\epsilon_e$  is given by (3.193a). When  $H_1$  is made infinite  $k_2$  becomes equal to  $k$ . The resultant structure is an unshielded coplanar line with a substrate having a finite thickness  $H$ .

**Example 3.8.** A coplanar line with upper and lower shielding and used in an MMIC circuit has the following dimensions:  $S = 50 \mu\text{m} = 0.05 \text{ mm}$ ,  $W = 50 \mu\text{m}$ ,  $H = 250 \mu\text{m}$ ,  $H_1 = 800 \mu\text{m}$ . The substrate material is gallium arsenide with  $\epsilon_r = 12.9$ . We want to find the effective dielectric constant and characteristic impedance. The first step is to find  $k_1$  and  $k_2$  using (3.193c) and (3.194c). A straightforward evaluation gives  $k_1 = 0.3547$ ,  $k_2 = 0.33547$ . We now use (III.13c) to find  $K(k_1)/K(k'_1) = 0.6573$ ,  $K(k_2)/K(k'_2) = 0.6414$ . By using (3.193a) and (3.193b), we get  $q = 0.506$  and  $\epsilon_e = 7.0228$ . The last calculation is for  $Z_c$  using (3.194) and gives  $Z_c = 54.77 \Omega$ . This example shows that for the shield spacings used very little effect on the coplanar-line characteristics occurred as is apparent from the fact that  $k_1 \approx k_2$  and  $q \approx 0.5$ , relationships that hold exactly when no shields are used.

## Attenuation

The attenuation in a coplanar line caused by dielectric loss is given by the same formula as for a microstrip line, i.e., by (3.171). By using the filling factor  $q$  this can be expressed as

$$\alpha_d = \frac{\pi}{\lambda_0} \frac{\epsilon'_r}{\sqrt{\epsilon_e}} q \tan \delta_l \quad (3.196)$$

This formula can be used for shielded and unshielded lines as long as the appropriate filling factor  $q$  is used.

For thin conductors with thickness  $T$  less than  $0.05S$  and with a slot width  $W > 0.3S$ , the formula for the unshielded coplanar-line attenuation derived in App. III can be used. The center conductor has a series resistance per unit length given by

$$R_1 = \frac{R_m}{4S(1 - k^2)K^2(k)} \left[ \pi + \ln \frac{4\pi S}{T} - k \ln \frac{1 + k}{1 - k} \right] \quad (3.197a)$$

The distributed series resistance of the ground planes is given by

$$R_2 = \frac{kR_m}{4S(1 - k^2)K^2(k)} \left[ \pi + \ln \frac{4\pi(S + 2W)}{T} - \frac{1}{k} \ln \frac{1 + k}{1 - k} \right] \quad (3.197b)$$

where  $k = S/(S + 2W)$ . The attenuation due to conductor loss is given by

$$\alpha_c = \frac{R_1 + R_2}{2Z_c} \quad (3.197c)$$

In normal situations the additional attenuation introduced by upper and lower shields is small if  $H$  and  $H_1$  are greater than  $4W$ .

**Example 3.9.** A coplanar line has a copper strip of width 0.6 mm, slot width  $W = 0.6$  mm, metal thickness  $T = 0.005S = 3 \mu\text{m}$ . The dielectric used is alumina with a dielectric constant of 9.7 and a loss tangent equal to  $2 \times 10^{-4}$ . We want to find the attenuation caused by dielectric loss and conductor loss at a frequency of 4 GHz. For this line  $k = S/(S + 2W) = 0.333$ . The effective dielectric constant, from (3.191), is 5.35. From (3.192) and (III.13c) we obtain

$$Z_c = \frac{120\pi}{4\sqrt{5.35}} \frac{1}{\pi} \ln 2 \frac{1 + \sqrt{k'}}{1 - \sqrt{k'}} = 63.7 \Omega$$

where we used  $k' = \sqrt{1 - k^2} = 0.9428$ . From (3.196) we obtain

$$\alpha_d = \frac{9.7\pi}{7.5\sqrt{5.35}} 0.5 \times 2 \times 10^{-4} \times 8.686 = 1.526 \times 10^{-3} \text{ dB/cm}$$

where  $q = (\epsilon_e - 1)/(\epsilon_r - 1) = 0.5$  was used. To evaluate  $K(k) = K(0.333)$ , we use (III.13d) to obtain

$$\begin{aligned} K(0.333) &= \frac{2}{1 + k'} K\left(\frac{1 - k'}{1 + k'}\right) = \frac{2}{1.9428} K(0.0294) = \frac{\pi}{1.9428} \\ &= 1.617 \end{aligned}$$

From (3.197) we get  $R_1 = 19.25R_m/\text{cm}$  and  $R_2 = 5.97R_m/\text{cm}$ . We now use  $R_m = 8.22 \times 10^{-3}\sqrt{f}$  and (3.197c) to get

$$\alpha_c = (2.158 \times 10^{-2} + 6.69 \times 10^{-3}) = 2.827 \times 10^{-2} \text{ dB/cm}$$

The ground planes contribute 23.7 percent of the conductor loss. The total attenuation is  $2.98 \times 10^{-2}$  dB/cm.

Jackson has made some loss calculations for coplanar and microstrip transmission lines at a frequency of 60 GHz and found that for typical line dimensions and characteristic impedances greater than  $50 \Omega$ , the coplanar line has a smaller attenuation.† The substrate considered had a dielectric constant of 12.8 and a loss tangent of  $6 \times 10^{-3}$ . The maximum strip width considered by Jackson was 0.3 mm. For these line dimensions the quasistatic formulas given above can be used. We have verified that indeed the quasistatic formulas give essentially the same attenuation. The lower loss in coplanar lines appears to be due to being able to use a wider center conductor for a given impedance as compared with that for a microstrip line. However, this is not always

†R. W. Jackson, Considerations in the Use of Coplanar Waveguide for Millimeter-Wave Integrated Circuits *IEEE Trans.*, vol. MTT-34, pp. 1450–1456, December, 1986.

necessarily true since the relative attenuation of the two types of transmission lines will depend on other factors such as substrate thickness and dielectric constant also.

## High-Frequency Dispersion

Coplanar transmission lines exhibit dispersion effects similar to that for microstrip lines. There are less available computed results for the effective dielectric constant and characteristic impedance for coplanar lines than what is available for the microstrip line. The coplanar line can be viewed as two coupled slot lines and from this point of view it is clear that there are two modes of propagation that are quasi-TEM in character. The reader is referred to the paper by Nakatani and Alexopoulos for typical dispersive properties of a coplanar line.<sup>†</sup> In many integrated microwave circuit applications, the line dimensions are so small relative to the wavelength that the quasi-TEM formulas can be used even though the frequency may be as high as 50 GHz.

## PART 3 RECTANGULAR AND CIRCULAR WAVEGUIDES

---

Hollow-pipe waveguides do not support a TEM wave. In hollow-pipe waveguides the waves are of the TE and TM variety. The waveguide with a rectangular cross section is the most widely used one. It is available in sizes for use at frequencies from 320 MHz up to 333 GHz. The WR-2300 waveguide for use at 320 MHz has internal dimensions of 58.42 in by 29.1 in and is a very large duct. By contrast, the WR-3 waveguide for use at 333 GHz has internal dimensions of 0.034 in by 0.017 in and is a very miniature structure. The standard WR-90 X-band waveguide has internal dimensions of 0.9 in by 0.4 in and is used in the frequency range of 8.2 to 12.5 GHz. The rectangular waveguide is widely used to couple transmitters and receivers to the antenna. For high-power applications the waveguide is filled with an inert gas such as nitrogen and pressurized in order to increase the voltage breakdown rating.

Circular waveguides are not as widely used as rectangular waveguides but are available in diameters of 25.18 in down to 0.239 in to cover the frequency range 800 MHz up to 116 GHz.

---

<sup>†</sup>A. Nakatani and N. G. Alexopoulos, Toward a Generalized Algorithm for the Modeling of the Dispersive Properties of Integrated Circuit Structures on Anisotropic Substrates, *IEEE Trans.*, vol. MTT-33, pp. 1436–1441, December, 1985.

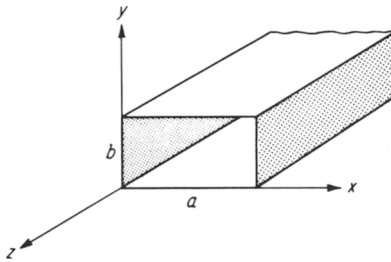


**FIGURE 3.36**  
Rectangular waveguide.

### 3.17 RECTANGULAR WAVEGUIDE

The rectangular waveguide with a cross section as illustrated in Fig. 3.36 is an example of a waveguiding device that will not support a TEM wave. Consequently, it turns out that unique voltage and current waves do not exist, and the analysis of the waveguide properties has to be carried out as a field problem rather than as a distributed-parameter-circuit problem.

In a hollow cylindrical waveguide a transverse electric field can exist only if a time-varying axial magnetic field is present. Similarly, a transverse magnetic field can exist only if either an axial displacement current or an axial conduction current is present, as Maxwell's equations show. Since a TEM wave does not have any axial field components and there is no center conductor on which a conduction current can exist, a TEM wave cannot be propagated in a cylindrical waveguide.

The types of waves that can be supported (propagated) in a hollow empty waveguide are the TE and TM modes discussed in Sec. 3.7. The essential properties of all hollow cylindrical waveguides are the same, so that an understanding of the rectangular guide provides insight into the behavior of other types as well. As for the case of the transmission line, the effect of losses is initially neglected. The attenuation is computed later by using the perturbation method given earlier, together with the loss-free solution for the currents on the walls.

The essential properties of empty loss-free waveguides, which the detailed analysis to follow will establish, are that there is a double infinity of possible solutions for both TE and TM waves. These waves, or modes, may be labeled by two identifying integer subscripts  $n$  and  $m$ , for example,  $TE_{nm}$ . The integers  $n$  and  $m$  pertain to the number of standing-wave interference maxima occurring in the field solutions that describe the variation of the fields along the two transverse coordinates. It will be found that each mode has associated with it a characteristic cutoff frequency  $f_{c, nm}$  below which the mode does not propagate and above which the mode does propagate. The cutoff frequency is a geometrical parameter dependent on the waveguide cross-sectional configuration. When  $f_c$  has been determined, it is found that the propagation factor  $\beta$  is given by

$$\beta = (k_0^2 - k_c^2)^{1/2} \quad (3.198)$$

where  $k_0 = \omega\sqrt{\mu_0\epsilon_0}$  and  $k_c = 2\pi f_c\sqrt{\mu_0\epsilon_0}$ . The guide wavelength is readily seen to be given by

$$\lambda_g = \frac{2\pi}{\beta} = \frac{\lambda_0}{(1 - \lambda_0^2/\lambda_c^2)^{1/2}} = \frac{\lambda_0}{\sqrt{1 - f_c^2/f^2}} \quad (3.199)$$

where  $\lambda_0$  is the free-space wavelength of plane waves at the frequency  $f = \omega/2\pi$ . Since  $k_c$  differs for different modes, there is always a lower band of frequencies for which only one mode propagates (except when  $k_c$  may be the same for two or more modes). In practice, waveguides are almost universally restricted to operation over this lower-frequency band for which only the dominant mode propagates, because of the difficulties associated with coupling signal energy into and out of a waveguide when more than one mode propagates. This latter difficulty arises because of the different values of the propagation phase constant  $\beta$  for different modes, since this means that the signal carried by the two or more modes does not remain in phase as the modes propagate along the guide. This necessitates the use of separate coupling probes for each mode at both the input and output and thus leads to increased system complexity and cost.

Another feature common to all empty uniform waveguides is that the phase velocity  $v_p$  is greater than the velocity of light  $c$  by the factor  $\lambda_g/\lambda_0$ . On the other hand, the velocity at which energy and a signal are propagated is the group velocity  $v_g$  and is smaller than  $c$  by the factor  $\lambda_0/\lambda_g$ . Also, since  $\beta$ , and hence  $\lambda_g$ ,  $v_p$ , and  $v_g$ , are functions of frequency, any signal consisting of several frequencies is dispersed, or spread out, in both time and space as it propagates along the guide. This dispersion results from the different velocities at which the different frequency components propagate. If the guide is very long, considerable signal distortion may take place. Group and signal velocities are discussed in detail in Sec. 3.19.

With some of the general properties of waveguides considered, it is now necessary to consider the detailed analysis that will establish the above properties and that, in addition, will provide the relation between  $k_c$  and the guide configuration, the expressions for power and attenuation, etc. The case of TE modes in a loss-free empty rectangular guide is considered first.

## TE Waves

For TE, or  $H$ , modes,  $e_z = 0$  and all the remaining field components can be determined from the axial magnetic field  $h_z$  by means of (3.71). The axial field  $h_z$  is a solution of

$$\nabla_t^2 h_z + k_c^2 h_z = 0$$

$$\text{or} \quad \frac{\partial^2 h_z}{\partial x^2} + \frac{\partial^2 h_z}{\partial y^2} + k_c^2 h_z = 0 \quad (3.200)$$



If a product solution  $h_z = f(x)g(y)$  is assumed, (3.200) becomes

$$\frac{1}{f} \frac{d^2 f}{dx^2} + \frac{1}{g} \frac{d^2 g}{dy^2} + k_c^2 = 0$$

after substituting  $fg$  for  $h_z$  and dividing the equation by  $fg$ . The term  $1/f d^2 f/dx^2$  is a function of  $x$  only,  $1/g d^2 g/dy^2$  is a function of  $y$  only, and  $k_c^2$  is a constant, and hence this equation can hold for all values of  $x$  and  $y$  only if each term is constant. Thus we may write

$$\frac{1}{f} \frac{d^2 f}{dx^2} = -k_x^2 \quad \text{or} \quad \frac{d^2 f}{dx^2} + k_x^2 f = 0$$

$$\frac{1}{g} \frac{d^2 g}{dy^2} = -k_y^2 \quad \text{or} \quad \frac{d^2 g}{dy^2} + k_y^2 g = 0$$

where  $k_x^2 + k_y^2 = k_c^2$  in order that the sum of the three terms may vanish. The use of the *separation-of-variables* technique has reduced the partial differential equation (3.200) to two ordinary simple-harmonic second-order equations. The solutions for  $f$  and  $g$  are easily found to be

$$f = A_1 \cos k_x x + A_2 \sin k_x x$$

$$g = B_1 \cos k_y y + B_2 \sin k_y y$$

where  $A_1, A_2, B_1, B_2$  are arbitrary constants. These constants, as well as the separation constants  $k_x, k_y$ , can be further specified by considering the boundary conditions that  $h_z$  must satisfy. Since the normal component of the transverse magnetic field  $\mathbf{h}$  must vanish at the perfectly conducting waveguide wall, (3.71b) shows that  $\mathbf{n} \cdot \nabla_t h_z = 0$  at the walls, where  $\mathbf{n}$  is a unit normal vector at the walls. When this condition holds, tangential  $\mathbf{e}$  will also vanish on the guide walls, as (3.71c) shows. The requirements on  $h_z$  are thus

$$\frac{\partial h_z}{\partial x} = 0 \quad \text{at } x = 0, a$$

$$\frac{\partial h_z}{\partial y} = 0 \quad \text{at } y = 0, b$$

where the guide cross section is taken to be that in Fig. 3.36. In the solution for  $f$ , the boundary conditions give

$$-k_x A_1 \sin k_x x + k_x A_2 \cos k_x x = 0 \quad \text{at } x = 0, a$$

Hence, from the condition at  $x = 0$ , it is found that  $A_2 = 0$ . At  $x = a$ , it is

necessary for  $\sin k_x a = 0$ , and this specifies  $k_x$  to have the values

$$k_x = \frac{n\pi}{a} \quad n = 0, 1, 2, \dots$$

In a similar manner it is found that  $B_2 = 0$  and

$$k_y = \frac{m\pi}{b} \quad m = 0, 1, 2, \dots$$

Both  $n$  and  $m$  equal to zero yields a constant for the solution for  $h_z$  and no other field components; so this trivial solution is of no interest.

If we use the above relations and put  $A_1 B_1 = A_{nm}$ , the solutions for  $h_z$  are seen to be

$$h_z = A_{nm} \cos \frac{n\pi x}{a} \cos \frac{m\pi y}{b} \quad (3.201)$$

for  $n = 0, 1, 2, \dots$ ;  $m = 0, 1, 2, \dots$ ;  $n = m \neq 0$ . The constant  $A_{nm}$  is an arbitrary amplitude constant associated with the  $nm$ th mode. For the  $nm$ th mode the cutoff wave number is designated  $k_{c, nm}$ , given by

$$k_{c, nm} = \left[ \left( \frac{n\pi}{a} \right)^2 + \left( \frac{m\pi}{b} \right)^2 \right]^{1/2} \quad (3.202)$$

and is clearly a function of the guide dimensions only. The propagation constant for the  $nm$ th mode is given by

$$\begin{aligned} \gamma_{nm} &= j\beta_{nm} = j(k_0^2 - k_{c, nm}^2)^{1/2} \\ &= j \left[ \left( \frac{2\pi}{\lambda_0} \right)^2 - \left( \frac{n\pi}{a} \right)^2 - \left( \frac{m\pi}{b} \right)^2 \right]^{1/2} \end{aligned} \quad (3.203)$$

When  $k_0 > k_{c, nm}$ ,  $\beta_{nm}$  is pure real and the mode propagates; when  $k_0 < k_{c, nm}$ , then  $\gamma_{nm}$  is real but  $\beta_{nm}$  is imaginary and the propagation factor is  $e^{-\gamma_{nm}|z|}$ , which shows that the mode decays rapidly with distance  $|z|$  from the point at which it is excited. This decay is not associated with energy loss, but is a characteristic feature of the solution. Such decaying, or evanescent, modes may be used to represent the local diffraction, or fringing, fields that exist in the vicinity of coupling probes and obstacles in waveguides. The frequency separating the propagation and no-propagation bands is designated the cutoff frequency  $f_{c, nm}$ . This is given by the solution of  $k_0 = k_{c, nm}$ ; that is,

$$f_{c, nm} = \frac{c}{\lambda_{c, nm}} = \frac{c}{2\pi} k_{c, nm} = \frac{c}{2\pi} \left[ \left( \frac{n\pi}{a} \right)^2 + \left( \frac{m\pi}{b} \right)^2 \right]^{1/2} \quad (3.204)$$

where  $c$  is the velocity of light. The cutoff wavelength is given by

$$\lambda_{c, nm} = \frac{2ab}{(n^2b^2 + m^2a^2)^{1/2}} \quad (3.205)$$

A typical guide may have  $a = 2b$ , in which case

$$\lambda_{c, nm} = \frac{2a}{(n^2 + 4m^2)^{1/2}}$$

and  $\lambda_{c, 10} = 2a$ ,  $\lambda_{c, 01} = a$ ,  $\lambda_{c, 11} = 2a/\sqrt{5}$ , etc. In this example there is a band of wavelengths from  $a$  to  $2a$ , that is, a frequency band

$$\frac{c}{2a} < f < \frac{c}{a}$$

for which only the  $H_{10}$  mode propagates. This is the dominant mode in a rectangular guide and the one most commonly used in practice. Above the frequency  $c/a$ , other modes may propagate; so the useful frequency band in the present case is a one-octave band from  $c/2a$  to  $c/a$ .

The remainder of the field components for the  $TE_{nm}$ , or  $H_{nm}$ , mode are readily found from (3.201) by using (3.71). The results for the complete  $nm$ th solution are

$$H_z = A_{nm} \cos \frac{n\pi x}{a} \cos \frac{m\pi y}{b} e^{\mp j\beta_{nm}z} \quad (3.206a)$$

$$H_x = \pm j \frac{\beta_{nm}}{k_{c, nm}^2} A_{nm} \frac{n\pi}{a} \sin \frac{n\pi x}{a} \cos \frac{m\pi y}{b} e^{\mp j\beta_{nm}z} \quad (3.206b)$$

$$H_y = \pm j \frac{\beta_{nm}}{k_{c, nm}^2} A_{nm} \frac{m\pi}{b} \cos \frac{n\pi x}{a} \sin \frac{m\pi y}{b} e^{\mp j\beta_{nm}z} \quad (3.206c)$$

$$E_x = Z_{h, nm} A_{nm} j \frac{\beta_{nm}}{k_{c, nm}^2} \frac{m\pi}{b} \cos \frac{n\pi x}{a} \sin \frac{m\pi y}{b} e^{\mp j\beta_{nm}z} \quad (3.206d)$$

$$E_y = -Z_{h, nm} A_{nm} j \frac{\beta_{nm}}{k_{c, nm}^2} \frac{n\pi}{a} \sin \frac{n\pi x}{a} \cos \frac{m\pi y}{b} e^{\mp j\beta_{nm}z} \quad (3.206e)$$

where the wave impedance for the  $nm$ th  $H$  mode is given by

$$Z_{h, nm} = \frac{k_0}{\beta_{nm}} Z_0 \quad (3.207)$$

When the mode does not propagate,  $Z_{h, nm}$  is imaginary, indicating that there is no net energy flow associated with the evanescent mode. A general field with  $E_z = 0$  can be described in a complete manner by a linear superposition of all the  $H_{nm}$  modes.

## Power

For a propagating  $H_{nm}$  mode the power, or rate of energy flow, in the positive  $z$  direction is given by

$$\begin{aligned}
 P_{nm} &= \frac{1}{2} \operatorname{Re} \int_0^a \int_0^b \mathbf{E} \times \mathbf{H}^* \cdot \mathbf{a}_z \, dx \, dy \\
 &= \frac{1}{2} \operatorname{Re} \int_0^a \int_0^b (E_x H_y^* - E_y H_x^*) \, dx \, dy \\
 &= \frac{1}{2} \operatorname{Re} Z_{h, nm} \int_0^a \int_0^b (H_y H_y^* + H_x H_x^*) \, dx \, dy \quad (3.208)
 \end{aligned}$$

If we substitute from (3.206*b*) and (3.206*c*) and note that

$$\begin{aligned}
 \int_0^a \int_0^b \sin^2 \frac{n\pi x}{a} \cos^2 \frac{m\pi y}{b} \, dx \, dy &= \int_0^a \int_0^b \cos^2 \frac{n\pi x}{a} \sin^2 \frac{m\pi y}{b} \, dx \, dy \\
 &= \begin{cases} \frac{ab}{4} & n \neq 0, m \neq 0 \\ \frac{ab}{2} & n \text{ or } m = 0 \end{cases}
 \end{aligned}$$

we find that

$$\begin{aligned}
 P_{nm} &= |A_{nm}|^2 \frac{\frac{1}{2}ab}{\epsilon_{0n} \epsilon_{0m}} \frac{\beta_{nm}^2}{k_{c, nm}^4} Z_{h, nm} \left[ \left( \frac{m\pi}{b} \right)^2 + \left( \frac{n\pi}{a} \right)^2 \right] \\
 &= \frac{|A_{nm}|^2 ab}{2\epsilon_{0n} \epsilon_{0m}} \left( \frac{\beta_{nm}}{k_{c, nm}} \right)^2 Z_{h, nm} \quad (3.209)
 \end{aligned}$$

where  $\epsilon_{0m}$  is the Neumann factor and equal to 1 for  $m = 0$  and equal to 2 for  $m > 0$ .

If two modes, say the  $H_{nm}$  and  $H_{rs}$  modes, were present simultaneously, it would be found that the power is the sum of that contributed by each individual mode, that is,  $P_{nm} + P_{rs}$ . This is a general property of loss-free waveguides. This power orthogonality arises because of the orthogonality of the functions (eigenfunctions) that describe the transverse variation of the fields when integrated over the guide cross section; e.g.,

$$\int_0^a \sin \frac{n\pi x}{a} \sin \frac{r\pi x}{a} \, dx = 0 \quad n \neq r$$

Even when small losses are present the energy flow may be taken to be that contributed by each individual mode, with negligible error in all cases except when two or more degenerate modes are present. Degenerate modes are modes which have the same propagation constant  $\gamma$ , and for these the presence of even small losses may result in strong coupling between the modes.

## Attenuation

If the waveguide walls have finite conductivity, there will be a continuous loss of power to the walls as the modes propagate along the guide. Consequently, the phase constant  $j\beta$  is perturbed and becomes  $\gamma = \alpha + j\beta$ , where  $\alpha$  is an attenuation constant that gives the rate at which the mode amplitude must decay as the mode progresses along the guide. For practical waveguides the losses caused by finite conductivity are so small that the attenuation constant may be calculated using the perturbation method outlined in Sec. 3.8 in connection with lossy transmission lines. The method will be illustrated for the dominant  $H_{10}$  mode only. For the  $H_{nm}$  and also the  $E_{nm}$  modes, the calculation differs only in that somewhat greater algebraic manipulation is required.

For the  $H_{10}$  mode, the fields are given by (apart from the factor  $e^{-j\beta_{10}z}$ )

$$\begin{aligned} h_z &= A_{10} \cos \frac{\pi x}{a} \\ h_x &= j \frac{\beta_{10}}{k_{c,10}^2} A_{10} \frac{\pi}{a} \sin \frac{\pi x}{a} \\ e_y &= -Z_{h,10} A_{10} \frac{j\beta_{10}}{k_{c,10}^2} \frac{\pi}{a} \sin \frac{\pi x}{a} \end{aligned}$$

as reference to (3.206) shows. From (3.209) the rate of energy flow along the guide is

$$P_{10} = |A_{10}|^2 \frac{ab}{4} \left( \frac{\beta_{10}}{k_{c,10}} \right)^2 Z_{h,10}$$

The currents on the lossy walls are assumed to be the same as the loss-free currents, and hence are given by

$$\mathbf{J}_s = \mathbf{n} \times \mathbf{H}$$

where  $\mathbf{n}$  is a unit inward directed normal at the guide wall. Thus, on the walls at  $x = 0, a$ , the surface currents are

$$\mathbf{J}_s = \begin{cases} \mathbf{a}_x \times \mathbf{H} = -\mathbf{a}_y A_{10} & x = 0 \\ -\mathbf{a}_x \times \mathbf{H} = -\mathbf{a}_y A_{10} & x = a \end{cases}$$

whereas on the upper and lower walls the currents are

$$\mathbf{J}_s = \begin{cases} \mathbf{a}_y \times \mathbf{H} = -\mathbf{a}_z \frac{j\beta_{10}}{k_{c,10}^2} A_{10} \frac{\pi}{a} \sin \frac{\pi x}{a} + \mathbf{a}_x A_{10} \cos \frac{\pi x}{a} & y = 0 \\ -\mathbf{a}_y \times \mathbf{H} = \mathbf{a}_z \frac{j\beta_{10}}{k_{c,10}^2} A_{10} \frac{\pi}{a} \sin \frac{\pi x}{a} - \mathbf{a}_x A_{10} \cos \frac{\pi x}{a} & y = b \end{cases}$$

With a finite conductivity  $\sigma$ , the waveguide walls may be characterized as exhibiting a surface impedance given by

$$Z_m = \frac{1 + j}{\sigma \delta_s} = (1 + j) R_m$$

where  $\delta_s$  is the skin depth. The power loss in the resistive part  $R_m$  of  $Z_m$  per unit length of guide is

$$\begin{aligned} P_l &= \frac{R_m}{2} \oint_{\text{guide walls}} \mathbf{J}_s \cdot \mathbf{J}_s^* dl \\ &= \frac{R_m |A_{10}|^2}{2} \left( 2 \int_0^b dy + 2 \int_0^a \frac{\beta_{10}^2}{k_{c,10}^4} \frac{\pi^2}{a^2} \sin^2 \frac{\pi x}{a} dx + 2 \int_0^a \cos^2 \frac{\pi x}{a} dx \right) \end{aligned}$$

Since  $k_{c,10} = \pi/a$ , the above gives

$$P_l = R_m |A_{10}|^2 \left[ b + \frac{a}{2} \left( \frac{\beta_{10}}{k_{c,10}} \right)^2 + \frac{a}{2} \right]$$

If  $P_0$  is the power at  $z = 0$ , then  $P_{10} = P_0 e^{-2\alpha z}$  is the power in the guide at any  $z$ . The rate of decrease of power propagated is

$$-\frac{dP_{10}}{dz} = 2\alpha P_{10} = P_l$$

and equals the power loss, as indicated in the above equation. The attenuation constant  $\alpha$  for the  $H_{10}$  mode is thus seen to be

$$\begin{aligned} \alpha &= \frac{P_l}{2P_{10}} = \frac{R_m \left[ b + \frac{a}{2} \left( \frac{\beta_{10}}{k_{c,10}} \right)^2 + \frac{a}{2} \right]}{\frac{ab}{2} \left( \frac{\beta_{10}}{k_{c,10}} \right)^2 Z_{h,10}} \\ &= \frac{R_m}{ab\beta_{10}k_0Z_0} (2bk_{c,10}^2 + ak_0^2) \text{ Np/m} \end{aligned} \quad (3.210)$$

The attenuation for other  $TE_{nm}$  modes is given by the formula in Table 3.4, which summarizes the solutions for  $TE_{nm}$  and also  $TM_{nm}$  modes. In Fig. 3.37 the attenuation for the  $TE_{10}$  mode in a copper rectangular guide is given as a function of frequency. To convert attenuation given in nepers to decibels, multiply by 8.686.

The theoretical formulas for attenuation give results in good agreement with experimental values for frequencies below about 5,000 MHz. For higher frequencies, measured values of  $\alpha$  may be considerably higher, depending on the smoothness of the waveguide surface. If surface imperfections of the order of magnitude of the skin depth  $\delta_s$  are present, it is readily

**TABLE 3.4**  
**Properties of modes in a rectangular guide†**

	TE modes	TM modes
$H_z$	$\cos \frac{n\pi x}{a} \cos \frac{m\pi y}{b} e^{-j\beta_{nm}z}$	0
$E_z$	0	$\sin \frac{n\pi x}{a} \sin \frac{m\pi y}{b} e^{-j\beta_{nm}z}$
$E_x$	$Z_{h,nm} H_y$	$\frac{-j\beta_{nm}n\pi}{ak_{c,nm}^2} \cos \frac{n\pi x}{a} \sin \frac{m\pi y}{b} e^{-j\beta_{nm}z}$
$E_y$	$-Z_{n,nm} H_x$	$\frac{-j\beta_{nm}m\pi}{bk_{c,nm}^2} \sin \frac{n\pi x}{a} \cos \frac{m\pi y}{b} e^{-j\beta_{nm}z}$
$H_x$	$\frac{j\beta_{nm}n\pi}{ak_{c,nm}^2} \sin \frac{n\pi x}{a} \cos \frac{m\pi y}{b} e^{-j\beta_{nm}z}$	$-\frac{E_y}{Z_{e,nm}}$
$H_y$	$\frac{j\beta_{nm}m\pi}{bk_{c,nm}^2} \cos \frac{n\pi x}{a} \sin \frac{m\pi y}{b} e^{-j\beta_{nm}z}$	$\frac{E_x}{Z_{e,nm}}$
$Z_{h,nm}$	$\frac{k_0}{\beta_{nm}} Z_0$	
$Z_{e,nm}$		$\frac{\beta_{nm}}{k_0} Z_0$
$k_{c,nm}$		$\left[ \left( \frac{n\pi}{a} \right)^2 + \left( \frac{m\pi}{b} \right)^2 \right]^{1/2}$
$\beta_{nm}$		$(k_0^2 - k_{e,nm}^2)^{1/2}$
$\lambda_{c,nm}$		$\frac{2ab}{(n^2b^2 + m^2a^2)^{1/2}}$
$\alpha$	$\frac{2R_m}{bZ_0(1 - k_{c,nm}^2/k_0^2)^{1/2}} \left[ \left( 1 + \frac{b}{a} \right) \frac{k_{c,nm}^2}{k_0^2} - \frac{2R_m}{bZ_0(1 - k_{c,nm}^2/k_0^2)^{1/2}} \frac{n^2b^3 + m^2a^3}{n^2b^2a + m^2a^3} \right]$ $+ \frac{b}{a} \left( \frac{\epsilon_{0m}}{2} - \frac{k_{c,nm}^2}{k_0^2} \right) \frac{n^2ab + m^2a^2}{n^2b^2 + m^2a^2}$	

†  $R_m = (\omega\mu_0/2\sigma)^{1/2}$ ,  $\epsilon_{0m} = 1$  for  $m = 0$  and 2 for  $m > 0$ . The expression for  $\alpha$  is not valid for degenerate modes.

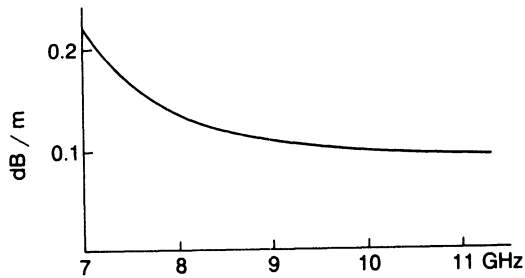


FIGURE 3.37

Attenuation of  $TE_{10}$  mode in a copper rectangular waveguide,  $a = 2.286$  cm,  $b = 1.143$  cm.

appreciated that the effective surface area is much greater, resulting in greater loss. By suitably polishing the surface, the experimental values of attenuation are found to be in substantial agreement with the theoretical values.†

### Dominant $TE_{10}$ Mode

Since the  $TE_{10}$  mode is the dominant mode in a rectangular guide, and also the most commonly used mode, it seems appropriate to examine this mode in more detail. From the results given earlier, the field components for this mode are described by the following (propagation in the  $+z$  direction assumed):

$$H_z = A \cos \frac{\pi x}{a} e^{-j\beta z} \quad (3.211a)$$

$$H_x = \frac{j\beta}{k_c} A \sin \frac{\pi x}{a} e^{-j\beta z} \quad (3.211b)$$

$$E_y = -jAZ_h \frac{\beta}{k_c} \sin \frac{\pi x}{a} e^{-j\beta z} \quad (3.211c)$$

where the subscript 10 has been dropped for convenience since this discussion pertains only to the  $TE_{10}$  mode. The parameters  $\beta$ ,  $k_c$ , and  $Z_h$  are given by

$$k_c = \frac{\pi}{a} \quad (3.212a)$$

$$\beta = \left[ k_0^2 - \left( \frac{\pi}{a} \right)^2 \right]^{1/2} \quad (3.212b)$$

$$Z_h = -\frac{E_y}{H_x} = \frac{k_0}{\beta} Z_0 \quad (3.212c)$$

†See J. Allison and F. A. Benson, Surface Roughness and Attenuation of Precision Drawn, Chemically Polished, Electropolished, Electroplated and Electroformed Waveguides, *Proc. IEE (London)*, vol. 102, pt. B, pp. 251–259, 1955.



The guide wavelength  $\lambda_g$  is

$$\lambda_g = \frac{2\pi}{\beta} = \frac{\lambda_0}{\left[1 - (\lambda_0/2a)^2\right]^{1/2}} \quad (3.212d)$$

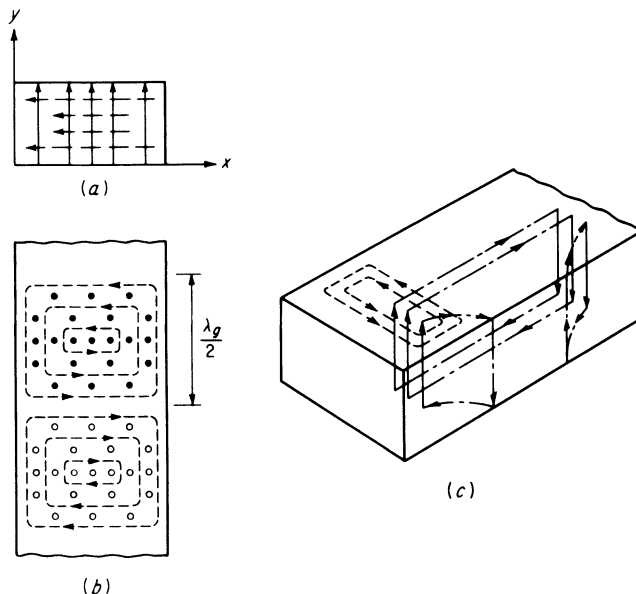
since the cutoff wavelength  $\lambda_c = 2a$ . The phase and group velocities are

$$v_p = \frac{\lambda_g}{\lambda_0} c \quad (3.212e)$$

$$v_g = \frac{\lambda_0}{\lambda_g} c \quad (3.212f)$$

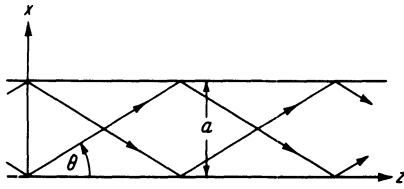
and are discussed in detail in Sec. 3.19.

In Fig. 3.38 the magnetic and electric field lines associated with the  $TE_{10}$  mode are illustrated. Note that the magnetic flux lines encircle the electric field lines; so these can be considered to be the source (displacement current) for the magnetic field. On the other hand, the electric field lines terminate in an electric charge distribution on the inner surface of the upper and lower waveguide walls. This charge oscillates back and forth in the axial and transverse directions and thus constitutes an axial and transverse conduction current that forms the continuation of the displacement current. The total current, displacement plus conduction, forms a



**FIGURE 3.38**

Magnetic and electric field lines for the  $TE_{10}$  mode. (a) Transverse plane; (b) top view; (c) mutual total current and magnetic field linkages.


**FIGURE 3.39**

 Decomposition of  $TE_{10}$  mode into two plane waves.

closed linkage of the magnetic field lines, and as such may be regarded as being generated by the changing magnetic flux these enclose. This completes the required mutual-support action between the electric and magnetic fields which is required for wave propagation.

The fields for a  $TE_{10}$  mode may be decomposed into the sum of two plane TEM waves propagating along zigzag paths between the two waveguide walls at  $x = 0$  and  $x = a$ , as in Fig. 3.39. For the electric field we have

$$E_y = -\frac{Z_h \beta}{2 k_c} (e^{j\pi x/a - j\beta z} - e^{-j\pi x/a - j\beta z})$$

If  $\pi/a$  and  $\beta$  are expressed as

$$\frac{\pi}{a} = k_0 \sin \theta \quad \beta = k_0 \cos \theta$$

the relation  $(\pi/a)^2 + \beta^2 = k_0^2$  still holds. The electric field is now given by

$$E_y = \frac{Z_h \beta}{2 k_c} (e^{-jk_0(x \sin \theta + z \cos \theta)} - e^{-jk_0(-x \sin \theta + z \cos \theta)})$$

which is clearly two plane waves propagating at angles  $\pm \theta$  with respect to the  $z$  axis, as illustrated. Alternatively, the field may be pictured as a plane wave reflecting back and forth between the two guide walls. As shown in Sec. 2.7, the constant phase planes associated with these obliquely propagating plane waves move in the  $z$  direction at the phase velocity  $c/\cos \theta = \beta c/k_0$ , and this is the reason why the phase velocity of the  $TE_{10}$  mode exceeds the velocity of light. Since the energy in a TEM wave propagates with the velocity  $c$  in the direction in which the plane wave propagates, this energy will propagate down the guide at a velocity equal to the component of  $c$  along the  $z$  axis. This component is  $v_g = c \cos \theta = (k_0/\beta)c$  and is the group velocity for the  $TE_{10}$  mode. When  $\theta = \pi/2$ , the plane waves reflect back and forth, but do not progress down the guide; so the mode is cutoff.

The above decomposition of the  $TE_{10}$  mode into two plane waves may be extended to the  $TE_{nm}$  modes also. When  $n$  and  $m$  are both different from zero, four plane waves result. Although such superpositions of plane waves may be used to construct the field solutions for rectangular guides, this is a rather cumbersome approach. However, it does lend insight into why the phase velocity exceeds that of light, as well as other properties of the modes.

## TM Modes

For TM modes,  $h_z$  equals zero and  $e_z$  plays the role of a potential function from which the remaining field components may be derived. This axial electric field satisfies the reduced Helmholtz equation

$$\nabla_t^2 e_z + k_c^2 e_z = 0 \quad (3.213)$$

of the same type encountered earlier for  $h_z$ , that is, (3.200). The solution may be found by using the separation-of-variables method. In the present case the boundary conditions require that  $e_z$  vanish at  $x = 0, a$  and  $y = 0, b$ . This condition requires that the solution for  $e_z$  be

$$e_z = A_{nm} \sin \frac{n\pi x}{a} \sin \frac{m\pi y}{b} \quad (3.214)$$

instead of a product of cosine functions which was suitable for describing  $h_z$ . Again, there are a doubly infinite number of solutions corresponding to various integers  $n$  and  $m$ . However, unlike the situation for TE modes,  $n = 0$  and  $m = 0$  are not solutions. The cutoff wave number is given by the same expression as for TE modes; i.e.,

$$k_{c, nm} = \left[ \left( \frac{n\pi}{a} \right)^2 + \left( \frac{m\pi}{b} \right)^2 \right]^{1/2} \quad (3.215)$$

and the propagation factor  $\beta_{nm}$  by

$$\beta_{nm} = (k_0^2 - k_{c, nm}^2)^{1/2} \quad (3.216)$$

The lowest-order propagating mode is the  $n = m = 1$  mode, and this has a cutoff wavelength equal to  $2ab/(a^2 + b^2)^{1/2}$ . Note that the TE<sub>10</sub> mode can propagate at a lower frequency (longer wavelength), thus verifying that this is the dominant mode.† It should also be noted that for the same values of  $n$  and  $m$ , the TE<sub>*nm*</sub> and TM<sub>*nm*</sub> modes are degenerate since they have the same propagation factor. Another degeneracy occurs when  $a = b$ , for in this case the four modes TE<sub>*nm*</sub>, TE<sub>*mn*</sub>, TM<sub>*nm*</sub>, and TM<sub>*mn*</sub> all have the same propagation constant. Still further degeneracies exist if  $a$  is an integer multiple of  $b$ , or vice versa.

The rest of the solution for TM modes is readily constructed using the general equations (3.72). A summary of this solution is given in Table 3.4. The TM modes are the dual of the TE modes and apart from minor differences have essentially the same properties. For this reason it does not seem necessary to repeat the preceding discussion.

---

†In any hollow waveguide the dominant mode is a TE mode because the boundary conditions  $e_z = 0$  for TM modes always require  $e_z$  to have a greater spatial variation in the transverse plane than that for  $h_z$  for the lowest-order TE mode, and hence the smallest value of  $k_c$  occurs for TE modes. Hence a TE mode has the lowest cutoff frequency, i.e., is the dominant mode.

### 3.18 CIRCULAR WAVEGUIDES

Figure 3.40 illustrates a cylindrical waveguide with a circular cross section of radius  $a$ . In view of the cylindrical geometry involved, cylindrical coordinates are most appropriate for the analysis to be carried out. Since the general properties of the modes that may exist are similar to those for the rectangular guide, this section is not as detailed.

#### TM Modes

For the TM modes a solution of

$$\nabla_t^2 e_z + k_c^2 e_z = 0$$

is required such that  $e_z$  will vanish at  $r = a$ . When we express the transverse laplacian  $\nabla_t^2$  in cylindrical coordinates (App. I), this equation becomes

$$\frac{\partial^2 e_z}{\partial r^2} + \frac{1}{r} \frac{\partial e_z}{\partial r} + \frac{1}{r^2} \frac{\partial^2 e_z}{\partial \phi^2} + k_c^2 e_z = 0 \quad (3.217)$$

The separation-of-variables method may be used to reduce the above to two ordinary differential equations. Consequently, it is assumed that a product solution  $f(r)g(\phi)$  exists for  $e_z$ . Substituting for  $e_z$  into (3.217) and dividing the equation by  $fg$  yield

$$\frac{1}{f} \frac{d^2 f}{dr^2} + \frac{1}{rf} \frac{df}{dr} + \frac{1}{r^2 g} \frac{d^2 g}{d\phi^2} + k_c^2 = 0$$

Multiplying this result by  $r^2$  gives

$$\frac{r^2}{f} \frac{d^2 f}{dr^2} + \frac{r}{f} \frac{df}{dr} + r^2 k_c^2 = -\frac{1}{g} \frac{d^2 g}{d\phi^2}$$

The left-hand side is a function of  $r$  only, whereas the right-hand side depends on  $\phi$  only. Therefore this equation can hold for all values of the variables only if both sides are equal to some constant  $\nu^2$ . As a result, (3.217) is seen to separate into the following two equations:

$$\frac{d^2 f}{dr^2} + \frac{1}{r} \frac{df}{dr} + \left( k_c^2 - \frac{\nu^2}{r^2} \right) f = 0 \quad (3.218a)$$

$$\frac{d^2 g}{d\phi^2} + \nu^2 g = 0 \quad (3.218b)$$

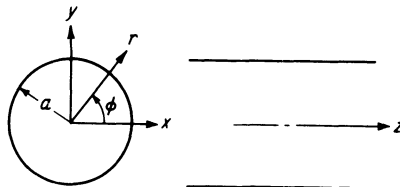


**FIGURE 3.40**

The circular cylindrical waveguide.

**TABLE 3.5**  
**Values of  $p_{nm}$  for TM modes**

$n$	$p_{n1}$	$p_{n2}$	$p_{n3}$
0	2.405	5.520	8.654
1	3.832	7.016	10.174
2	5.135	8.417	11.620

In this case the field inside the waveguide must be periodic in  $\phi$  with period  $2\pi$ , that is, single-valued. It is therefore necessary to choose  $\nu$  equal to an integer  $n$ , in which case the general solution to (3.218*b*) is

$$g(\phi) = A_1 \cos n\phi + A_2 \sin n\phi$$

where  $A_1$  and  $A_2$  are arbitrary constants.

Equation (3.218*a*) is Bessel's differential equation and has two solutions (a second-order differential equation always has two independent solutions)  $J_\nu(k_c r)$  and  $Y_\nu(k_c r)$ , called Bessel functions of the first and second kind, respectively, and of order  $\nu$ .† For the problem under investigation here, only  $J_n(k_c r)$  is a physically acceptable solution since  $Y_n(k_c r)$  becomes infinite at  $r = 0$ . The final solution for  $e_z$  may thus be expressed as

$$e_z(r, \phi) = (A_1 \cos n\phi + A_2 \sin n\phi)J_n(k_c r) \quad (3.219)$$

Reference to App. II shows that  $J_n(x)$  behaves like a damped sinusoidal function and passes through zero in a quasiperiodic fashion. Since  $e_z$  must vanish when  $r = a$ , it is necessary to choose  $k_c a$  in such a manner that  $J_n(k_c a) = 0$ . If the  $m$ th root of the equation  $J_n(x) = 0$  is designated  $p_{nm}$ , the allowed values (eigenvalues) of  $k_c$  are

$$k_{c, nm} = \frac{p_{nm}}{a} \quad (3.220)$$

The values of  $p_{nm}$  for the first three modes for  $n = 0, 1, 2$  are given in Table 3.5. As in the case of the rectangular guide, there are a doubly infinite number of solutions.

Each choice of  $n$  and  $m$  specifies a particular TM $_{nm}$  mode (eigenfunction). The integer  $n$  is related to the number of circumferential variations in the field, whereas  $m$  relates to the number of radial variations. The propagation constant for the  $nm$ th mode is given by

$$\beta_{nm} = \left( k_0^2 - \frac{p_{nm}^2}{a^2} \right)^{1/2} \quad (3.221)$$

---

† $Y_\nu$  is also called a Neumann function.

the cutoff wavelength by

$$\lambda_{c, nm} = \frac{2\pi a}{p_{nm}} \quad (3.222)$$

and the wave impedance by

$$Z_{e, nm} = \frac{\beta_{nm}}{k_0} Z_0 \quad (3.223)$$

A cutoff phenomenon similar to that for the rectangular guide exists. For the dominant TM mode,  $\lambda_c = 2\pi a/p_{01} = 2.61a$ , a value 30 percent greater than the waveguide diameter.

Expressions for the remaining field components may be derived by using the general equations (3.72). Energy flow and attenuation may be determined by methods similar to those used for the rectangular guide. A summary of the results is given in Table 3.6.

## TE Modes

The solution for TE modes parallels that for the TM modes with the exception that the boundary conditions require that  $\partial h_z/\partial r$  vanish at  $r = a$ . An appropriate solution for  $h_z$  is

$$h_z(r, \phi) = (B_1 \cos n\phi + B_2 \sin n\phi) J_n(k_c r) \quad (3.224)$$

with the requirement that

$$\frac{dJ_n(k_c r)}{dr} = 0 \quad \text{at } r = a \quad (3.225)$$

The roots of (3.225) will be designated by  $p'_{nm}$ ; so the eigenvalues  $k_{c, nm}$  are given by

$$k_{c, nm} = \frac{p'_{nm}}{a} \quad (3.226)$$

Table 3.7 lists the values of the roots for the first few modes. Note that  $p'_{0m} = p_{1m}$  since  $dJ_0(x)/dx = -J_1(x)$ , and hence the TE<sub>0m</sub> and TM<sub>1m</sub> modes are degenerate.

The first TE mode to propagate is the TE<sub>11</sub> mode, having a cutoff wavelength  $\lambda_{c, 11} = 3.41a$ . This mode is seen to be the dominant mode for the circular waveguide, and is normally the one used. A sketch of the field lines in the transverse plane for this mode is given in Fig. 3.41. The attenuation constant for the dominant TE<sub>11</sub> mode is given by

$$\alpha = \frac{R_m}{aZ_0} \left( 1 - \frac{1.841^2}{k_0^2 a^2} \right)^{-1/2} \left( \frac{1.841^2}{k_0^2 a^2} + 0.4185 \right) \quad (3.227)$$

**TABLE 3.6**  
**Properties of modes in circular waveguides**

	TE modes	TM modes
$H_z$	$J_n\left(\frac{p'_{nm}r}{a}\right)e^{-j\beta_{nm}z}\begin{cases} \cos n\phi \\ \sin n\phi \end{cases}$	0
$E_z$	0	$J_n\left(\frac{p_{nm}r}{a}\right)e^{-j\beta_{nm}z}\begin{cases} \cos n\phi \\ \sin n\phi \end{cases}$
$H_r$	$-\frac{j\beta_{nm}p'_{nm}}{ak_{c,nm}^2}J_n'\left(\frac{p'_{nm}r}{a}\right)e^{-j\beta_{nm}z}\begin{cases} \cos n\phi \\ \sin n\phi \end{cases}$	$-\frac{E_\phi}{Z_{e,nm}}$
$H_\phi$	$-\frac{jn\beta_{nm}}{rk_{c,nm}^2}J_n\left(\frac{p'_{nm}r}{a}\right)e^{-j\beta_{nm}z}\begin{cases} -\sin n\phi \\ \cos n\phi \end{cases}$	$\frac{E_r}{Z_{e,nm}}$
$E_r$	$Z_{h,nm}H_\phi$	$-\frac{j\beta_{nm}p_{nm}}{ak_{c,nm}^2}J_n'\left(\frac{p_{nm}r}{a}\right)e^{-j\beta_{nm}z}\begin{cases} \cos n\phi \\ \sin n\phi \end{cases}$
$E_\phi$	$-Z_{h,nm}H_r$	$-\frac{jn\beta_{nm}}{rk_{c,nm}^2}J_n\left(\frac{p_{nm}r}{a}\right)e^{-j\beta_{nm}z}\begin{cases} -\sin n\phi \\ \cos n\phi \end{cases}$
$\beta_{nm}$	$\left[k_0^2 - \left(\frac{p'_{nm}}{a}\right)^2\right]^{1/2}$	$\left[k_0^2 - \left(\frac{p_{nm}}{a}\right)^2\right]^{1/2}$
$Z_{h,nm}$	$\frac{k_0}{\beta_{nm}}Z_0$	
$Z_{e,nm}$		$\frac{\beta_{nm}}{k_0}Z_0$
$k_{c,nm}$	$\frac{p'_{nm}}{a}$	$\frac{p_{nm}}{a}$
$\lambda_{c,nm}$	$\frac{2\pi a}{p'_{nm}}$	$\frac{2\pi a}{p_{nm}}$
Power	$\frac{Z_0 k_0 \beta_{nm} \pi}{2k_{c,nm}^4 \epsilon_{0n}} (p_{nm}'^2 - n^2) J_n^2(p_{nm}')$	$\frac{Y_0 k_0 \beta_{nm} \pi}{2k_{c,nm}^4 \epsilon_{0n}} p_{nm}^2 [J_n'(k_{c,nm} a)]^2$
$\alpha$	$\frac{R_m}{aZ_0} \left(1 - \frac{k_{c,nm}^2}{k_0^2}\right)^{-1/2} \times \left[\frac{k_{c,nm}^2}{k_0^2} + \frac{n^2}{(p_{nm}')^2 - n^2}\right]$	$\frac{R_m}{aZ_0} \left(1 - \frac{k_{c,nm}^2}{k_0^2}\right)^{-1/2}$

**TABLE 3.7**  
**Values of  $p'_{nm}$  for TE modes**

$n$	$p'_{n1}$	$p'_{n2}$	$p'_{n3}$
0	3.832	7.016	10.174
1	1.841	5.331	8.536
2	3.054	6.706	9.970

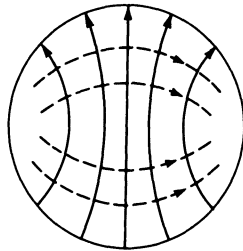


**FIGURE 3.41**  
 Field lines for the  $TE_{11}$  mode in a circular waveguide.

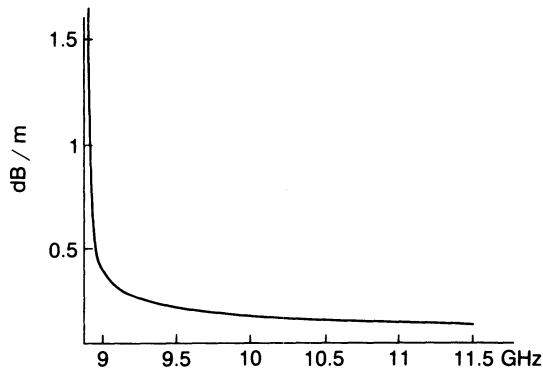


**FIGURE 3.42**  
 Attenuation of dominant  $TE_{11}$  mode in a circular waveguide. Diameter = 2 cm.

Figure 3.42 shows the attenuation in decibels per meter for a copper waveguide with an internal diameter of 2 cm. For this guide the cutoff frequency is 8.79 GHz. In the normal operating range from 9 to 11 GHz, the attenuation drops from 0.36 dB/m at 9 GHz to 0.11 dB/m at 11 GHz.

### 3.19 WAVE VELOCITIES

In any system capable of supporting propagating waves, a number of wave velocities occur that pertain to signal propagation, energy propagation, wavefront propagation, etc. These various velocities are examined below in the context of propagation in waveguides.



## Phase Velocity

The phase velocity of a wave in a waveguide was introduced earlier and shown to be equal to

$$v_p = \frac{\lambda_g}{\lambda_0} c \quad (3.228)$$

for an air-filled guide. Here  $\lambda_g$  is the guide wavelength,  $\lambda_0$  the free-space wavelength, and  $c$  the velocity of light. The phase velocity is the velocity an observer must move with in order to see a constant phase for the wave propagating along the guide. It is noted that the phase velocity is greater than the velocity of light, and since the principle of relativity states that no signal or energy can be propagated at a velocity exceeding that of light, the physical significance of the phase velocity might very well be questioned.

The clue to the significance of the phase velocity comes from the recognition that this velocity entered into wave solutions that had a steady-state time dependence of  $e^{j\omega t}$ . A pure monochromatic (single-frequency) wave of this type exists only if the source was turned on at  $t = -\infty$  and is kept on for all future time as well. This is clearly not a physically realizable situation. In actual fact the source must be turned on at some finite time, which can be chosen as  $t = 0$ . The generated signal is then of the form illustrated in Fig. 3.43. Associated with the sudden steplike beginning of the signal is a broad frequency band, as a Fourier analysis shows. If this signal is injected into the guide at  $z = 0$ , an observer a distance  $l$  farther along the guide will, in actual fact, see no signal until a time  $l/c$  has elapsed. In other words, the wavefront will propagate along the guide with a velocity  $c$ . At the time  $l/c$ , the observer will begin to see the arrival of the transient associated with the switching on of the signal. After a suitable period of time has elapsed, the transient will have died out, and the observer will then see the steady-state sinusoidally varying wave. Once steady-state conditions prevail, the phase velocity can be introduced to describe the velocity at which a constant phase point appears to move along the guide. Note, however, that there is no information being transmitted along the guide once steady-state conditions have been established. Thus the phase velocity is not associated with any physical entity such as a signal, wavefront, or energy flow velocity. The term signal is used here to denote a time function that can convey

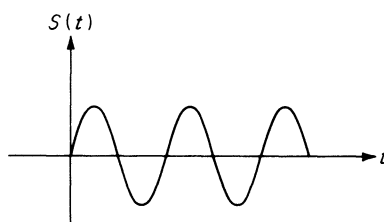


**FIGURE 3.43**  
Sinusoidal signal applied at time  $t = 0$ .

information to the observer. Thus the step change at  $t = 0$  is a signal, but once steady-state conditions are achieved, the observer does not receive any more information. A better understanding of the above features will be obtained after the group velocity, discussed below, has been examined.

## Group Velocity

The physical definition of group velocity is the velocity with which a signal consisting of a very narrow band of frequency components propagates. The appropriate tool for the analysis of this situation is the Fourier transform. If a time function is denoted by  $f(t)$ , this function of time has associated with it a frequency spectrum  $F(\omega)$  given by the Fourier transform of  $f(t)$ ,

$$F(\omega) = \int_{-\infty}^{\infty} f(t) e^{-j\omega t} dt \quad (3.229a)$$

Conversely, if the spectrum  $F(\omega)$  is known, the time function may be found from the inverse Fourier transform relation

$$f(t) = \frac{1}{2\pi} \int_{-\infty}^{\infty} F(\omega) e^{j\omega t} d\omega \quad (3.229b)$$

From Eq. (3.229b) it is seen that the Fourier transform represents  $f(t)$  as a superposition of steady-state sinusoidal functions of infinite duration. These relations are a generalization of the Fourier series relations. If the time function is passed through a device having a response  $Z(\omega)$  that is a function of frequency, e.g., filter, the output time function  $f_o(t)$  will have a frequency spectrum  $F(\omega)Z(\omega)$ , and hence, by (3.229b), is given by

$$f_o(t) = \frac{1}{2\pi} \int_{-\infty}^{\infty} F(\omega) Z(\omega) e^{j\omega t} d\omega$$

In general,  $Z(\omega) = |Z(\omega)|e^{-j\psi(\omega)}$ ; so

$$f_o(t) = \frac{1}{2\pi} \int_{-\infty}^{\infty} |Z(\omega)| F(\omega) e^{j(\omega t - \psi)} d\omega \quad (3.230)$$

If the output  $f_o$  is to be an exact reproduction of the input, then in (3.230) it is necessary for  $|Z|$  to equal a constant  $A$ , and  $\psi$  must be a linear function of  $\omega$ , say  $a\omega + b$ . In this case

$$f_o(t) = \frac{A}{2\pi} e^{-jb} \int_{-\infty}^{\infty} F(\omega) e^{j\omega(t-a)} d\omega \quad (3.231a)$$

If we put  $t - a = t'$ , the above becomes

$$f_o(t' + a) = \frac{Ae^{-jb}}{2\pi} \int_{-\infty}^{\infty} F(\omega) e^{j\omega t'} d\omega = Ae^{-jb} f(t') \quad (3.231b)$$

as comparison with (3.229*b*) shows. Thus the output time function is

$$f_o(t' + a) = f_o(t) = Ae^{-jb}f(t') = Ae^{-jb}f(t - a) \quad (3.232)$$

i.e., an exact duplicate of the input, apart from a constant multiplier and a time delay  $a$ . Thus the conditions given on  $|Z|$  and  $\psi$  are those sufficient for a distortion-free system.

Now, in a waveguide, the transverse variations of the field are independent of frequency. The only essential frequency-dependent part of the field solution is the propagation factor  $e^{-j\beta z}$  since

$$\beta = (k_0^2 - k_c^2)^{1/2} = \left( \frac{\omega^2}{c^2} - k_c^2 \right)^{1/2}$$

is a function of frequency. Thus a waveguide of length  $l$ , in which the field has a time dependence  $e^{j\omega t}$ ,  $\omega > 0$ , can be considered as a frequency filter with a response  $e^{-j\beta l}$ . Since  $\beta$  is not a linear function of  $\omega$ , it may be anticipated that some signal distortion will occur for propagation in a waveguide. For an ideal TEM-wave transmission line,  $\beta = k_0 = \omega/c$  and distortion-free transmission is possible. However, practical lines have an attenuation which depends on frequency ( $R_m \propto \sqrt{f}$ ), and this will produce distortion. Fortunately, for narrowband signals neither waveguides nor transmission lines produce significant distortion unless very long lines are used.

Consider now a time function  $f(t)$  having a band of frequencies between  $-f_m$  and  $f_m$ . This signal is used to modulate a carrier of frequency  $f_c \gg f_m$ . The resultant is

$$S(t) = f(t) \cos \omega_c t = \text{Re} [ f(t) e^{j\omega_c t} ] \quad (3.233)$$

If  $F(\omega)$  is the spectrum of  $f(t)$ , the spectrum of  $S(t)$  is

$$\begin{aligned} F_s(\omega) &= \int_{-\infty}^{\infty} e^{-j\omega t} f(t) \frac{e^{j\omega_c t} + e^{-j\omega_c t}}{2} d\omega \\ &= \frac{1}{2} [ F(\omega - \omega_c) + F(\omega + \omega_c) ] \end{aligned} \quad (3.234)$$

These spectra are illustrated in Fig. 3.44.

For positive  $\omega$  the waveguide response is  $e^{-j\beta(\omega)l}$ . For negative  $\omega$  the response must be chosen as  $e^{j\beta(\omega)l}$  since, if the time variation is  $e^{-j\omega t}$ , the sign in front of  $\beta$  must be positive for propagation in the positive  $z$  direction. In other words, all physical systems will have a response such that  $|Z(\omega)|$  is an even function of  $\omega$  and  $\psi(\omega)$  is an odd function of  $\omega$ . Since  $\beta$  is an even function, the sign must be changed for  $\omega < 0$ . These even and odd symmetry properties are required simply so that the output time function is real, a physical requirement. The output spectrum for the

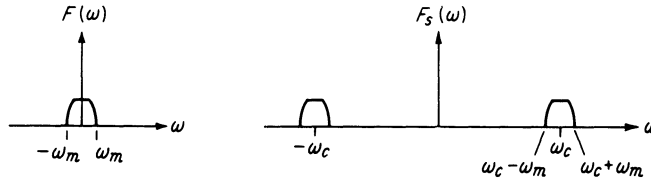


**FIGURE 3.44**  
Spectrum of  $f(t)$  and  $S(t)$ .

waveguide is thus

$$F_o(\omega) = \frac{1}{2} [F(\omega - \omega_c)e^{-j\beta(\omega)l} + F(\omega + \omega_c)e^{j\beta(\omega)l}]$$

and the output signal is

$$S_o(t) = \frac{1}{2\pi} \int_{-\infty}^{\infty} F_o(\omega) e^{j\omega t} d\omega \quad (3.235)$$

The analysis that follows is simplified if the signal is represented in complex form as  $f(t)e^{j\omega_c t}$  with a spectrum  $F(\omega - \omega_c)$ . In this case only the positive half of the spectrum needs to be considered, and the output signal is given by

$$S_o(t) = \text{Re} \frac{1}{2\pi} \int_{\omega_c - \omega_m}^{\omega_c + \omega_m} F(\omega - \omega_c) e^{j\omega t - j\beta(\omega)l} d\omega \quad (3.236)$$

since  $F(\omega - \omega_c)$  is zero outside the band  $\omega_c - \omega_m \leq \omega \leq \omega_c + \omega_m$ . If the band is very narrow,  $\omega_m \ll \omega_c$ , then  $\beta(\omega)$  may be approximated by the first few terms in a Taylor series expansion about  $\omega_c$ . Thus

$$\beta(\omega) = \beta(\omega_c) + \left. \frac{d\beta}{d\omega} \right|_{\omega_c} (\omega - \omega_c) + \frac{1}{2} \left. \frac{d^2\beta}{d\omega^2} \right|_{\omega_c} (\omega - \omega_c)^2 + \cdots \quad (3.237)$$

Retaining the first two terms only and letting  $\beta(\omega_c) = \beta_0$  and  $d\beta/d\omega_c = \beta'_0$  at  $\omega_c$ , (3.236) gives

$$S_o(t) = \text{Re} \frac{1}{2\pi} \int_{\omega_c - \omega_m}^{\omega_c + \omega_m} F(\omega - \omega_c) e^{j\omega(t - \beta'_0 l)} e^{-j\beta_0 l + j\beta'_0 l \omega_c} d\omega$$

If this is compared with (3.231) and (3.232), it is seen that

$$\begin{aligned} S_o(t) &= \text{Re} [e^{-j\beta_0 l + j\beta'_0 l \omega_c} f(t - \beta'_0 l) e^{j\omega_c(t - \beta'_0 l)}] \\ &= f(t - \beta'_0 l) \cos(\omega_c t - \beta_0 l) \end{aligned} \quad (3.238)$$

To the order of approximation used here, the input modulating signal  $f(t)$  is reproduced without distortion but with a time delay  $\beta'_0 l$ . This is to be anticipated since  $\beta$  was approximated by a linear function of  $\omega$  in the band

$\omega_c - \omega_m$  to  $\omega_c + \omega_m$  (distortion-free condition). The signal delay defines the group velocity  $v_g$ , which is equal to the distance  $l$  divided by the delay time; thus

$$v_g = \frac{l}{l\beta'_0} = \left( \frac{d\beta}{d\omega} \right)^{-1} \quad (3.239)$$

This is also the signal velocity. Note, however, that this velocity has significance only if the band, or "group," of frequencies making up the signal is so narrow that  $\beta$  may be approximated by a linear function throughout the frequency band of interest. If this is not the case, more terms in the expansion (3.237) must be retained and signal distortion will occur. In this case the group velocity as given by (3.239) is no longer the signal velocity. In fact, because of signal distortion, no unique signal velocity exists any longer. Different portions of the signal will travel with different velocities, and the resultant signal becomes dispersed in both time and space.

In the case of a waveguide,

$$\begin{aligned} v_g &= \left( \frac{d\beta}{d\omega} \right)^{-1} = c \frac{dk_0}{d\beta} = \left[ \frac{d(\omega^2/c^2 - k_c^2)^{1/2}}{d\omega} \right]^{-1} \\ &= \frac{\beta c^2}{\omega} = \frac{\beta}{k_0} c = \frac{\lambda_0}{\lambda_g} c \end{aligned} \quad (3.240)$$

It is seen that  $v_g < c$  and that  $v_g v_p = c^2$  for a waveguide.

A typical plot of  $k_0$  versus  $\beta$  for a waveguide is given in Fig. 3.45. From this plot it can be seen that for a narrow band of frequencies a linear approximation for  $\beta$  is good. Also note that for high frequencies (large  $k_0$ )  $\beta$  becomes equal to  $k_0$ . Thus frequencies well above the cutoff frequency  $f_c$  suffer very little dispersion and propagate essentially with the velocity of light  $c$ . No frequency components below the cutoff frequency  $f_c$  can propagate along the guide.

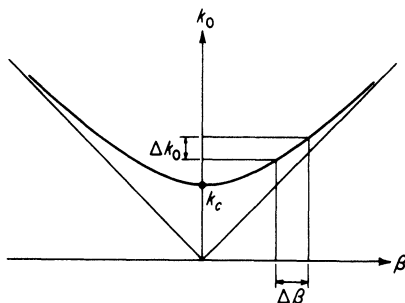


**FIGURE 3.45**  
Plot of  $k_0$  versus  $\beta$  for a waveguide.

The equality of the wavefront velocity and the velocity of light can be readily explained by means of Fig. 3.45. The switching on of a signal results in an initial transient that has a spectrum of frequencies extending out to infinity. Any small group of frequencies at the high end of the spectrum will have a group velocity equal to  $c$  since  $dk_0/d\beta$  equals unity for  $k_0$  near infinity. Thus the high-frequency part of the transient will propagate along the guide with a velocity  $c$ . The lower-frequency components will propagate with smaller group velocities and arrive later.

## Energy-Flow Velocity

Power is a flow of energy, and consequently there is a velocity of energy flow such that the average energy density in the guide multiplied by this velocity is equal to the power. In a waveguide it turns out that this velocity of energy flow is equal to the group velocity. A proof for the case of  $E$  modes will be given below, that for  $H$  modes being very similar.

For  $E$  modes the field is given by [see (3.72)]

$$\mathbf{E}_t = -\frac{j\beta}{k_c^2} \nabla_t e_z e^{-j\beta z} \quad \mathbf{H}_t = \frac{k_0 Y_0}{\beta} \mathbf{a}_z \times \mathbf{E}_t$$

The average rate of energy flow, or power, is given by

$$P = \frac{1}{2} \int_S Y_e |\mathbf{E}_t|^2 dS = \frac{1}{2} \frac{k_0 Y_0}{\beta} \int_S |\mathbf{E}_t|^2 dS \quad (3.241)$$

where the integration is over the guide cross section.

The energy density in the magnetic field per unit length of guide is

$$U_m = \frac{\mu_0}{4} \int_S |\mathbf{H}_t|^2 dS = \frac{\mu_0}{4} \frac{k_0^2 Y_0^2}{\beta^2} \int_S |\mathbf{E}_t|^2 dS \quad (3.242)$$

The energy density in the electric field per unit length of guide is equal to that in the magnetic field. This is readily shown to be the case by using the complex Poynting vector theorem, which states that (Sec. 2.5)

$$\frac{1}{2} \int_S \mathbf{E} \times \mathbf{H}^* \cdot \mathbf{a}_z dS = P + 2j\omega(W_m - W_e)$$

where the integration is over the guide cross section, and the term on the right gives the power transmitted past the plane  $S$  plus  $2j\omega$  times the net reactive energy stored in the guide beyond the plane  $S$ . Since the integral of the complex Poynting vector over a cross section  $S$  for a propagating mode in a loss-free guide is real, it follows that  $W_m = W_e$ . In addition, since the location of the transverse plane  $S$  is arbitrary, it also follows that the energy densities  $U_m$  and  $U_e$  per unit length of guide are equal.

The velocity of energy flow may now be found from the relation

$$\begin{aligned} v &= \frac{P}{U_e + U_m} = \frac{P}{2U_m} = \frac{k_0 Y_0}{\beta} \frac{\beta^2}{\mu_0 k_0^2 Y_0^2} \\ &= \frac{\beta}{\mu_0 k_0 Y_0} = \frac{\beta}{k_0 \sqrt{\mu_0 \epsilon_0}} = \frac{\beta}{k_0} c = v_g \end{aligned} \quad (3.243)$$

and comes out equal to the group velocity as stated earlier.

### 3.20 RIDGE WAVEGUIDE

For a rectangular waveguide with a width  $a$  equal to twice the height  $b$ , the maximum bandwidth of operation over which only the dominant  $TE_{10}$  mode propagates is a 2 : 1 band. For some system applications it is necessary to have a waveguide that operates with only a single mode of propagation over much larger bandwidths. A transmission line supporting only a TEM mode can fulfill this requirement but must then have cross-sectional dimensions that are small relative to the shortest wavelength of interest. A coaxial transmission line will support higher-order TE and TM modes in addition to the TEM mode. Thus, to avoid excitation of a higher-order mode of propagation, the outer radius must be kept small relative to the wavelength. The small cross section implies a relatively large attenuation; so some other form of waveguide is needed. The ridge waveguide illustrated in Fig. 3.46 was developed to fulfill this need for a single-mode waveguide capable of operating over a very broad band. Physically, it is easy to understand why the ridge waveguide has a very large frequency band of operation. The center section of width  $W$  and spacing  $S$  functions very much like a parallel-plate transmission line and consequently the ridge waveguide has a much lower cutoff frequency for the same width and height as does the

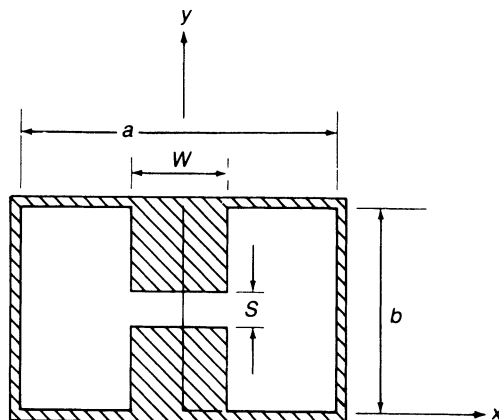


**FIGURE 3.46**  
Ridge waveguide.

conventional rectangular waveguide. Operation over bandwidths of 5 to 1 or more is possible.

The ridge waveguide, when uniformly filled with dielectric, which can be air, has the same general properties as the rectangular and circular waveguides discussed earlier. If we can determine the cutoff wavelength  $\lambda_c$  for the dominant mode, then at any frequency above the cutoff frequency the propagation constant  $\beta$  is given by

$$\beta = \sqrt{k_0^2 - (2\pi/\lambda_c)^2}$$

At the cutoff frequency  $\beta = 0$  and the electromagnetic field has no variation with the axial coordinate  $z$ . The cutoff wave number  $k_c = 2\pi/\lambda_c$  can be found using the transverse-resonance method as described below.

The transverse-resonance method is based on finding the resonant frequency for the transmission-line circuit that provides a model for the waveguide cross section. At cutoff we can view the electromagnetic field as a uniform plane wave with components  $E_y$  and  $H_z$  that propagates in the  $x$  direction and is incident onto a second parallel-plate transmission line of reduced height. The equivalent transmission-line circuit is that of two parallel-plate transmission lines of height  $b$ , length  $(a - W)/2$ , and short-circuited at  $x = 0$  and  $a$ . These two transmission lines are connected to another parallel-plate line of height  $S$  and length  $W$  and placed between the first two as shown in Fig. 3.47. At the junction where the height changes, a local fringing electric field occurs and stores electric field energy in the vicinity of the step. The effect of this local fringing electric field is taken into account by a shunt capacitive susceptance  $jB$  at each junction as shown in Fig. 3.47.

The standing-wave field pattern along the  $x$  direction can exist only at the resonant frequency for the transmission-line circuit shown in Fig. 3.47. For the dominant mode the voltage is a maximum and the current is zero at the midsection. Thus, at  $x = a/2$ , the impedance looking in the  $x$  direction toward the short circuit must be infinite. The corresponding input admittance will be zero. At the step the admittance looking toward the short circuit is

$$Y = -jY_{c1} \cot k_c \frac{a - W}{2} + jB$$

By using the formula for admittance transformation along a transmission

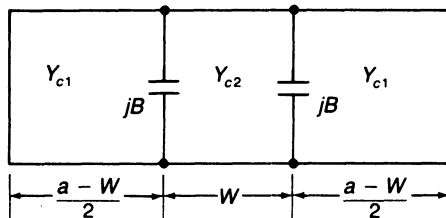


**FIGURE 3.47**  
Equivalent transmission-line circuit of cross section of ridge waveguide.



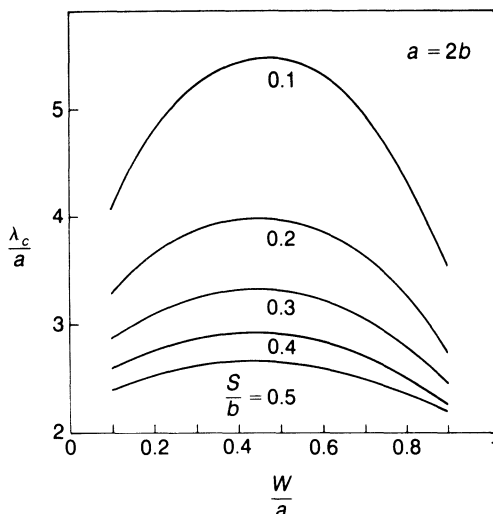


**FIGURE 3.48**  
Normalized cutoff wavelength  $\lambda_c/a$  for a ridge waveguide.

line, we obtain

$$Y_{\text{in}} = Y_{c2} \frac{Y + jY_{c2} \tan k_c W/2}{Y_{c2} + jY \tan k_c W/2}$$

In order for  $Y_{\text{in}}$  to vanish, we must have

$$jB - jY_{c1} \cot k_c \frac{a - W}{2} + jY_{c2} \tan k_c \frac{W}{2} = 0 \quad (3.244)$$

which is the transverse-resonance condition. The two characteristic admittances are inversely proportional to the parallel-plate spacing; thus  $Y_{c2} = (b/S)Y_{c1}$ . An approximate expression for the normalized shunt capacitive susceptance can be found using quasistatic conformal mapping and is<sup>†</sup>

$$\frac{B}{Y_{c1}} = \frac{2b}{\lambda_c} \left[ 1 - \ln 4u + \frac{1}{3}u^2 + \frac{1}{2}(1 - u^2)^4 \frac{b^2}{\lambda_c^2} \right] \quad u = \frac{S}{b} < 0.5 \quad (3.245)$$

The eigenvalue equation (3.244) is a transcendental equation. The computer program RIDGEWG solves (3.244) for the normalized cutoff wavelength  $\lambda_c/a$ .

Figure 3.48 shows typical results that are obtained. The numerical results obtained from (3.244) agree within 1 percent of the values given by Hopfer and Hoefler and Burton over the commonly used range of parameters.<sup>‡</sup>

<sup>†</sup>N. Marcuvitz, "Waveguide Handbook," MIT Radiation Lab Series, vol. 10, reprinted by Boston Technical Publishers, Inc., 1964.

<sup>‡</sup>S. Hopfer, The Design of Ridged Waveguides *IRE Trans.*, vol. MTT-3, pp. 20-29, October, 1955.

W. J. R. Hoefler and M. N. Burton, Closed Form Expression for the Parameters of Finned and Ridged Waveguides, *IEEE Trans.*, vol. MTT-30, pp. 2190-2194, December 1982.

### 3.21 FIN LINE

If the width  $W$  of the ridges in the ridge waveguide is very small, we obtain a fin line as shown in Fig. 3.49a. Usually the fins are metal foils on a thin dielectric substrate mounted in the  $E$  plane of a rectangular waveguide. For the dominant mode the current flows in the axial direction; so good electrical contact between the fins and the waveguide is not essential. The fin line is a shielded slot line. The fin line can be matched to the rectangular waveguide by means of a tapered section or by using one or more quarter-wave impedance transformers as shown in Figs. 3.49b and c.

The fin line is suitable for use in microwave circuits that incorporate two-terminal devices such as diodes. Transistors cannot be connected to a fin line since they are three-terminal devices.

The cutoff wavelength for a fin line may also be found by using the transverse-resonance method. The fins produce a shunt normalized capacitive susceptance across the center of the waveguide given by†

$$\frac{B}{Y_c} = \frac{2b}{\lambda_c} \left[ \ln \frac{1}{\alpha_2} + \sum_{n=1}^4 \left( \frac{\pi}{\Gamma_n b} - \frac{1}{n} \right) P_n^2 + \frac{\left( \frac{\pi}{\Gamma_1 b} - 1 \right) P_1^2}{1 + \left( \frac{\pi}{\Gamma_1 b} - 1 \right) \alpha_2^2} \right] \quad (3.246)$$

where

$$P_1 = \alpha_1$$

$$P_2 = 2\alpha_1^2 + \alpha_2^2 - 1$$

$$P_3 = 4\alpha_1^3 + 6\alpha_1\alpha_2^2 - 3\alpha_1$$

$$P_4 = 8\alpha_1^4 + 3\alpha_2^4 + 24\alpha_1^2\alpha_2^2 - 8\alpha_1^2 - 4\alpha_2^2 + 1$$

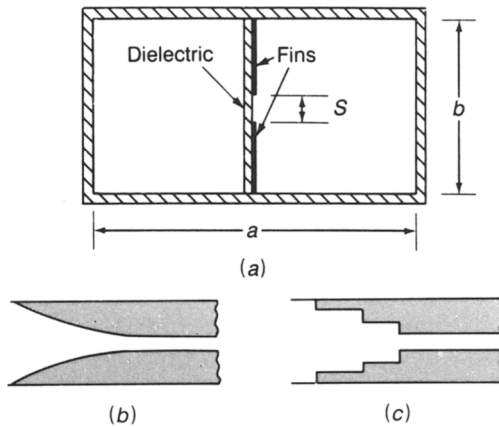
$$\alpha_1 = \cos^2 \frac{\pi S}{2b}$$

$$\alpha_2 = \sin^2 \frac{\pi S}{2b}$$

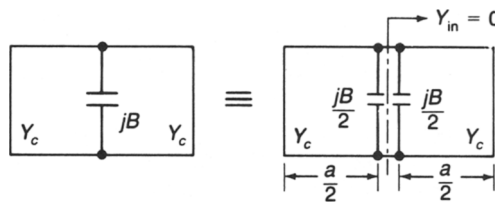
$$\Gamma_n = \left[ \left( \frac{n\pi}{b} \right)^2 - \left( \frac{2\pi}{\lambda_c} \right)^2 \right]^{1/2}$$

The equivalent circuit of the fin-line cross section consists of two short-circuited transmission lines of length  $a/2$  with  $jB$  connected at the center as

†R. E. Collin, "Field Theory of Guided Waves," 2nd ed., chap. 8, IEEE Press, Piscataway, N.J., 1990.


**FIGURE 3.49**

(a) Fin line; (b) tapered matching section; (c) quarter-wave matching section.


**FIGURE 3.50**

Equivalent circuit of fin-line cross section.

shown in Fig. 3.50. The resonance condition is

$$\frac{Y_{in}}{Y_c} = \frac{jB}{2Y_c} - j \cot \frac{\pi a}{\lambda_c} = 0 \quad (3.247)$$

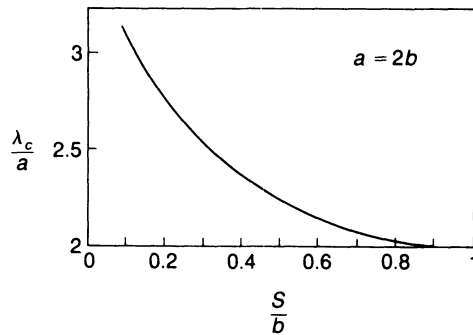
The computer program FINLINE solves this transcendental equation for the normalized cutoff wavelength  $\lambda_c/a$  for  $S/b = 0.1$  to  $0.9$ . Typical numerical results are shown in Fig. 3.51 for the case where  $a = 2b$ . These numerical results agree within 1 percent or better with those given by Hoefler and Burton.<sup>†</sup>

The propagation constant  $\beta$  is given by the same formula as for a conventional waveguide, i.e.,

$$\beta = (k_0^2 - k_c^2)^{1/2}$$

When the fins are mounted on a dielectric substrate, a correction is needed for the propagation constant if the dielectric has an appreciable thickness

<sup>†</sup>W. J. R. Hoefler and M. N. Burton, *loc. cit.*

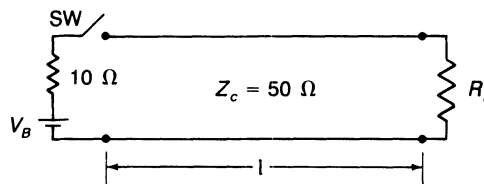

**FIGURE 3.51**

 Normalized cutoff wavelength  $\lambda_c/a$  for a fin line.

and a large dielectric constant. Empirical formulas for this case are available.†

## PROBLEMS

- 3.1.** For the ideal transmission line shown in Fig. P3.1, the switch is closed at  $t = 0$  and opened  $1 \mu\text{s}$  later. The characteristic impedance of the line is  $50 \Omega$ . The load resistance is also  $50 \Omega$ . The battery has an internal resistance of  $10 \Omega$ .
- Sketch the voltage across  $R_L$  as a function of time for a line  $300 \text{ m}$  long. The wave velocity  $v = 3 \times 10^8 \text{ m/s}$ .
  - Sketch the voltage waveform across  $R_L$  when  $R_L = 25 \Omega$  and the line is  $900 \text{ m}$  long.
  - Sketch the voltage waveform across  $R_L$  when  $R_L = 100 \Omega$  and the line is  $900 \text{ m}$  long.
  - Repeat (b) and (c) for a line  $75 \text{ m}$  long.


**FIGURE P3.1**

- 3.2.** Let a generator with internal resistance  $R_g$  be connected to a transmission line of length  $l$  and having a characteristic impedance  $Z_c$ . The line is terminated in a load resistance  $R_L$ . Let  $\tau = l/v$  be the one-way propagation time delay. The generator produces a pulsed waveform  $P(t)$ ,  $0 \leq t \leq T$ . Show that the voltage across  $R_L$  is given by

$$V_L = \frac{Z_c}{Z_g + Z_c} (1 + \Gamma_L) \left[ P(t - \tau) + \Gamma_L \Gamma_g P(t - 3\tau) + \Gamma_L^2 \Gamma_g^2 P(t - 5\tau) + \cdots \right]$$

†K. Chang (ed.), "Handbook of Microwave and Optical Components," vol. 1, pp. 38–39, John Wiley & Sons, Inc., New York, 1989.

*Hint:* See (3.12) and consider the total line voltage at  $z = l$ .

- 3.3.** A pulse generator produces a sawtooth pulse  $P(t) = 10t/T$ ,  $0 \leq t \leq T$ , where  $T = 10^{-8}$  s. The generator has an internal resistance  $R_g = 200 \Omega$  and is connected to a transmission line with  $Z_c = 50 \Omega$ . The line is  $l$  meters long and terminated in a load resistance  $R_L$ . The wave velocity equals  $3 \times 10^8$  m/s.
- Find and sketch the load voltage as a function of time when  $l = 3$  m and  $R_L = 200 \Omega$ .
  - Repeat (a) when  $R_L = 12.5 \Omega$ .
  - Find an analytic expression for the voltage across  $R_L$  when  $R_L = 200 \Omega$  and  $l = 12$  m.
  - Make a distance-time plot of the line voltage for (c).
- 3.4.** A battery with voltage of 10 V is connected in series with a 50- $\Omega$  resistor to the input of a 50- $\Omega$  transmission line at time  $t = 0$ . The transmission line, of length 12 m, is terminated in a 1- $\mu$ F capacitor. Find and sketch the voltage across the capacitor as a function of time.

*Hint:* Apply Thévenin's theorem.

*Answer:*

$$V_c = 10[1 - e^{-(t-0.04)/50}] \quad t \text{ in microseconds}$$

- 3.5.** In the circuit illustrated in Fig. P3.5, the battery is connected at  $t = 0$ . Find and sketch the voltage across  $R_L$  as a function of time. Assume that  $R_L = R_g = Z_c = 50 \Omega$ ,  $C = 1 \mu\text{F}$ ,  $l = 300$  m, and  $v = 3 \times 10^8$  m/s.

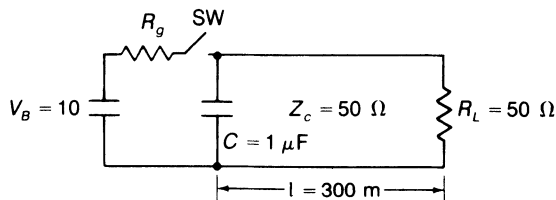


**FIGURE P3.5**

- 3.6.** The resistor  $R_L$  is replaced by a capacitor  $C_L = 1 \mu\text{F}$  in Fig. P3.5. Find the voltage across  $C_L$  during the time interval  $1 \mu\text{s} \leq t \leq 3 \mu\text{s}$ .

*Answer:*

$$V_L = 5[1 + e^{-(t-1)/25}] - 10e^{-(t-1)/50}$$

where  $t$  is in microseconds.

- 3.7.** Consider an ideal loss-free transmission line of length  $l$ , as shown in Fig. P3.7. The far end is short-circuited. At the input end a battery of voltage  $V_0$  is switched across the line at time  $t = 0$ . Sketch the voltage wave on the line at the middle over the time interval  $0 \leq t \leq 7l/c$ .

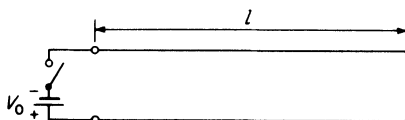


**FIGURE P3.7**

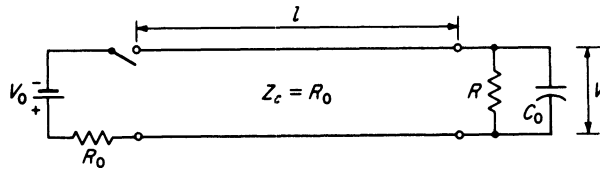


FIGURE P3.8

- 3.8. Consider the transmission-line circuit illustrated in Fig. P3.8. At time  $t = 0$ , a battery of voltage  $V_0$  is switched across the line at the input. Determine the output load voltage  $V$  as a function of time.

*Hint:* This transient problem may be solved in a manner similar to that used in low-frequency circuit theory. The governing equations for the transmission line are

$$\frac{\partial V}{\partial z} = -L \frac{\partial \mathcal{I}}{\partial t} \quad \frac{\partial \mathcal{I}}{\partial z} = -C \frac{\partial V}{\partial t}$$

The time derivative may be eliminated by taking the Laplace transform. The transformed solutions for  $V$  and  $\mathcal{I}$  are

$$V^+ e^{-sz/v} + V^- e^{sz/v} \quad I^+ e^{-sz/v} + I^- e^{sz/v}$$

By transforming the circuit equations for the load termination and the input voltage, the resultant equations may be solved for the Laplace transform of the load voltage. The inverse transform then gives the load voltage as a function of time.

The foregoing procedure may be simplified by first replacing the battery by a source  $V_0 e^{j\omega t}$  and obtaining the transfer function  $V/V_0 = Z_t(j\omega)$  as a function of  $\omega$  for this steady-state problem. Replacing  $j\omega$  by  $s$  then gives the transfer function in the  $s$  domain. The Laplace transform of the output voltage is then

$$V(s) = \frac{V_0}{s} Z_t(j\omega = s)$$

since the Laplace transform of the input step voltage is  $V_0/s$ . The output voltage is obtained from the inverse Laplace transform of  $V(s)$ .

- 3.9. Obtain expressions for the voltage and current standing-wave patterns on a lossless open-circuited transmission line. Sketch these patterns. Assume an  $e^{j\omega t}$  time dependence.
- 3.10. A transmission line with  $Z_c = 50 \Omega$  is terminated in an impedance  $25 + j25 \Omega$ . Find the reflection coefficient, standing-wave ratio, and fraction of the incident power delivered to the load.  
*Answer:* VSWR = 2.618, 80 percent.
- 3.11. Verify (3.47) and compute  $Z_{in}$  at a distance  $\lambda_0/4$  from the termination given in Prob. 3.10.
- 3.12. On a transmission line with  $Z_c = 50 \Omega$ , the voltage at a distance  $0.4\lambda_0$  from the load is  $4 + j2$ . The corresponding current is 0.1 A. Determine the normalized load impedance.  
*Answer:*  $0.145 + j0.397$ .
- 3.13. A  $50\text{-}\Omega$  transmission line is terminated by a  $75\text{-}\Omega$  load resistor. Find the distance  $l$  from the load at which  $Y_{in} = 0.02 + jB$ . By connecting a shunt

susceptance  $-jB$  across the line at this point, the load will be matched to the transmission line. Explain why this is so. The distance  $l$  can be expressed in terms of the wavelength  $\lambda_0$ .

- 3.14.** Figure P3.14 illustrates a three-conductor transmission line. Since potential is arbitrary to within an additive constant, the shield  $S_0$  can be chosen to be at zero potential. Show that there are two linearly independent solutions for TEM waves in this transmission line. If  $S_0$  encloses  $N$  conductors, how many TEM-wave solutions are possible?

*Hint:* Note that the potential can be arbitrarily specified on  $S_1$  and  $S_2$ .

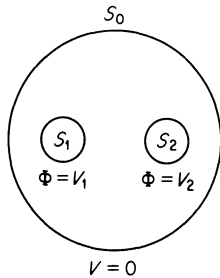


**FIGURE P3.14**

- 3.15.** Show that power transmitted along a transmission line is given by

$$P = \frac{Y_0}{2} \int |\nabla_t \Phi|^2 dx dy$$

For Prob. 3.14 show that this equals  $\frac{1}{2}(V_1 I_1 + V_2 I_2)$  by using Green's first identity (App. I) to convert the surface integral to a contour integral around the conductor boundaries.  $I_1$  and  $I_2$  are the total currents on  $S_1$  and  $S_2$ .

- 3.16.** Consider a three-conductor transmission line as shown in Fig. P3.14 but assume that the cross sections of  $S_1$  and  $S_2$  are not the same. Let  $\Phi_a$  and  $\Phi_b$  be two different solutions for the potential field. For  $\Phi_a$  let  $V_{a1}$ ,  $I_{a1}$  and  $V_{a2}$ ,  $I_{a2}$  be the voltage and currents on  $S_1$  and  $S_2$ . Similarly, for  $\Phi_b$  let  $V_{b1}$ ,  $I_{b1}$  and  $V_{b2}$ ,  $I_{b2}$  be the voltages and currents on  $S_1$  and  $S_2$ . For the TEM modes derived from  $\Phi_a + \Phi_b$ , show that the power flow is given by

$$\frac{1}{2}(V_{a1} + V_{b1})(I_{a1} + I_{b1}) + \frac{1}{2}(V_{a2} + V_{b2})(I_{a2} + I_{b2})$$

It is convenient to choose the potentials so that the two TEM modes obtained from  $\Phi_a$  and  $\Phi_b$  have independent power flow. Show that this will be the case if the interaction term

$$(V_{a1} I_{b1} + V_{b1} I_{a1}) + (V_{a2} I_{b2} + V_{b2} I_{a2})$$

equals zero. Furthermore, show that the interaction term will vanish if the potentials are chosen so that

$$\frac{V_{a1}}{V_{a2}} = -\frac{V_{b1}}{V_{b2}} = \left[ \frac{C_{22} + C_{12}}{C_{11} + C_{12}} \right]^{1/2}$$

where  $C_{11}$  is the capacitance between  $S_1$  and  $S_0$ ,  $C_{22}$  is the capacitance between  $S_2$  and  $S_0$ , and  $C_{12}$  is the capacitance between  $S_1$  and  $S_2$ . For a

symmetrical line,  $C_{11} = C_{22}$  and the two modes correspond to the even and odd modes.

*Hint:* Use the relations  $Q_{a1} = C_{11}V_{a1} + C_{12}(V_{a1} - V_{a2})$ ,  $Q_{a2} = C_{22}V_{a2} + C_{12}(V_{a2} - V_{a1})$  and similar ones for the total charge  $Q_{b1}$  and  $Q_{b2}$  on  $S_1, S_2$  in terms of  $V_{b1}$  and  $V_{b2}$ . Also note that  $I_{a1} = (Y_0/\epsilon_0)Q_{a1}$ , etc.

- 3.17.** Show that, for an air-filled coaxial line, minimum attenuation occurs when  $x \ln x = 1 + x$ ,  $x = b/a$ . What is the corresponding characteristic impedance?

*Hint:* Hold the outer radius  $b$  constant and find  $da/da$ .

- 3.18.** Evaluate  $Z_c$  for a lossy coaxial line using (3.28) and computed values of  $R, G, L$ , and  $C$ . Assume  $b = 3a = 1$  cm,  $f = 10^9$  Hz,  $\sigma = 5.8 \times 10^7$  S/m, and  $\epsilon = (2.56 - j0.001)\epsilon_0$ . Verify that

$$\text{Im } Z_c \ll \text{Re } Z_c \quad \text{and} \quad Z_c \approx \left(\frac{L}{C}\right)^{1/2}$$

See Table 3.1 for coaxial-line parameters.

- 3.19.** Use the energy definitions of  $L$  and  $C$  [Eqs. (3.112)] to derive the results given by (3.106) and (3.108) for a coaxial transmission line.

- 3.20.** A microstrip line has a substrate 1 mm thick and with a dielectric constant  $\epsilon_r = 8$ . The strip width  $W = 2.5$  mm. Find the low-frequency effective dielectric constant and characteristic impedance.

*Answer:*  $\epsilon_e = 5.953$ ,  $Z_c = 32.13 \Omega$ .

- 3.21.** A microstrip line uses an anisotropic dielectric substrate with  $\epsilon_r = 10$  and  $\epsilon_y = 8$ . The substrate is 0.5 mm thick and the strip width  $W = 0.75$  mm. Find the low-frequency effective dielectric constant and characteristic impedance.

*Answer:*  $\epsilon_e = 5.895$ ,  $Z_c = 42.97 \Omega$ .

- 3.22.** A microstrip line has a 1-mm-thick dielectric substrate with a dielectric constant of 6. Use the computer program MSTP to generate data giving the effective dielectric constant and characteristic impedance as a function of strip width  $W$ . Use these data to design a microstrip system with an input line having  $Z_c = 50 \Omega$ , an output line having  $Z_c = 75 \Omega$ , and an intermediate quarter-wave transformer section with  $Z_c = \sqrt{50 \times 75} \Omega$ . Specify the three strip widths  $W_1, W_2, W_3$  and the length of the quarter-wave transformer at a frequency  $f = 2$  GHz (see Fig. P3.22).

*Answer:* Widths are 1.505 mm, 1.0125 mm, 0.649 mm, length = 1.83 cm.

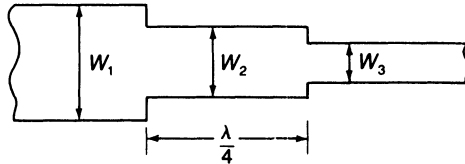


**FIGURE P3.22**

- 3.23.** Find the effective dielectric constant, characteristic impedance, and attenuation at 2 GHz for a microstrip line with the following parameters:  $\epsilon_r = 9.5$ , loss tangent =  $2 \times 10^{-3}$ , substrate thickness  $H = 1$  mm, strip width = 1.5 mm, and strip thickness  $T = 0.01$  mm. Use the computer program MSTP.



- 3.24.** Use the computer program MSTPD to generate dispersion data for the effective dielectric constant for a microstrip line having the following parameters: dielectric constant = 6, substrate thickness  $H = 0.5$  mm, and strip width  $W = 2$  mm. At what frequency has the effective dielectric constant increased by 5 percent more than the quasistatic value?
- 3.25.** In a monolithic microwave integrated circuit, gallium arsenide with  $\epsilon_r = 12.9$  is used as a substrate material. Find the effective dielectric constant, characteristic impedance, and attenuation at 10 GHz for a microstrip line with the following parameters: substrate thickness = 0.1 mm, strip width = 0.05 mm, strip thickness = 0.002 mm, and loss tangent =  $6 \times 10^{-3}$ . For these dimensions the quasistatic parameters are accurate. The computer program MSTP can be used for the evaluation. What is the attenuation in decibels per wavelength (microstrip) for this microstrip line?
- 3.26.** A microstrip line has the following parameters: strip width  $W = 1$  mm, substrate thickness = 1 mm, and anisotropic dielectric with  $\epsilon_r = 6.5$ ,  $\epsilon_y = 6$ . Find the following: distributed capacitance  $C$  and inductance  $L$  per centimeter, characteristic impedance, effective dielectric constant, and the quasi-TEM-mode wavelength at 2 GHz.
- 3.27.** Use the computer program CMSTP to find the even- and odd-mode characteristic impedances and the voltage coupling coefficient  $C$  for a coupled microstrip line having the following parameters: strip width  $W = 1$  mm, strip spacing  $S = 0.1$  mm, substrate thickness = 1 mm, and substrate dielectric constant = 9.7.
- 3.28.** A strip line has a ground-plane spacing of 2 mm, a strip width of 1 mm, and is filled with a dielectric medium with dielectric constant 2.3. Find the characteristic impedance.
- 3.29.** Use the computer program STPL to evaluate the characteristic impedance and attenuation of a strip line with the following parameters: ground-plane spacing = 2 mm, strip width  $W = 0.5$  mm, strip thickness  $T = 0.01$  mm, dielectric constant = 6, loss tangent = 0.006, and frequency of operation = 5 GHz. What is the ratio of the attenuation due to dielectric loss relative to that of conductor loss?
- 3.30.** A broadside coupled strip line is required for a 3-dB directional coupler. The even-mode characteristic impedance is to be 50  $\Omega$ . The voltage coupling coefficient is 0.707. From this information determine the required odd-mode characteristic impedance. Find the required strip width  $W$  and spacing  $S$  for this coupled strip line. The ground-plane spacing is 4 mm and the dielectric constant of the dielectric filling is 5. The strip thickness  $T = 0.05$  mm. Use the computer program CSTPL. You will need to follow an iterative procedure to arrive at the required parameters. An accuracy of  $\pm 0.5$  percent is adequate.  
*Hint:* Begin with  $W = 3.5$  mm,  $S = 0.5$  mm.
- 3.31.** In a monolithic microwave integrated circuit, a coplanar transmission line with the following parameters is used: strip width  $S = 0.1$  mm, slot width  $W = 0.1$  mm, strip thickness = 0.002 mm, substrate thickness = 0.5 mm, dielectric constant = 12.9, loss tangent = 0.0008, and frequency = 10 GHz. Use the computer program CPW to determine the characteristic impedance

and attenuation. If the strip thickness is increased to 0.005 mm, will this significantly reduce the attenuation?

- 3.32.** Figure P3.32 shows a coplanar-transmission-line circuit for use in a MMIC amplifier circuit. The required input- and output-line characteristic impedances are  $50 \Omega$  and  $72 \Omega$ . The impedance of the quarter-wave section is  $\sqrt{50 \times 72} = 60 \Omega$ . The ground-plane spacing  $2W + S$  is kept constant at 0.3 mm. The strip thickness is 0.002 mm. The substrate thickness is 0.4 mm and the dielectric constant is 12.9 with a loss tangent of 0.001. Use the computer program CPW to determine the required strip widths  $S_1$ ,  $S_2$ , and  $S_3$ . Determine the length  $l$  of the quarter-wave matching section at a frequency of 10 GHz. How much attenuation occurs in the quarter-wave section? An accuracy of  $\pm 0.25$  percent is sufficient.

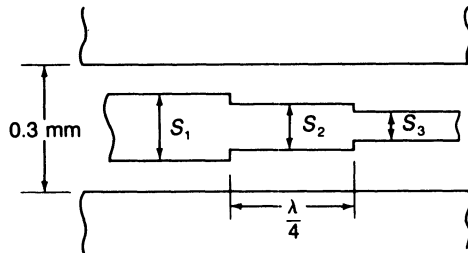


FIGURE P3.32

- 3.33.** In a planar transmission line, the attenuation is 0.25 dB/cm. By what fraction is the wave amplitude reduced in propagating a distance of 1 cm on this transmission line?
- 3.34.** Derive the equations (3.72) for TM waves.
- 3.35.** Find the cutoff frequency for the  $TE_{10}$  mode in a rectangular waveguide with dimensions 4 cm by 2 cm. Find the guide wavelength  $\lambda_g$  and phase velocity at a frequency 25 percent higher than the cutoff frequency.
- 3.36.** Derive the solution for a  $TE_{10}$  mode in a rectangular guide of wide dimension  $a$  and height  $b$  when the guide is filled with dielectric of permittivity  $\epsilon$ . Show that the cutoff frequency is given by  $f_c = c/2a\epsilon_r^{1/2}$ , where  $c$  is the free-space velocity of light and  $\epsilon_r$  is the dielectric constant. Show that the guide wavelength is smaller for a dielectric-filled guide than for an air-filled guide.
- 3.37.** Obtain an expression for the attenuation of a  $TE_{10}$  mode in a dielectric-filled guide when  $\epsilon = \epsilon_1 - j\epsilon_2$  but the walls are perfectly conducting. Obtain an exact expression and compare it with the results deduced by an application of the perturbation method.
- 3.38.** Obtain a solution for an  $H$  wave in the parallel-plate transmission line with centered dielectric slab as illustrated in Fig. P3.38. Assume that the plates are perfectly conducting and infinitely wide. Can a TEM wave propagate in this structure? Why?

*Hint:* Assume  $h_z = \cos k_d x$  for  $|x| \leq a/2$  and  $h_z = Ae^{-p|x|}$  for  $|x| > a/2$ . Verify that  $k_d^2 + p^2 = (\epsilon_r - 1)k_0^2$ . Match the tangential fields at  $x = a/2$  to obtain an equation for  $A$  and one relating the parameters  $p$  and  $k_d$ .

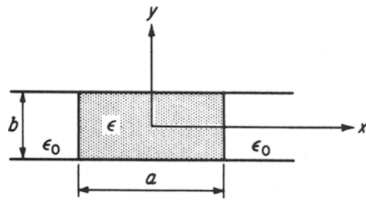


FIGURE P3.38

- 3.39.** Obtain solutions for  $TE_{n,0}$  modes in the partially filled waveguide illustrated in Fig. P3.39.

*Hint:* Assume that

$$h_z = \begin{cases} \cos k_d x & 0 < x < t \\ A \cos p(a - x) & t < x < a \end{cases}$$

and match the tangential fields at  $x = t$ . Thus show that

$$\beta^2 = k_0^2 - p^2 = \epsilon_r k_0^2 - k_d^2$$

and that

$$p \tan k_d t = -k_d \tan p d$$

Note that there are an infinite number of solutions for  $p$  and  $k_d$  corresponding to various  $TE_{n,0}$  modes. Obtain numerical values for  $\beta$ ,  $p$ , and  $k_d$  when  $k_0 = 2$ ,  $t = 1$  cm,  $d = 1.5$  cm, and  $\epsilon_r = 4$ . Note that there is a lowest-order solution for  $p$  pure imaginary.

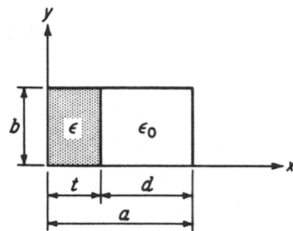


FIGURE P3.39

- 3.40.** Obtain expressions for the surface currents of a  $TE_{1,0}$  mode in a rectangular guide. A narrow slot may be cut in a waveguide along a current flow line without appreciably disturbing the field. Show that, for the  $TE_{1,0}$  mode, narrow centered axial slots may be cut in the broad face of a rectangular guide. This principle is used in standing-wave detectors to provide suitable points of entry for a probe used to sample the interior waveguide field.
- 3.41.** Use the computer program RECTWG to evaluate the parameters of a rectangular waveguide with width  $a = 1$  cm, height  $b = 0.4$  cm at a frequency of 20 GHz. How much attenuation will occur in a waveguide 5 m long?
- 3.42.** For TE modes in a waveguide, write  $\mathbf{H}_t = -I(z)\nabla_t h_z$ ,  $\mathbf{E}_t = V(z)\mathbf{a}_z \times \nabla_t h_z$ . Use Maxwell's equations to show that  $V(z)$  and  $I(z)$  satisfy the transmission-

line equations

$$\frac{dV}{dz} = -j\omega\mu_0 I \quad \frac{dI}{dz} = -\left(j\omega\epsilon_0 + \frac{k_c^2}{j\omega\mu_0}\right)V$$

Construct an equivalent distributed-parameter circuit for these modes. For TM modes put  $\mathbf{E}_t = -V(z)\nabla_t e_z$ ,  $\mathbf{H}_t = -I(z)\mathbf{a}_z \times \nabla_t e_z$ , and show that

$$\frac{dV}{dz} = -\left(j\omega\mu_0 + \frac{k_c^2}{j\omega\epsilon_0}\right)I \quad \frac{dI}{dz} = -j\omega\epsilon_0 V$$

Construct an equivalent distributed-parameter circuit for these modes.†

- 3.43.** Consider an infinitely long rectangular guide. The guide is filled with dielectric for  $z \geq 0$ , having a dielectric constant  $\epsilon_r$ . An  $H_{10}$  mode is incident from  $z < 0$ . At  $z = 0$ , a reflected  $H_{10}$  mode and a transmitted  $H_{10}$  mode are produced because of the discontinuity. Show that the reflection coefficient is given by  $(Z_2 - Z_1)/(Z_2 + Z_1)$ , where  $Z_1$  is the wave impedance in the empty guide and  $Z_2$  is the wave impedance in the dielectric-filled guide. Show that the ratio of the wave impedances equals the ratio of the guide wavelengths.
- 3.44.** Find the surface currents for the  $H_{01}$  mode in a circular guide.
- 3.45.** Obtain an expression for power in a  $TE_{11}$  mode in a circular guide. (See App. II for Bessel-function integrals.)
- 3.46.** Derive an expression for attenuation for  $TE_{0m}$  modes in a circular waveguide.  
*Answer:*  $\alpha = R_m f_{c,0m}^2 / [aZ_0 f(f^2 - f_{c,0m}^2)^{1/2}]$ .
- 3.47.** Find the attenuation in decibels per mile for an  $H_{01}$  mode in a circular copper guide of 1 in diameter when operated at a frequency of 10 times the cutoff frequency.
- 3.48.** Show that, in a coaxial line with inner radius  $a$  and outer radius  $b$ , there are solutions for  $TE_{nm}$  and  $TM_{nm}$  modes. A suitable solution for  $e_z$  and  $h_z$  is

$$[AJ_n(k_c r) + Y_n(k_c r)]\cos n\phi$$

Obtain equations (transcendental in nature) for determining the cutoff wave number  $k_c$  by imposing proper boundary conditions at  $r = a, b$ .

- 3.49.** Use the computer program RIDGEWG to find the cutoff wavelength and frequency for a ridge waveguide with dimensions  $a = 1$  cm,  $b = 0.4$  cm, ridge width = 0.5 cm, and ridge spacing  $S = 0.1$  cm. Compare this with the cutoff frequency of a standard waveguide with  $a = 1$  cm and  $b = 0.4$  cm.
- 3.50.** Use the transverse-resonance technique to derive the eigenvalue equation for  $TE_{n0}$  modes in the partially filled rectangular guide of Prob. 3.39. Verify that the wave impedances in the  $x$  direction in the two regions are  $k_0 Z_0/p$  and  $kZ/k_d = k_0 Z_0/k_d$ .
- 3.51.** A rectangular waveguide with internal dimensions  $a = 0.9$  in and  $b = 0.4$  in (standard X-band waveguide) has a centered fin with a slot spacing  $S = 2$  mm. Find the cutoff wavelength and compare it with that for the waveguide without fin loading. Use the computer program FINLINE.

†S. A. Schelkunoff, *Bell System Tech. J.*, vol. 34, p. 995, September, 1955.

- 3.52. The permittivity  $\epsilon$  is generally a function of  $\epsilon(\omega)$  of  $\omega$ . Obtain an expression for the group velocity of a coaxial line filled with dielectric. Neglect the frequency dependence of the attenuation due to conductor loss.
- 3.53. A rectangular guide of dimensions  $a = 2b = 2.5$  cm is operated at a frequency of  $10^{10}$  Hz. A pulse-modulated carrier of the above frequency is transmitted through the guide. How much pulse delay time is introduced by a guide 100 m long?

## REFERENCES

1. Ramo, S., J. R. Whinnery, and T. Van Duzer: "Fields and Waves in Communication Electronics," 2nd ed., John Wiley & Sons, Inc., New York, 1984.
2. Liboff, R. L., and G. C. Dalman: "Transmission Lines, Waveguides, and Smith Charts," MacMillan Publishing Company, New York, 1985.
3. Pozar, D. M.: "Microwave Engineering," Addison-Wesley Publishing Company, Reading, Mass. 1990.
4. Rizzi, P. A.: "Microwave Engineering—Passive Circuits," Prentice-Hall, Inc., Englewood Cliffs, N.J., 1988.
5. Edwards, T. C.: "Foundations for Microstrip Circuit Design," John Wiley & Sons, Inc., New York, 1987.
6. Bahl, I., and P. Bhartia: "Microwave Solid State Circuit Design," John Wiley & Sons, Inc., New York, 1988.
7. Chang, K. (ed.): "Handbook of Microwave and Optical Components," vol. 1, John Wiley & Sons, Inc., New York, 1989.
8. Ishii, T. K.: "Microwave Engineering," 2nd ed., Harcourt Brace Jovanovich, New York, 1989.
9. Wolff, E. A., and R. Kaul: "Microwave Engineering and Systems," John Wiley & Sons, Inc., New York, 1988.
10. Baden Fuller, A. J.: "Microwaves," 3rd ed., Pergamon Press, New York, 1990.